Aspects of porcine immunological response to Nipah virus

by

Beata Boczkowska

A Thesis submitted to the Faculty of Graduate Studies of

The University of Manitoba

in partial fulfilment of the requirements of the degree of

Doctor of Philosophy

Department of Medical Microbiology

University of Manitoba

Winnipeg, Manitoba

ABSTRACT

Nipah virus (NiV) is a highly pathogenic and zoonotic paramyxovirus in the subfamily *Paramyxovirinae*, genus *Henipavirus*. The virus causes outbreaks of severe febrile encephalitis with a high mortality rate in humans, and of encephalitic and respiratory disease but with a low mortality rate in pigs.

The innate immune response has a critical role in limiting viral infection by activating antiviral state and adaptive immune response. As pigs are able to overcome the infection with NiV, the working hypothesis was that IFN induced signaling pathways are not completely inhibited by NiV in infected porcine cells enabling an antiviral state to be established. Indeed, there was no block of eIF2α phosphorylation in porcine fibroblast (ST) and monocytic-like (IPAM) cells, and interestingly also not in human fibroblast (MRC5) cells, suggesting no differences in the establishment of an antiviral state. To address the potential activation of an alternative IFN induced pathway, the MAPK signaling pathways were examined. The findings revealed that NiV infection triggers different kinetics of phosphorylation of ERK and p38 MAPK in the selected cell types. The data indicates that p38 MAPK to be indispensable for NiV replication *in vitro* especially in immune cells.

Previous studies did suggest the involvement of immune cells in viral spread and in immune modulation of porcine adaptive immune response. The next hypothesis stated that NiV infects immune cells and affects the population frequencies of PBMC in pigs. The objectives were to determine the permissiveness of porcine immune cells to NiV *in vitro* and if a subpopulation frequency of PBMC is affected *in vivo*. *In vitro*, productive viral replication was detected in monocytes, CD6+CD8+ T lymphocytes and NK cells, by recovery of infectious

virus, anti-genomic RNA and detection of structural N and non-structural C proteins within the infected cells. B lymphocytes, CD4-CD8-, as well as CD4+CD8- T lymphocytes were not permissive to NiV. In NiV infected piglets, the expansion of the CD4+CD8- T cells early post infection was consistent with a functional humoral response. In contrast, significant drop in CD4+CD8- T cell frequency was observed in piglets which succumbing to experimental infection, supporting vaccine studies that antibody development is a critical component of protective immune response. Thus in the porcine host, both aspects of innate and adaptive immune response are affected and contribute to NiV pathogenesis. These findings will help researchers to design and establish vaccination programs that would be more effective in pigs.

Acknowledgements

First, I would like thank my advisor Dr. Hana Weingartl for her unfailing mentorship, support, and enthusiasm for both my research and academic success. I am grateful for her patience and the trust she repeatedly invested in me. I am also appreciative of the financial support provided for my studies from National Science and Engineering Research Council grant and from the internal Canadian Food Inspection Agency Research partnership strategy project.

Many thanks to my committee members, Drs. Fowke and Rodriguez-Lecompte for their suggestions and advice throughout the years. It was a great experience to have you both on my committee.

All the BSL4 work was done at the National Centre for Animal Disease (NCFAD), Canadian Food Inspection agency (CFIA), with help from members of Special Pathogen Unit and Animal Care Unit (Dr. Melanie van der Loop, Kevin Tierney, Cory Nakamura) and U of M, T.K. Cheung Centre for Animal Science Research (Robert Stuski). A special thanks to Peter Marszal for being my BSL4 buddy and never refusing any of my time points. Without his generosity of time a lot of the experiments would not have been possible.

Finally, I wish to express my gratitude to my friends and family. Thanks to all my friends in Winnipeg and Julie (BFF) for making my off-work life enjoyable and filled with amazing stories. This period of my life was transformative and very difficult but with the help of David, the lessons learned here are now an integral part of my life. This accomplishment is a small tribute to my exceptional family who continue to guide my life through their wisdom and love. Especially to my mom and sis who showed me early in life that obstacles are made to be overcome and no hardship or person should break your desire to succeed in life. They are my source of daily inspiration and belief in things seemingly impossible is possible.

Table of Contents

List of Tables

List of Figures

Abbreviations

ALCAM	Activated leukocyte cell adhesion molecule
AP-1	Activator protein-1
APC	Antigen presenting cell
ATF	Activating transcription factor
ASV	African swine fever
BBB	Blood brain barrier
BSL4	Biosafety level 4
CARD	Caspase activation and recruitment domain
CD	Cluster of differentiation
CDV	Canine distemper virus
CMC	Carboxymethylcellulose
COX	Cyclooxygenase
ConA	Concanavalin A
CPE	Cytopathic effect
CNS	Central nervous system
CSF	Cerebrospinal fluid
CTL	Cytotoxic T lymphocyte
DC	Dendritic cell
DMEM	Dulbecco's modified eagles medium
DMSO	Dimethylsulfoxide
DPI	Days post inoculation
DTT	Dithiothreitol
EEA	Early endosomal antigen

eIF	Eukaryotic initiation factor
ELK-1	E-26-like protein 1
EMCV	Encephalomyocarditis virus
EMEM	Eagle minimal essential medium
ER	Endoplasmic reticulum
ERK	Extracellular regulated kinase
FBS	Foetal bovine serum
FITC	Fluorescein isothiocyanate
FMDV	Foot and mouth disease virus
GAS	IFN-γ activated sequence
GAF	IFN-γ activated factor
GE	Gene end sequence
GFP	Green fluorescent protein
GPCR	G protein coupled receptors
GTP	Guanosine-5'-triphosphate
GS	Gene start sequence
HCV	Hepatitis C virus
HEp-2	Hepatocellular carcinoma, human cell line
HEV	High endothelial venules
HeV	Hendra virus
HIV	Human immunodeficiency virus
hpi	Hours post inoculation
HPIV	Human parainfluenza virus
HPRT	Hypoxanthine-guanine phosphoribosytransferase
hrs	hours

IFN	Interferon
IFNAR	Interferon associated receptor
Ig	Immunoglobulin
IKK	IκB kinase
IKKi	Inducible IκB kinase
IκB	Inhibitor of NF-κB
IL	Interleukin
IN	Intranasal
iNOS	Inducible nitric oxide synthase
IP	Intraperitoneal
IPAM	Immortalized porcine alveolar macrophage
IPS-1	Interferon-beta promoter stimulator 1
IRF	Interferon regulatory factor
IRAK	Interleukin-1-receptor-associated kinase
ISG	Interferon stimulated gene
ISRE	Interferon stimulated response element
JAK	Janus activated kinase
JEV	Japanese encepathilitis virus
JNK	c-Jun N-terminal kinase
LPG2	Laboratory of genetics and physiology 2
MDA5	Melanoma differentiation associated gene 5
MAPK	Mitogen activated protein kinase
MAPKKK	MAPK kinase kinase
MAPKAPK	MAPK activated protein kinase

MAVS	Mitochondrial antiviral signaling adaptor
MCP-1	Monocyte chemotactic protein-1
MEF	Mouse embryonic fibroblast
MEK	Mitogen activated kinase
MeV	Measles virus
MHC	Major histocompatibility complex
min	Minutes
MK	MAPK activated protein kinase
MKP	MAPK phosphatase
MLK1	Mixed lineage kinase-1
MNK	MAPK interacting kinase
MOI	Multiplicity of Infection
MRAD	Milliradian
MRC5	Human lung fibroblast
mRNA	Messenger RNA
MSK	Mitogen and stress activated protein kinase
Myc	Myelocytomatosis oncogene cellular homolog
MyD88	Myeloid differentiation factor 88
MxA	Myxovirus resistance A
NES	Nuclear export sequence
NEMO	NF-κB essential modifier
NFAT	Nuclear factor of activated T cells
NF-κB	Nuclear factor kappa B
NiV	Nipah virus
NK	Natural killer cell

NLS	Nuclear localization sequence
NOS	Nitric oxide synthase
nt	Nucleotides
OAS	Oligoadenylate-synthetase
ORF	Open reading frame
PMA	Phorbol 12-myristate 13-acetate
PAMP	Pathogen associated molecular pattern
PAX	Paired box
PBMC	Peripheral blood mononuclear cell
pDC	Plasmacytoid dendritic cell
PE	Phycoerythrin
PLK	Polo-like kinase
PKR	Double-stranded RNA-dependent protein kinase
PIV	Parainfluenza virus
PMA	Phorbol 12-myristate 13-acetate
PFU	Plaque forming unit
PP	Ser/Thr Phosphatases
PRR	Pathogen recognition receptor
PRRSV	Porcine reproductive and respiratory syndrome virus
PTP	Tyrosine phosphatases
Rab	Small GTPase
RAF-1	Rapidly accelerated fibrosarcoma kinase
RANTES	Regulated on Activation, Normal T cell Expressed and Secreted
RAS	Small G protein
RdRp	RNA dependent RNA polymerase

RIG	Retinoic acid inducible gene
RIP-1	Receptor interacting protein-1
RLR	RIG-1 like receptor
ROS	Reactive oxygen species
RNA	Ribonucleic acid
RNase L	Cellular endoribonuclease
RNP	Ribonucleocapsid
RPV	Rinderpest virus
RSK	Ribosomal S6 kinase
RSV	Respiratory syncytial virus
RT	Room temperature
RTK	Tyrosine kinase receptor
RT-PCR	Reverse transcriptase-PCR
Ser	Serine
SeV	Sendai virus
SH2	Tyrosine-protein kinase homology
SIV	Swine influenza virus
ST	Swine testis fibroblast
STAT	Signal transducer and activator of transcription
TANK	TRAF family member-associated NF-kappa B activator
TAK1	Transforming growth factor-β activating kinase 1
TBK1	(TANK)-binding kinase 1
TCID	Tissue culture infective dose
TCR	T cell receptor
Th	T helper cell subset

THP-1	Human monocytic cell line
Thr	Threonine
TIR	Translocated intimin receptor
TLR	Toll-like receptor
TNF	Tumor necrosis factor
TRIF	TIR domain containing adaptor inducing IFN-β
TRAF	TNF receptor-associated factor
Tyk	Protein-tyrosine kinase 2
UTR	Untranslated region
VCAM	Vascular cell adhesion molecule
Vero	African green monkey kidney cell line
VISA	Virus-induced signaling adapter

1.0 Introduction

Nipah virus is a zoonotic, highly pathogenic, biosafety level 4 (BSL4) virus within the family *Paramyxoviridae*, genus *Henipavirus* (1). Humans infected with NiV suffer primarily from severe encephalitis with pulmonary involvement in a high percentage of patients, and with fatal outcomes in about 40 or more percent of laboratory confirmed cases, depending on the outbreak (2, 3). All human cases during the initial 1998–1999 outbreak in Malaysia and Singapore were due to transmission of NiV from infected pigs (4, 5). In Bangladesh, transmission of the virus from its natural reservoir, the *Pteropus* bat to humans is by ingestion of contaminated date palm sap or fruit. In addition, nosocomial and human to human transmission have also been reported (6, 7, 8).

1.1 History of Nipah virus outbreaks

In the second half of 1998, Malaysia reported an outbreak of encephalitis, initially thought to be caused by Japanese encephalitis virus (JEV) (2). The outbreak had epidemiologic characteristics which were unlike those of the endemic mosquito-borne JEV, and in March 1999, Nipah virus (NiV) was identified as the etiologic agent of the outbreak (4, 9). Characteristics of this outbreak included exposure to swine as the principal risk factor for infection; the occupations, racial groups and age groups were also considered when the association was made with the infection (4, 9). The disease primarily involved the central nervous system with patients progressing to coma and death. The outbreak was eventually brought to a halt by instituting a system of surveillance and culling in excess of 1.1 million swine. The culling resulted in huge economic losses (10). In 1998-1999 in both Malaysia and Singapore, there were a total of 265

human cases and 105 deaths due to zoonotic transmission of NiV from pigs to humans (2, 11-13).

In 2001, an outbreak of disease occurred in Siliguri, India, where transmission of the disease included family members and attending medical staff (14). The etiology of the outbreak remained unknown until serum specimens were tested and discovered to have IgM antibodies to NiV. Subsequently, NiV viral RNA was detected by RT-PCR in the urine of patients and the viral identity was confirmed by sequencing. Unlike the previous outbreaks in Malaysia, no intermediate animal host was readily identifiable. Beginning in 2001, Bangladesh had a number of relatively small outbreaks in an area bordering India to the east (7, 15, 16, 17). The mortality rates in these subsequent regional outbreaks were as high as 75% compared to the 40% seen in other documented cases (7, 18). To date it is estimated that there were 582 human cases of NiV with an overall 315 human fatalities accounted (16, 19, 20). Epidemiological investigations suggested a number of routes for human infection including direct or indirect contact with fruit bats (*Pteropus giganteus* being the predominate species in this region) in roosting or feeding areas (21, 22), contamination through food products by the bats (partially eaten fruits or palm sap tapped from trees) (15, 23), and person to person transmission (6, 18, 24).

1.2 Nipah virus reservoir

During the initial outbreaks the suspected route of transmission of NiV was from bats to pigs via pig feed, contaminated by bats feces and saliva (2, 5, 21, 25). Bat feces and urine were also the primary risk factor of NiV infection in outbreaks in Bangladesh (26, 27), where several *P. giganteus* samples were identified to be positive (27). Shortly after the Malaysian outbreak, samples taken from bats from the following species were also found to be seropositive: *Cynopterus brachyotis, Eonyveteris spelaea, Scotophuilus, Pteropus vampyrus and Pteropus*

hypomelanus (25). Overall, the highest prevalence of neutralizing antibodies was detected in fruit bats from the species of *P. hypomelanus* and *P. vampyrus* (25). *P. vampyrus* bat species are widely found in South Asia and are able to move hundreds of miles within days (28); therefore it is thought to be the most important host for NiV (26). A growing list of *Pteropus* species with antibodies against NiV reinforced the hypothesis that *Pteropus* species (Order Chiroptera, Family Pteropodidae) act as a host reservoir for Nipah virus (22, 25, 26, 27, 29). In experimentally NiV infected bats, NiV was detected in urine (30). The successful isolation of NiV from *Pteropus* spp. bats was depended on seasonal factors which could be interpreted as evidence for seasonal dependent variation of virus concentration or prevalence (31, 32). Outbreaks in Northern India and Bangladesh occur repeatedly in January/February (7, 15, 23); and in Thailand, the virus was consistently found in May from *P. lylei* urine (29). These months coincided with the bat's breeding seasons. The breeding cycle/season of *Pteropus* spp. bats commences in December and pups are delivered in February, followed by pup separation from mother which starts in May (33, 34). The breeding season overlapping with the early palm sap harvest season likely result in a high risk period for spillover of NiV (35, 36).

1.3 Classification

Nipah virus belongs to the family *Paramyxoviridae*, has a non-segmented, negative strand RNA genome surrounded by an envelope forming relatively spherical, pleomorphic virus particles (4). There are two subfamilies within the family *Paramyxoviridae*, the *Paramyxovirinae* and the *Pneumovirinae*. The subfamily *Paramyxovirinae* is divided into 5 genera: *Rubulavirus* (prototype, mumps virus), *Respirovirus* (prototype, human parainfluenza virus 1), *Morbillivirus* (prototype, Measles virus), *Avulavirus* (prototype Newcastle disease virus), and with the emergence of NiV and its counterpart Hendra virus (HeV), a relatively new genus *Henipavirus*

(Fig.1) (37, 38). The henipaviruses genetic organization does resemble viruses found in the Respirovirus and Morbillivirus genera (37, 38).

The most prominent molecular feature of henipaviruses is the large genome of 18,246 nucleotides (nt) compared to other members of the *Paramyxoviridae* family (37, 39, 40). The prototypical genomes of NiV and HeV are 18,246 nt and 18,234 nt long respectively (37, 40). There are two distinct strains of NiV isolated from the Malaysian and Bangladesh outbreaks. Sequence analysis revealed that there is a nucleotide variation range of 6.32% - 9.15% and an amino acid variation range of 1.42% - 9.87% between the Malaysian and Bangladesh strains (41). Recently, a new virus with a similar genome size of (18,162 nt) to NiV and HeV referred to Cedar virus (CedPV) was also isolated from pteropid bats (42).

1.4 Viral structure and genomic organization

Nipah virions share common morphological characteristics with the rest of the family Paramyxoviridae, such as pleomorphic structure with spike like projections. Nipah virus particles are larger in average diameter (500 nm) with surface spikes of 10 nm in length (43, 44). The attachment glycoprotein (G) and fusion (F) proteins are the surface spikes that protrude from the surface of the lipid bilayer membrane. The matrix protein (M) is at the inner surface of the lipid bilayer envelope and stabilizes the structure by interacting with the surface glycoproteins and ribonucleocapsid (RNP). The RNP is inside the viral membrane consisting of viral genome surrounded tightly by nucleoprotein (N), the phosphoprotein (P) and the RNA-dependent RNA polymerase (L) (45). The complete structure of NiV and its individual components are shown in Figure 2.

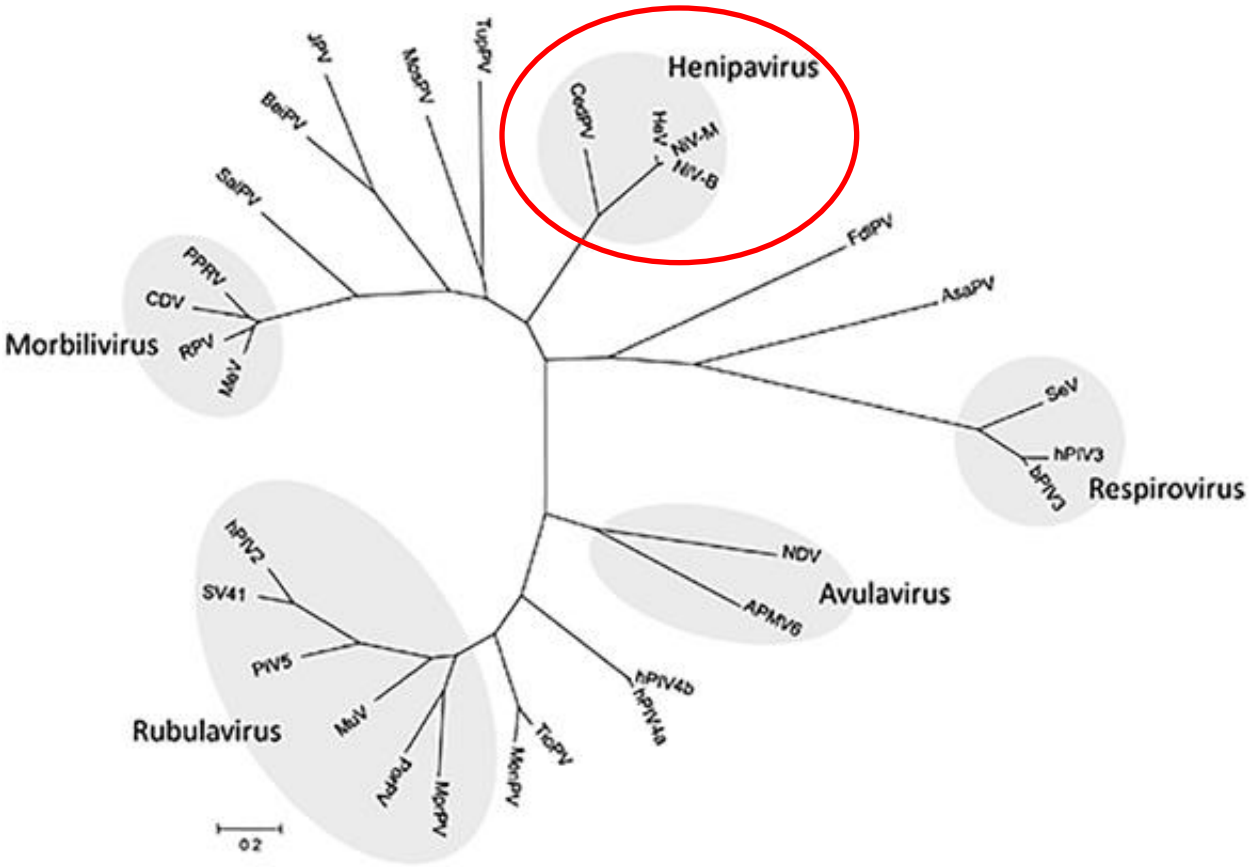

Figure 1 Phylogenetic tree of *Paramyxoviridae* family based on the N amino acid sequences. The *Morbilivirus* and *Respirovirus* genera have similar genetic organization to *Henipavrus* genus. The *Henipavirus* genus is highlighted to accent the comparison of nucleotides of Malaysian and Bangladesh NiV strains, HeV and newly added CedPV. Adapted from **(42).**

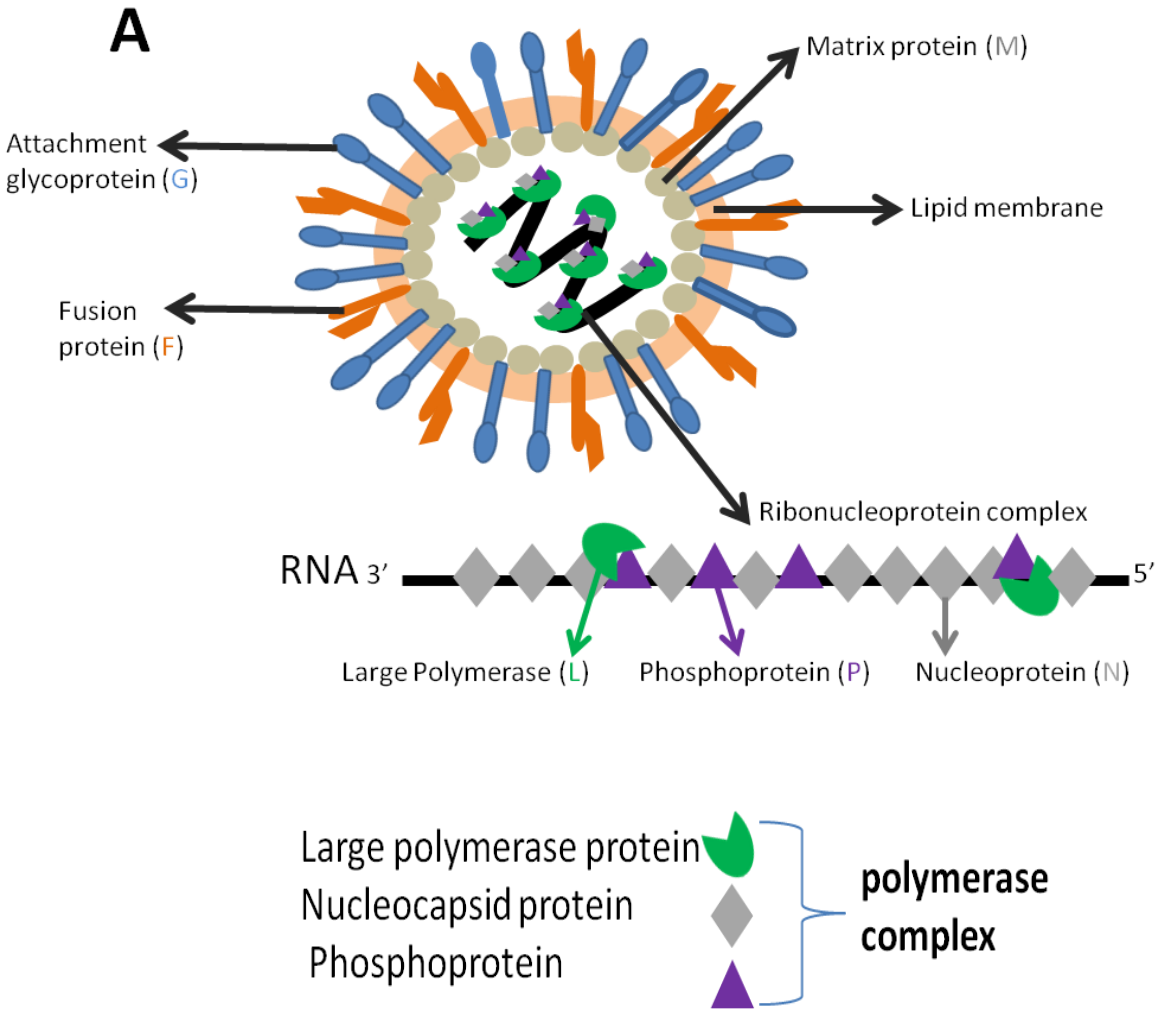

Figure 2 Nipah virus structure and the viral polymerase complex that is required for transcription of genomic RNA into mRNA and anti-genome RNA.

The organization of the henipavirus genome is shown in Figure 3A. The viral genome encodes for six genes in the following order: 3` leader - nucleocapsid (N), phosphoprotein (P), matrix (M), fusion (F), glycoprotein (G), and RNA-dependent RNA polymerase (L) - trailer-5' (46, 47, 48). Like other paramyxoviruses, 3' leader and 5' trailer regions are present for both transcription and replication and each gene is flanked by gene-start (GS) and gene-end (GE) sequences with untranslated regions (UTRs) (45). Nipah genome size is attributed to the large UTRs at the 3' end of most genes with unknown functions (40). Recently, the 3' UTR of NiV N function was revealed to play a role in posttranscriptional regulation by binding of hnRNP (heterogeneous nuclear ribonucleoproteins) which are endogenous host protein present in the cytoplasm of cells (49). The GS signals initiation and capping whereas the GE is essential for polyadenylation and termination of each mRNA (45). The genomic promoters have similar 12-13 nt at the end of the genome and antigenome and are important for virus replication (50). The NiV P gene produces three non-structural proteins referred to as C, V, and W. The NiV V and W proteins are produced from edited RNA transcripts by insertion a non template G's into NiV P reading frame by polymerase stuttering (51). Transcripts with one added G express the V protein and transcripts with two added two G's will express the NiV W (51). NiV C protein is encoded by an internal open reading frame (ORF) that initiates 23 nt downstream of the translational initiation site for the NiV P ORF (52) as represented in Figure 3B.

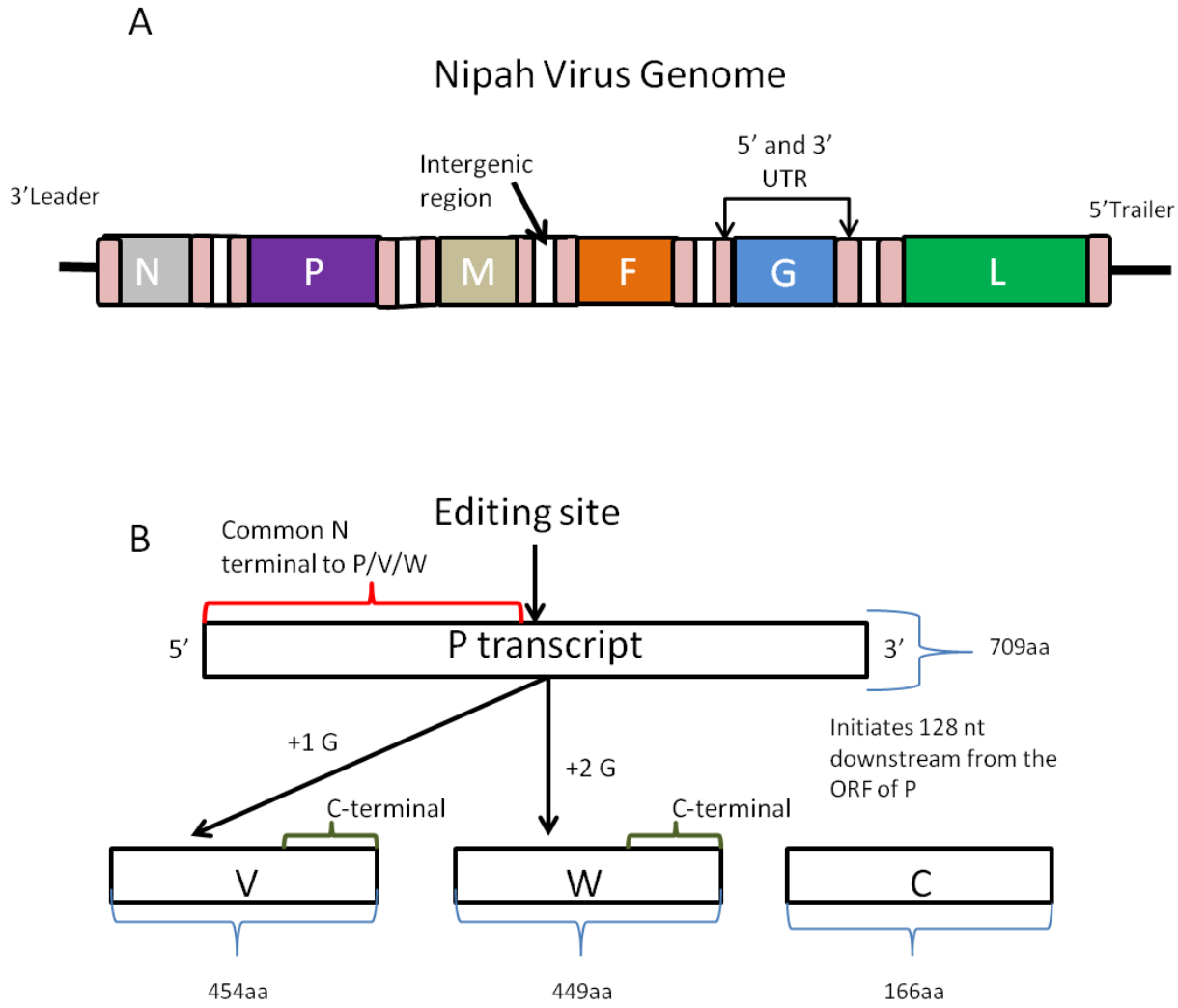

Figure 3 **A**. NiV genome consists of six structural genes with unique genus specific 3' leader and 5' trailer sequences **B**. Gene processing of the NiV P transcript produces three non structural proteins, NiV V (454 aa), W (449aa) and C (166aa). NiV C is produced from an entirely different reading frame within the P gene and NiV V and W are transcribed with insertion of non templated G's inserted into NiV P reading frame. The P protein of 709 aa is produced from the unedited P transcript. The red bracket indicates the common N –terminal region and the green bracket indicates the unique C terminal region of each non-structural protein.

1.5 Nipah structural proteins - physical characterization and function

The nucleocapsid (N) proteins of NiV and HeV are 532 amino acids in length and responsible for encapsidating the viral genome and mRNA during replication and transcription (53). The NiV N protein has the ability to assemble itself in the absence of other viral proteins into a ring like structure (54, 55). The N proteins of the subfamily *Paramyxovirinae* cover exactly six nucleotides to enable for effective viral replication (56). Due to structural constraints imposed by the binding between the RNA and the N protein, mutations in the NiV N protein can lead to inefficient viral replication (53, 55). The nucleoproteins of paramyxoviruses including NiV N are usually comprised of two domains; the amino-terminal domain is responsible for specific interaction with the RNA genome and other N proteins, and the carboxy-terminal domain interacts with the P protein (57). The C-terminal domain of N is mostly disordered allowing for flexibility to exert multiple biological effects along with binding to the C-terminal X domain (XD) of the homologous P protein (58). For maximal replication, NiV N protein needs to be phosphorylated as demonstrated in studies on effective minigenome replication (59). The turnover rate of NiV-N residue phosphorylation is quick suggesting the involvement of host cellular activity regulation of NiV N phosphorylation (59). Another important feature of NiV N proteins is its strong immunogenic properties and high abundance making it ideal for diagnostic purposes (54, 60).

The phosphoprotein (P) is generated from the P gene along with three other distinct non-structural proteins (45). The NiV P protein is least conserved NiV protein and is about 100 to 400 amino acids longer than other paramyxovirus P proteins (57). Biochemical and structural studies of NiV P revealed disordered and order domains required to complex with the nucleocapsid (58). These regions on the NiV P are essential to interact with N protein for

replication and the transcription of mRNA as part of the RNA dependent RNA polymerase (RdRp)(57, 61). In addition, the P protein is phosphorylated on serine residues by cellular kinases in order to interact with N protein during virus replication and transcription (62).

The NiV matrix (M) protein has a length of 352 amino acids (1). By interacting with the inner surface of the viral envelope, F protein and ribonucleoprotein complex, the M protein provides stability to the virion structure (63). The N terminal domains on the NiV M protein are essential for virus budding and are retained near the inner surface of the envelope (63, 64). In epithelial cells, once syncytia are formed the M protein moves from the cytoplasm to accumulate on the apical surfaces to facilitate the release of newly replicated virus (65). Proper nuclear and cytoplasmic trafficking of NiV M is essential for virus budding and is regulated by putative bipartite nuclear localization sequence (NLS), containing a lysine rich nuclear export sequence (NES). This lysine rich NES is involved in import and export as well as required for plasma membrane targeting of NiV M for incorporation into the virion (66). Therefore, the ubiquitination of the NiV M protein is required for export from the nucleus but it remains to be demonstrated why NiV M requires nuclear transit and possible post translation modification for virus assembly and budding (66).

Nipah G (attachment) glycoproteins are type II membrane proteins (602 amino acids) that serve primarily for binding to cellular receptor (1, 67). NiV G structure is comprised of a globular head connected to its transmembrane anchor and short cytoplasmic tail via a stalk domain (68). The globular head of the G protein folds as a β-propeller consisting of six blades and is maintained by disulfide bonds between each blade (68). The globular head of the G protein binds with ephrin B2 cellular receptors, which are expressed on lymphocytes, neurons, smooth muscle cells, and endothelial cells surrounding small arteries (69 -73). The normal

cellular function of ephrin B2 is to regulate cellular processes such angiogenesis (to form new blood vessels through endothelial sprouting), proliferation and remodeling processes (74). This cellular receptor is important in mammalian host development and is a highly conserved protein across mammalian species. Due to the expression of these ubiquitous receptors, NiV can enter into a number of host cells. In addition, ephrin B3 is also a receptor for NiV G and this receptor is found predominately in brain on brain stem neurons (70, 71, 72, 75) as well as human monocytes (69). Stimulation due to Eph binding to ephrin known as reverse signaling is accompanied by ERK phosphorylation (76). The reverse signaling including the ERK pathway may be speculated to be also activated by binding of NiV G in its tetrameric form to ephrin B. While the binding domain of NiV G is required for binding to both cellular receptors (68), it is the stalk region of NiV G that possess the receptor activation site that will enable the F protein to initiate fusion (77, 78). The NiV G globular head is vital in preventing F protein triggering by the G stalk domain. Only upon attachment of the G globular head to the cellular receptor will the G stalk domain trigger the F protein (79, 80). In contrast to the attachment glycoproteins of other paramyxoviruses, NiV G lacks both hemagglutinin and neuraminidase activities (81, 82).

The fusion (F) proteins of NiV are type I transmembrane protein composed of 546 amino acids. The F glycoprotein is required for fusion of the viral envelope with cell membrane and cell to cell fusion. Fusion is pH-independent process in viral entry (83). To promote fusion, the F protein precursor (F_0) must be proteolytically cleaved into 2 subunits (F1 and F2) by specific enodosomal cellular proteases known as cathepsins thereby releasing the fusion peptide of the F1 subunit (83- 86). The F1 subunit protein structure is comprised of N-terminal hydrophobic peptide domain, two heptad repeat domains, a transmembrane domain and cytoplasmic tail (87). In polarized epithelial cells, the cytoplasmic domain of the F tail region and the transmembrane

domain require specific tyrosine residues to become functional to increase fusion activity and trafficking of F protein (88, 89). The proteolytic process takes place during F transport in early endosomes indicated by early endosomal antigen 1 (EEA-1), Rab4, and Rab11, and recycling endosomes while NiV F trafficking is through late endosomal compartments (90). A functionally mature F protein is transported back to the plasma membrane, and can be triggered to initiate rearrangement of heptad repeat domains of the F1 subunit (91). The triggering of F protein to form the six- helix bundle will only take place when the NiV G undergoes conformational changes to expose the C terminal stalk domain of G (79). Once triggered, the F fusion peptide is exposed and inserted into the cell membrane to form a pre-hairpin intermediate to initiate conformation changes to form a six-helix bundle to mediate membrane fusion (91). Data does suggest that greater levels of F triggering occur via NiV G binding to ephrin B2 than with ephrin B3 in turn resulting in faster membrane fusion (92).

The L protein is the largest viral protein of paramyxoviruses; the L gene is the last to be transcribed as it is the most distal in transcription located at the 5' end of the NiV genome. As result the L protein is produced at low levels in NiV infected cells (40). The NiV L protein forms a complex with P protein required for polymerase activity with N:RNA templates (45). The L protein functions include initiation, elongation and termination in both mRNA transcription (capping, methylation, and polyadenylation of mRNA) and in genome replication (45, 93). However, it is suggested to be more important for maintaining the overall polymerase complex structure rather than for its catalytic activity (48).

1.6 Nipah non-structural proteins- physical characterization and function

The P gene of henipaviruses encodes three non-structural proteins (C, V, and W) in addition to the P protein. Co-transcriptional RNA editing of the P gene produces V and W

proteins by inserting one additional G in mRNA coding for V and two extra G into the mRNA coding for W (Fig. 3B) (45, 52). High frequency of RNA editing of the P gene was observed in all NiV strains (Malaysian or Bangladesh) (94). However, the frequency of editing is lower at early time points of infection and increases over time (52). The C protein is encoded by an internal open reading frame (ORF) that is 23 nt downstream of the translational initiation site for the P ORF (45, 52). All the non- structural proteins (C, V, and W) are detected in infected cells; however they have different cellular locations (94, 95). In NiV infected VERO cell lines along with recombinant studies of the proteins, P and V are localized in the cytoplasm while W was found in the nucleus (51, 94, 96, 97). A difference in the localization of W was in NiV infected human endothelial cell lines where W was detected only in the cytoplasm but translocated to the nucleus in NiV infected neuroblastoma cell lines (95). The C protein was scattered in perinuclear region of NiV infected VERO cell lines (94).

These non-structural proteins are involved in NiV life cycle by regulating replication (98, 99) and hindering the JAK-STAT signaling pathway (96, 97, 100). By mapping the binding domains of NiV V and W, it was found that the N terminal of P/V/W proteins bind to STAT1 (Fig. 3B). The interaction with NiV P and STAT1 as observed by quantification of protein expression was less strong than with NiV V and W (97, 101). The Shaw *et al*. (101) study also characterized the V nuclear export sequence (NES) that is required for its accumulation in the cytoplasm and subsequent sequestering of STAT1 and STAT2. Conversely, W has a nuclear localization sequence (NLS) which enables it to act in the nucleus of the infected cells (100). This NLS is located in the unique region on the C terminal end of the NiV W protein (101). The inhibition of IFN α and IFN γ reporter genes was demonstrated by recombinant NiV V protein. NiV V protein sequestered STAT 1 and 2 in large molecular weight complexes in the cytoplasm,

unlike other viruses that block the downstream effects of STAT signaling pathway by STAT1 degradation (96, 102). In NiV V expressing cells both STAT1 and STAT2 remained cytoplasmic even after the addition of IFN (96). The STAT1 and STAT2 binding domain on V were mapped between 100-160 amino acids (100). Mutations in the binding region of STAT1 of the NiV V coding sequence confirmed that this region is needed for association with STAT1 in porcine and human cells (103). NiV P and W also co-localized with STAT1 with NiV W in the nucleus and cytoplasm whereas P protein binds to STAT1 only in the cytoplasm (97).

The nuclear localization of NiV W is necessary for the impairment of TLR3/TRIF pathway by blocking TRIF mediated activation of IRF-3 responsive promoter to initiate the production of IFN β (101). NiV V proteins bind to the MDA5 helicase along with LGP2 to suppress RLR signaling thereby inhibiting the downstream signaling events leading to IFN β synthesis (104, 105).

The C protein of NiV was first shown to have less of an ability to inhibit the activation of the JAK-STAT pathway when compared to V and W proteins (106). With the use of recombinant NiV with specific mutations introduced into the C protein, it was proposed that NiV C protein is more important for viral replication and the W protein was the primary inhibitor of JAK-STAT pathway (107). A more recent study by Mathieu *et al*. (108) revealed an added function to the C protein which suggests it can also regulate cytokine balance in transfected cells. These data was corroborated by using reverse genetics to show that the C mutant NiV induces early and heightened induction of IFN β and antiviral gene expression (109). However, NiV C also exhibits inhibitory activity against TRL7/9 dependent IFNα induction by binding to IKKs and inhibiting phosphorylation of IRF-7 (110). Hence, the NiV C protein along with NiV V and

W proteins play important roles in early induction of pro-inflammatory cytokines and IFN antagonism during NiV infection.

1.7 Overview of NiV replication cycle

Figure 4 describes schematically the life cycle of NiV which follows the same replication mechanisms as other paramyxoviruses. First, Nipah virions attach to specific host cellular receptors, known as ephrin B2 or ephrin B3 (70, 71, 72, 75). Following attachment, the virus can enter cells either via macropinocytosis (111) or fusion with the plasma membrane (82, 92, 112). Upon receptor binding NiV G undergoes conformational changes to expose the C terminal stalk domain of G in turn triggering F to form the six- helix bundle and initiate membrane fusion (79). NiV G binding to ephrin B phosphorylates specific tyrosine kinases during virus entry in turn, recruiting and initiating cellular signaling pathways (76,113). Only upon the release of the ribonucleocapsid into the cytoplasm can NiV replication cycle begin with the transcription of viral genome (82, 112). The viral polymerase begins all RNA synthesis at the 3' end of the genome and transcribes the gene into mRNA sequentially (N to the L gene) by terminating and reinitiating at each of the gene junctions (45). Incomplete processivity results in a gradient of mRNA synthesis that is inversely proportional to the distance of the gene from the 3' end of the genome. The GE signals direct polyadenylation and termination of each mRNA and the poly-A tails of the mRNA are synthesized by repeated reading of a short U stretch by the viral polymerase. At the end of each gene, the polymerase falls off the RNA and starts over at the next GS signal (45). When the polymerase ignores these GE, it produces proteins downstream (45). The P gene is not monocistronic as it encodes for non-structural proteins which are synthesized by insertion of additional non templated G's to the reading frame to express V and W proteins

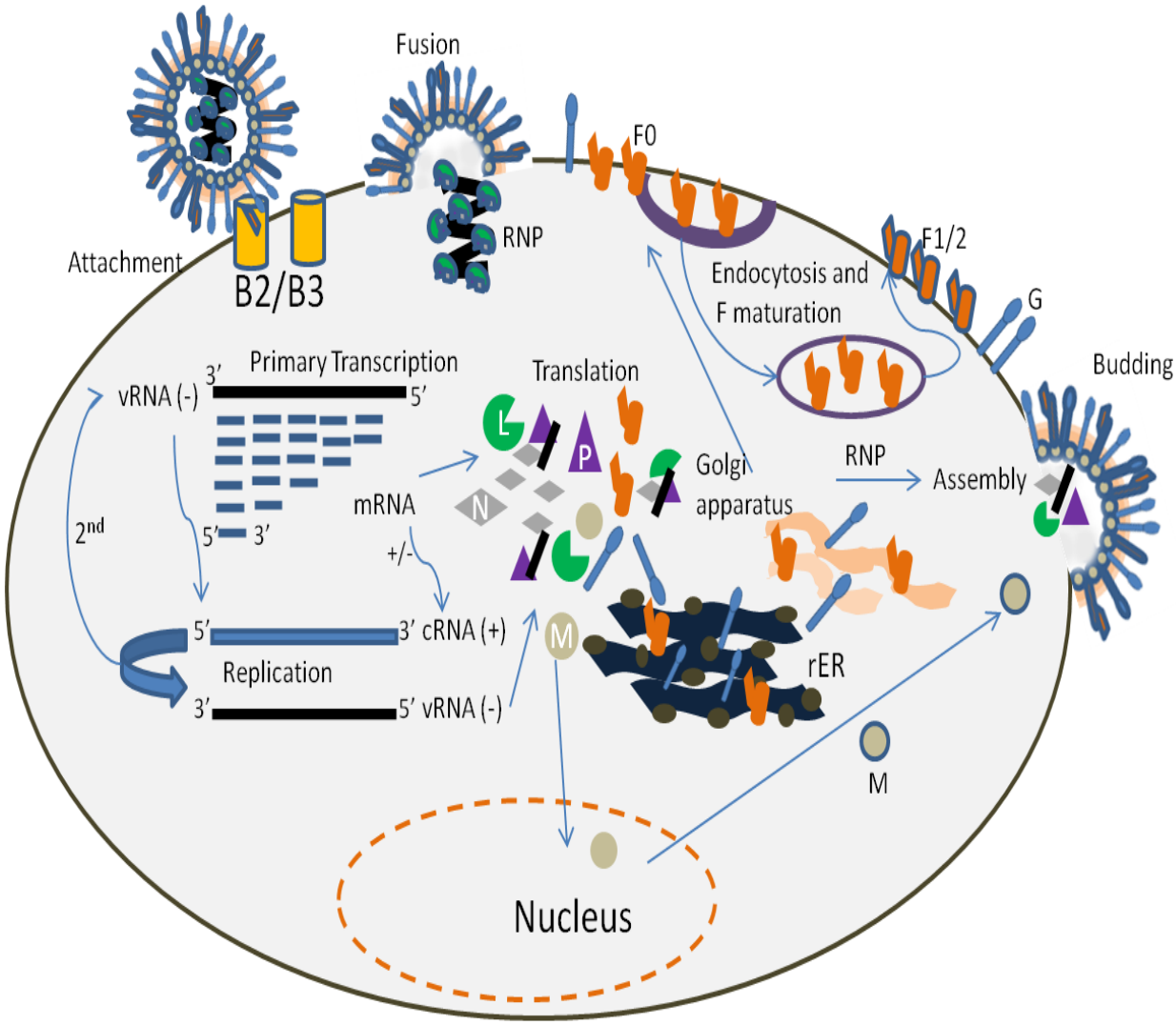

Figure 4 A general description of NiV replication cycle. Nipah virus binds to cellular receptors ephrin B2/B3 via the G glycoprotein (A) and F protein mediates fusion of the viral membrane to the cell membrane for the virus to enter the cells (B). The viral RNP complex is released into the cytoplasm followed by primary transcription (C) and translation (D). Secondary viral transcription begins with the negative genome generation followed by a 3'- 5' gradient of viral mRNA from N to L. Complementary cRNA becomes a template for replication of more viral vRNA (E). All viral proteins are synthesized by ribosomes in the cytoplasm. Following translation of viral proteins, F and M proteins are modified post translationally and are directed to specific cellular locations to complete maturation. Assembly and budding follow.

whereas the C protein is expressed from an alternative reading (Fig. 3B) (45, 52). In addition to individual viral proteins, full length progeny, negative sense RNA is also produced by the viral polymerase. Only when enough unassembled N protein is present, the polymerase start to transcribe a full length positive-sense antigenome by a similar process to transcription, with one exception that the mRNA transcriptional signal at each gene junctions is not recognized (45, 93). The genome then associates with nucleocapsids, which are formed consisting of the N and P proteins (114). All viral proteins are synthesized by ribosomes in the cytoplasm. Though, F and G proteins require association with the endoplasmic reticulum (ER) for transport through the Golgi apparatus to the cell membrane. The F protein must be proteolytical cleaved in endosome in order for conformational change to take place to be functional mature and is recycled back to the cell membrane (83, 84, 85, 90). NiV M protein mediates virus assemblage and budding of new virions to complete the viral replication cycle (66).

1.8 NiV infection in humans

In humans, the main symptomatic signs of NiV infection are severe acute encephalitis and respiratory disease. The prevalence of respiratory symptoms differs between the Bangladesh and India outbreaks and the Malaysian outbreak (2, 3). Only 40% of Malaysian and Singaporean patients reported respiratory distress, while close to 70% of Bangladesh and Indian patients reported these symptoms (2, 3, 115). A majority (90%) of cases from the 2001-2004 Bangladesh outbreaks had altered mental status, while only 21% of patients presented this sign during the Malaysian outbreak (3). From the Malaysian outbreak, it was determined that 7.5% of patients who had recovered from NiV infection developed relapse encephalitis, while 3.7% of patients who had non-encephalitic or symptomatic infection developed late-onset encephalitis. Patients who experienced relapsed or late-onset encephalitis had a lower mortality rate (18%) than those

who suffered acute Nipah encephalitis (40%) (115, 116). However, those with relapse or late-onset encephalitis tended to have worse residual neurological deficits (61%) than those who had acute encephalitis (22%). These relapses of encephalitis in humans are considered to be recrudescent due to replication of NiV in the central nervous system (CNS) (115, 116). To date it is unknown how the virus can remain in humans to cause disease after months or years post initial infection.

Nipah is detected in bronchiolar cells early in infections and is shed through nasopharyngeal and tracheal secretions (114, 117). An acute infection with NiV leads to a systemic multi-organ vasculitis associated with endothelial cells and involving the CNS. Vasculitis of small blood vessels in brain and lungs is the main pathologic feature of NiV infection in humans (114, 118). In the vascular endothelium reports showed intense immunohistochemical staining of endothelial and multinucleated giant cells (11, 114). However, evidence of endothelial infection and vasculitis was also observed in other organs, including lung, heart, spleen, and kidney (11,114). Multiple organ failure is attributed to NiV entering the bloodstream and disseminating throughout the host by either free form or binding to leukocytes (119). Cells like neutrophils, macrophages and lymphocytes are found in the vicinity of necrotic plaques in the CNS. Viremia appears to be the main route of CNS invasion by NiV in humans (114). In humans, infection of the CNS is characterized by vasculitis, thrombosis, parenchymal necrosis and presence of viral inclusion bodies (11, 114, 120).

Animal models have provided suitable models to resemble human NiV disease. There are several animal models for NiV infection including the IFNAR-KO mouse model (121); the guinea pig model (122-124); the cat model (125-127); the golden Syrian hamster model (128-130); and the ferret model (131, 132). Each of these small animal models share some aspects of

NiV infection in humans but only two animal models. African green monkeys (133) and ferret models (129, 130) have the closest and complete pathogenesis as observed in humans. These models show both severe respiratory and neurological disease along with generalized vasculitis as observed in human NiV infection. Currently, these two models are being used for efficacy testing for human vaccine studies against NiV infection (discussed in Section 1.13).

1.9 NiV infection in pigs

During the initial outbreak in 1998 - 1999 in Malaysia, pig infection rate was 100% in affected farms but mortality rates were between 1 - 5%. The incubation period was estimated to be between 7-14 days (5). The mode of transmission was suspected to be airborne or due to direct exposure to infected pigs. This was later supported by the detection of NiV in upper and lower respiratory tract (5, 134, 135). The clinical disease and the signs varied depending on age of the pig. Signs of neurological and respiratory distress were more frequently observed (5). On gross examination, the lungs, kidneys, and brain showed edema and congestion with petechial to ecchymotic hemorrhages on the serosal surfaces. Vasculitis and syncytial cell formations were observed in endothelial cells of the small blood vessels and lymphatic vessels in histopathological examination. By immunohistochemistry, NiV antigen was detected in alveolar macrophages with infiltration of lymphocytes in both peribronchial and peribronchiolar areas; in addition, syncytia formation was also observed in epithelial cells of the respiratory tract (5, 134,135).

In experimental pig models of NiV infections, the age of the pigs ranges between 5-9 weeks old. These pigs were inoculated by either subcutaneous or the oral-nasal route (125, 136,137). Clinical signs varied from subclinical to body temperature elevations, increased respiratory rates and mild cough (125, 136, 137,138). Inoculations by subcutaneous or nasal

route with virus doses of 5 X 10^4 to 5 X 10^5 pfu/pig had consistent outcomes of advanced neurological signs and required euthanasia in some pigs (125, 136, 137). The proportion of pigs requiring euthanasia represented about 15% or more than observed in field infections (125, 136, 137, 138). In some of the experimentally inoculated pigs, bacterial infections were suspected due to the appearance of whitish cloudy cerebrospinal fluid which was subsequently confirmed as bacterial meningitis caused by *Streptococcus suis* and *Enterococcus faecalis* (137).

Many of the pathological signs are similar to the ones reported in natural infection of pigs with NiV. In the lung lesions, infiltrations of mononuclear cells were observed in the peribronchiolar and perivascular regions with vasculitis leading to interstitial pneumonia. NiV antigen was detected in several different cell types; these included endothelial cells, smooth muscle cells of tunica media (blood vessels), macrophages, and cells of bronchiolar epithelial and to a lesser extent in alveolar epithelial cells (125, 134, 136, 137). Although NiV will stain for antigen in endothelial cells, it is rare to observe syncytia and multicleated giant cells in pig specimens whereas epithelial syncytia were more readily observed (125, 134). In the brain and the meninges, noticeable perivascular cuffing consists mostly of neutrophils, monocytes and lymphocytes (125, 134, 136, 137). NiV antigen was detected in ependymal cells, choroid plexus and meninges as well as in neurons and glial cells (125, 134, 136). As with the lung, NiV antigen was found in the endothelial cells of small blood vessels such as arterioles, capillaries and venules of CNS, smooth muscle cell of tunica media and mononuclear cells (125, 134, 136). With the use of experimentally NiV infected pigs, a clearer understanding was established as to how the virus initiates the progression of infection of the cells of the CNS. It was observed that with nasal inoculations of NiV, the virus was able to gain access to the CNS via cranial nerves from the nasal cavity (136). It was demonstrated that after initial replication in the oro-nasal

cavity, NiV has the potential of crossing blood brain barrier to gain access to the CNS (136, 138). In addition, the nasal cavity is an important region for dissemination of virus since drainage into the submandibular lymph nodes from the nasal cavity would allow the virus to enter into the blood and/or lymphatic vessels.

As with natural NiV infections in pigs, the lymph nodes of experimentally infected NiV pigs were also affected and infected. As early as 6-7 days post inoculation (dpi) the highest viral load was determined in lymph nodes associated with the lungs. Pathological findings revealed that early post inoculation lymph nodes had notable necrosis whereas later in the infection (28 dpi) necrotic cells were not visible but lymphoid depletion was present and affecting both the cortical sinusoids and germinal centres (136, 137, 138). Immunohistochemistry analysis confirmed NiV antigen was present in endothelial cells of blood and lymphatic vessels, dendritic cells and a small percentage of lymphocytes in the lymph nodes (136, 137, 138). Pathological lesions were also evident in the spleen but not in the thymus (137). The humoral immune response was represented by the development of antibodies in pigs that recovered and cleared the virus (138). Pigs started to develop neutralizing antibodies against NiV around 7- 10 dpi (137). In surviving animals neutralizing antibodies were at a high titer by 16 dpi. Although virus appeared to be cleared from the tissues of the infected animals by 23 dpi, low amount of NiV RNA was detected in submandibular and bronchial lymph nodes of three pigs and olfactory bulb of one animal. Despite the presence of neutralizing antibodies, virus RNA was still recovered (137). NiV infected pigs possess neutralizing antibodies which demonstrates response of the humoral immunity and possibly the importance of CD4+ T cells upon infection. However, there was a delay in the development of antibodies compared to other viruses such as influenza (137), (139) and signs of bacterial infections normally associated with immune comprised pigs (137)

suggesting that NiV infection in pigs may cause immune modulation of the adaptive immune response.

1.10 Innate Immune Response

The outcome of a virus infection is a complex struggle between virus replication and the antiviral response of the host. The innate immunity is the initial and crucial response against virus infection and plays an important role in antiviral protection and activation of the adaptive immune response. The innate immune cells include natural killer (NK) cells, monocytes, dendritic cells (DC), macrophages and neutrophils (140). The common features of all innate immune cells is the expression of pattern-recognition receptors that are capable of recognizing pathogen associated molecular patterns (PAMP) on foreign invaders of host cells (141). Viral RNA is recognized inside endosomes by TLR 3 and TLR 7 triggering a cascade of signals (Fig. 5) for the activation of IFN and pro-inflammatory genes (142). NiV W protein can impair the TLR3/TRIF pathway and the initiation of production of IFN by translocation into the nucleus to block TRIF mediated activation of IRF-3 responsive promoter (101). The only difference in the IFN induction signaling cascade is in plasmacytoid DC (pDC) where IFN genes are activated via IRF7 and not IRF3 (Fig. 5) (143). NiV C and V protein exhibits inhibitory activity against TRL 7 dependent IFN α induction potentially in pDC by binding to IKKs and inhibiting phosphorylation of IRF7 (110, 144). Activation of TRL 4 activation also recruits both TRIF and MyD88 as shown in Figure 5 leading to signaling through both MyD88-dependent pathways utilized by TLR 7 and the MyD88 independent pathway shared with TLR 3 to induce IFN and pro-inflammatory cytokines (145). Currently, there is no evidence that NiV proteins have the ability to initiate or inhibit TLR 4 activation.

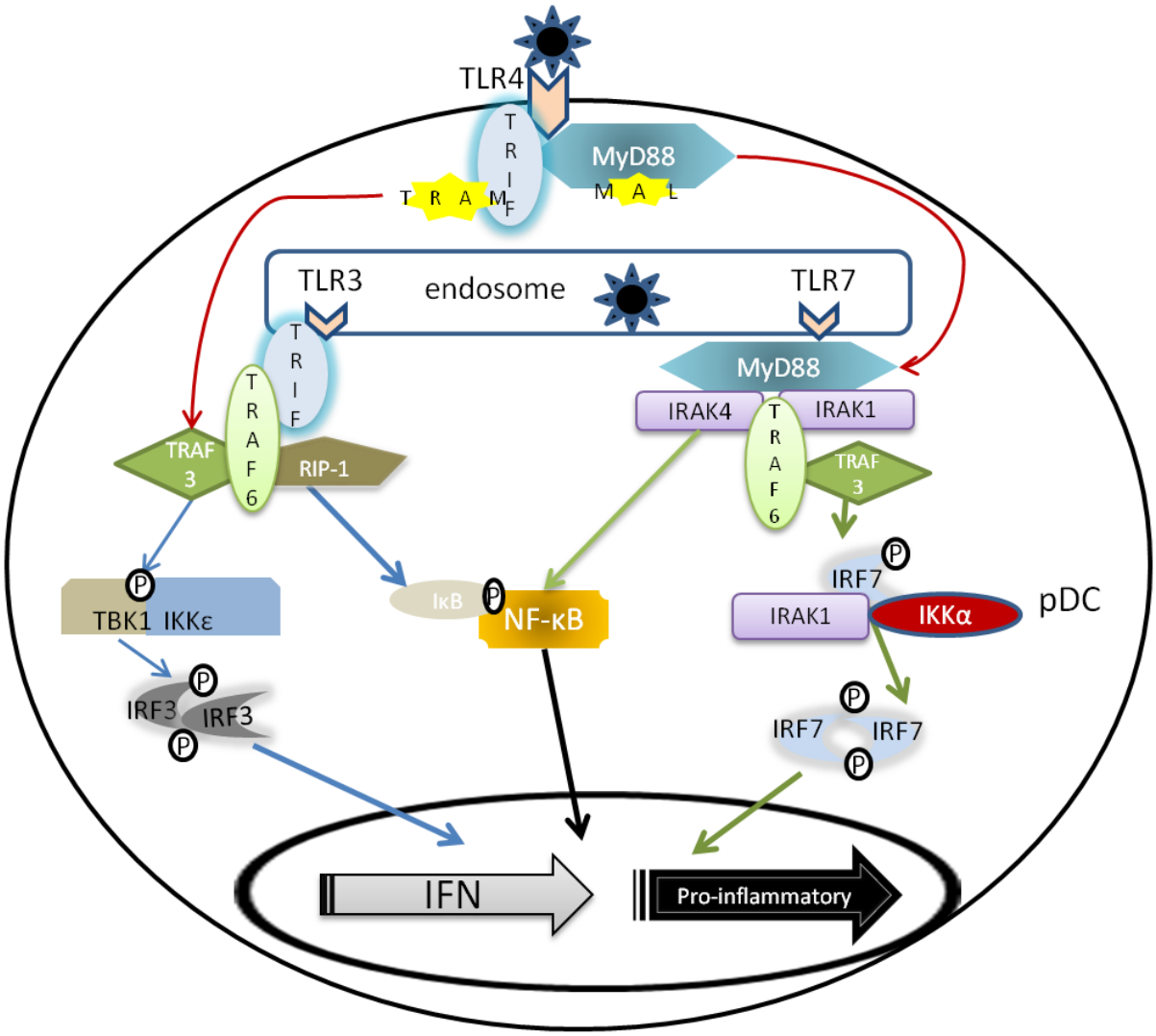

Figure 5 Signaling cascade following TLR4, TLR3, and TLR7 activation with envelope glycoprotein, ssRNA and dsRNA respectively. MyD88 and TRIF are the adaptor proteins for the TLRs to initiate the different pathways for the activation of IRF3, IRF7 (pDC only) and NF-κB for the induction and transcription of interferon and pro-inflammatory cytokine production. The blue line represents: TLR3; green line: TLR7; red line: TLR4 of the respective signaling cascades leading to the activation of IFN gene transcription. The black line indicates the activation pro-inflammatory cytokine transcription as a result of TRLs activation. Adapted from (142).

The cytoplasmic sensors, RIG-1 and MDA5 also initiate signaling pathways leading to the synthesis and release of type I IFNs and pro-inflammatory cytokines required to launch an antiviral inflammatory response (146-149,150). As with other RNA viruses, NiV viral genome and anti-genome possess foreign motifs, 5' triphosphates, which can be recognized by RIG-1 (142). Activation of RIG-1 was shown using RNA extracted from NiV and transfected into 293T cells (151) but this work did not exclude other helicase or TRLs. However, NiV V protein can antagonize MDA5 ATPase activity along with LGP2 to suppress RLR signaling in turn induces IFN responses (105).

Once IFN is produced and secreted from the cell, the type I IFNs bind to the IFN-α/β receptor on the same cell (autocrine signaling) as well as adjacent cells (paracrine signaling) leading to downstream signaling to create a broadly effective antiviral state (152, 153). Figure 6 shows the signaling cascade induced by type I and II IFN (153). Type I IFNs (α and β) share a common (IFNAR) receptor which is ubiquitously expressed on many different cell types (154). This receptor is associated with Janus family tyrosine kinases, JAK1 (Janus –activated kinase) and TYK2 (tyrosine kinase). These kinases phosphorylate specific tyrosine residues on the receptor via their Src homology 2 (SH2) domains (155). The activation of the signal transducer, phosphorylates the receptor-associated STAT proteins atY690 (STAT2) or Y701 (STAT1) leading to the formation of STAT1–STAT2 complex (156). The heterodimerized STAT1 and STAT2 complex joins with a third protein, the DNA-binding subunit IRF-9, to form a heterotrimeric complex known as the ISGF-3 (157, 158). ISGF-3 rapidly translocates to the nucleus and binds to the conserved IFN-stimulated response element (ISRE) sequences on IFN-α/β-stimulated gene (ISG) promoters inducing transcription of numerous associated antiviral genes (159-161). Not surprising as with other paramyxoviruses, NiV non-structural

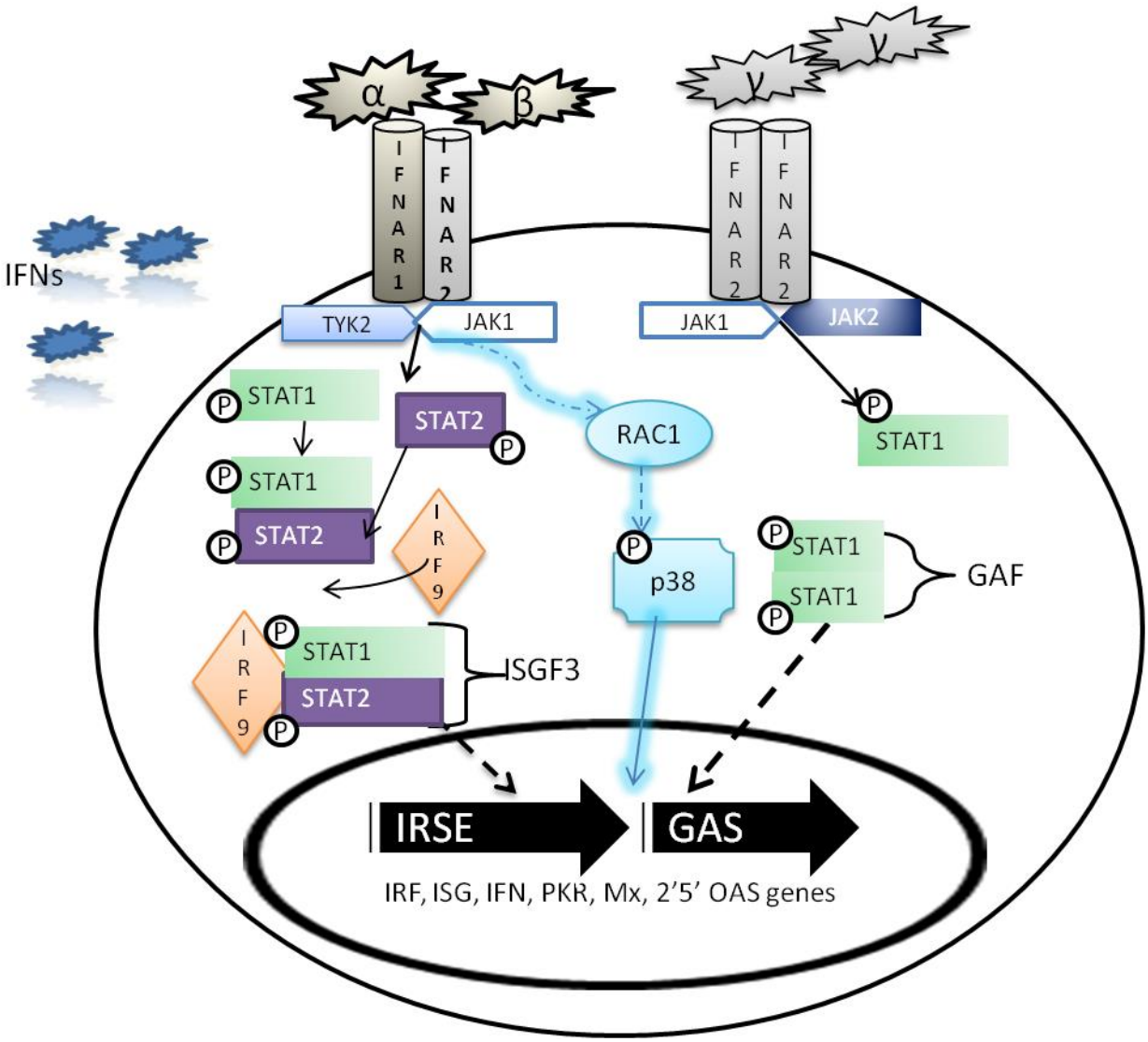

Figure 6 Pathways activated by type I and II interferons. Interferons engage with interferon receptors to activate JAK-signal transducer and activate STATs and p38 signaling pathways. The activated STATs make homodimers or heterodimers to induce gene by binding via interferon stimulated response elements (IRSE) or IFN gamma activate site (GAS) dependent promoters. The p38 MAPK is activated via a different series of signaling cascade initiated by IFN and is necessary for induction of genes of both ISRE and GAS dependent promoters as represented by dashed blue glow lines. The solid blue glow line (p38) and the black dashed (ISGF3 and GAF) translocation into the nucleus for activation of the IRSE or GAS promoters. Adapted from (153).

proteins counter regulate the JAK-STAT pathway. Initially in recombinant studies, NiV non-structural proteins were observed to co-localize with STAT1 with NiV W in the nucleus and cytoplasm whereas P protein would bind to STAT1 only in the cytoplasm (97). A difference in the localization of W protein was observed in NiV infected human cell lines. In endothelial human cell lines, the W was only detected in the cytoplasm whereas in neuron cell lines it was also detected in the nucleus suggesting tissue-specific antagonism of the JAK-STAT pathway (95). It is unknown if in NiV infected cells, the W protein has also species specific as in porcine cells. The NiV V protein can sequester STAT 1 and 2 in large molecular weight complexes in the cytoplasm to disrupt the IFN induced JAK-STAT signaling pathway (96, 102).

The type II IFN responses (IFN-γ) are induced in a similar manner but typically in immune cells (T lymphocytes and NK cells). Upon binding of IFN-γ to its receptor, STAT1 is phosphorylated to form a homodimers of STAT1-STAT1 (162) known as the IFN gamma activated factor (GAF) (163). As shown in Figure 6 these complexes translocate to the nucleus where ISGF3 binds ISRE and GAF binds to the promoters of gamma activated sequences (GAS). As a result of the complex binding to GAS promoters, transcription of numerous IFN induced genes involved in antiviral effect response are initiated within the affected host. The inhibition of IFN γ reporter genes were demonstrated by recombinant NiV V protein (96, 102). Hence, NiV non-structural proteins have the ability to interrupt the IFN induced JAK-STAT signaling pathway to counteract the host ability to evade viral infection. The role of the JAK-STAT pathway in NiV infected porcine animal cells or immune cells are not well characterized.

In addition to classical JAK-STAT pathway, MAPK pathways are also activated by IFNs binding to IFNAR (Fig. 6) (164, 165, 166). In particular, the p38 MAP kinase which belongs to the MAPK signaling pathway family is activated during treatment with IFNα or IFNβ, co-

stimulation with IFNγ and IFNα, or by the cyclic peptide of IFNα in various cell lines (164, 167, 168, 169). In addition, enveloped viruses such as influenza virus and RSV also benefit by early activation of p38 MAPK pathway to augment viral endocytic uptake and entry depending on the levels of intensity of p38 activation (170). The sequential activation of the signaling pathways begins with MAPKKK to MAPKK to MAPK to MAPKAPK (MAPK activated protein kinase) as shown in Figure 7. All downstream kinases are activated by MAPK in the cytoplasm and are in the mitogen kinase (MK) family (Fig. 7) (171). There are two other major MAPK signaling pathway which include ERK 1, 2 (extracellular signal regulated kinase) (172) and the JNK 1-3 (c-Jun N-terminal kinases) (173). The JNK 1/2 pathway is phosphorylated by specific stimuli and can also activate p38 MAPK pathway leading to the same biological functions (113). While, the ERK pathway can be activated by ligands binding to cellular receptors; virus binding to its cellular receptor may also begin the signaling cascade depending on the nature of the cellular receptor (174, 175 , 176). Members of the *Paramyxoviridae* family such as measles virus (MeV) and respiratory syncytial virus (RSV) require both the early and late activation of ERK pathway for efficient replication (177, 178). The ERK pathway is also crucial in innate immunity to trigger inflammation and mucus production in epithelial cells (179, 180). But more commonly, the activation of p38 MAPK pathway by viruses prompts the production of pro-inflammatory cytokines such as TNFα, IL-1β and IL-8 that can influence the immune response (181- 184). Extensive research of p38 MAP kinase indicates that it also plays an important role in the immune response by regulating respiratory burst of macrophages and neutrophils, chemotaxis, T cell differentiation and apoptosis by regulating IFN γ production (185, 186, 187). Hence, the activation of p38 MAP kinases can mediate transcriptional regulation of ISG genes to induce

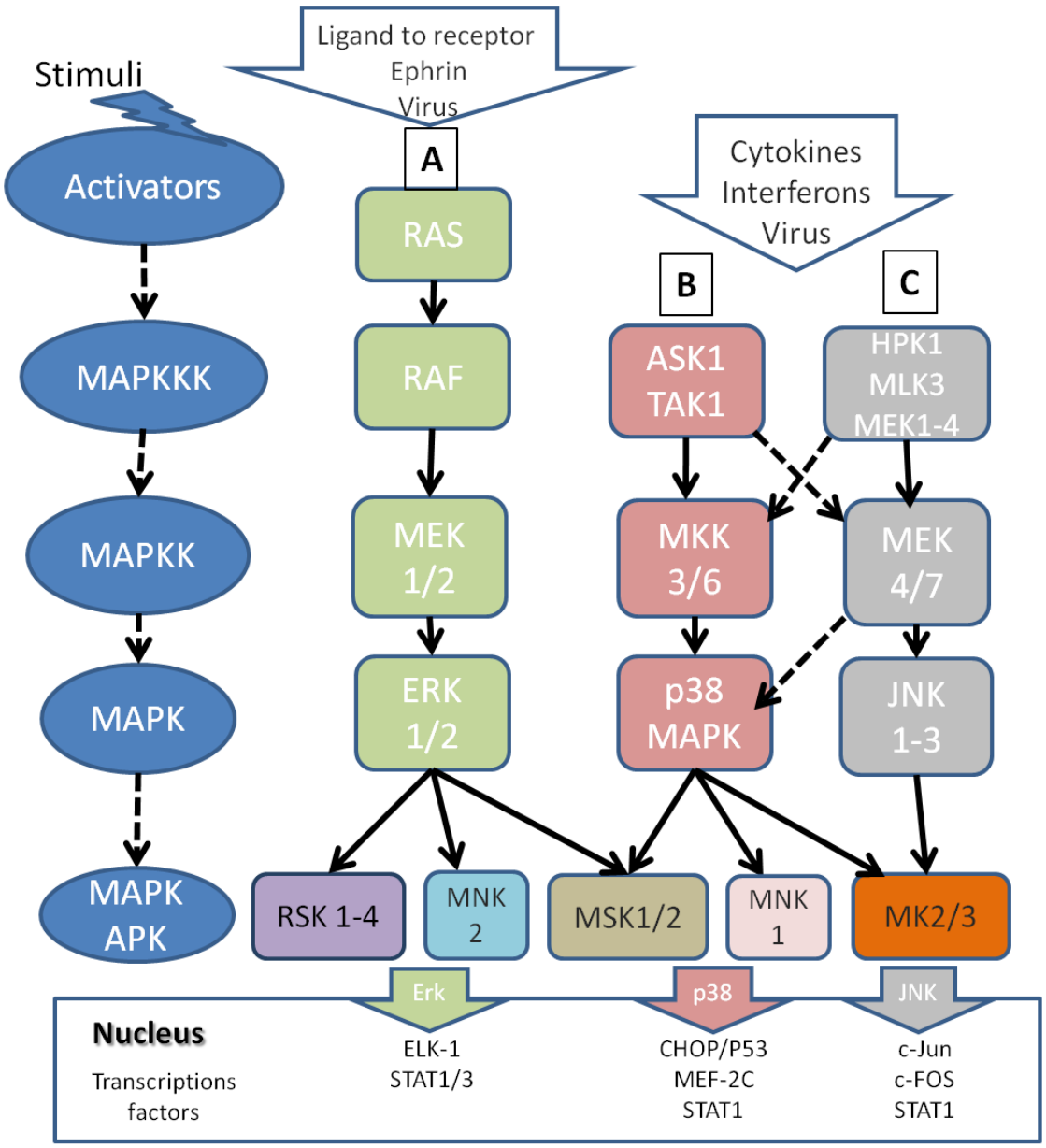

Figure 7 Three common MAPK signaling pathway cascades leading to the activation of protein kinases (MAPK and MAPKAPK) and transcription factors. Depending on the stimuli, different MAPK pathways are activated which in turn activate kinases that can translocate into the nucleus to promote and regulate numerous transcription factors. Examples of transcription factors activated by phosphorylated MAPK (ERK, p38, and JNK) are indicated in the figure. The solid arrows – direct interactions, dashed arrows- cross interactions of pathways. The compound arrows - direct interaction of the general cascade of MAPK signaling pathway. Adapted from 171.

antiviral activity and pro-inflammatory cytokine production to have an impact on the outcome of viral infections and the immune response.

1.11 Activation of an antiviral state

Both the JAK-STAT and p38 MAPK signaling pathways can initiate the transcription of more than 300 IFN-α/β-stimulated genes by IFN binding to IFNAR, including genes encoding for oligoadenylate-synthetase (OAS), PKR (double-stranded RNA‑dependent protein kinase), MxA (myxovirus resistance A), ISG15 and ISG56 (153, 164, 188). These proteins elicit an antiviral state by inhibiting different stages of virus life cycle. The ISGs mediate an IFN-induced ubiquitin-like protein response referred to as ISGylation. All components of the ISGylation pathway are induced by type I IFNs (189). In contrast to studies using transient expression of NiV proteins, interferon signaling pathways in human HEp-2 and 293T cells were only partially blocked. This was demonstrated by the expression of endogenous, IFN inducible ISG 54 and 56 genes in NiV infected cells with a MOI of 1 along with the addition of IFN (190).

Two other important proteins that can elicit an antiviral state have not been studied in NiV infected cells. The PKR is a ubiquitously expressed serine/threonine protein kinase present at low levels in quiescent cells; upon activation by IFN, this kinase becomes a key mediator of cellular antiviral action (191, 192). In addition to IFN, PKR activation is also triggered by binding of viral RNA and viral ribonucleoprotein (191, 193, 194). The activated PKR forms a dimer and phosphorylates downstream eukaryotic initiation factor 2 (eIF2α) at serine 51 (195) thereby inactivating translation and inhibiting protein synthesis (192). The phosphorylation of eIF2α not only halts the translation of viral proteins but may also lead to apoptosis which makes this kinase another important checkpoint against viral invasion (196, 197).

The 2, 5 OAS is another antiviral enzyme activated by dsRNA which polymerizes ATP, generating 2'-5' oligoadenylates, which in turn, activates RNase L (cellular endoribonuclease) (198). RNase L cleaves single strand RNA to inhibit translation of mRNA. This in turn stops protein synthesis leading to apoptosis and the limiting of viral replication (198).

1.12 Adaptive immune response

The innate and adaptive immunity are linked by induction of cellular pathways to produce IFNs and cytokines that have an immediate impact on the host immune response (199). Macrophages, DC and NK cells are stimulated by IFN in turn activating and amplifying the adaptive T cell response (200). Along with IFN, the activation of the p38 MAPK in both macrophages and DC cells plays a significant role in IL-12 production to drive naïve CD4+ T cells to become mature helper T cells. In general, upon encountering a foreign antigen, naïve CD8+ T cells proliferate and expand into effector cells primarily in lymph nodes (201). The doubling time of CD8+ T cell *in vivo* in response to an infectious antigen was estimated to be as fast as 4 hrs (202). Naïve CD4+ T cells complex with antigen presented via MHC II on APC followed by extensive proliferation and differentiation into specific T helper cell subsets (Th). The two major subsets are Th1 and Th2 which help to determine the direction of the response. Th1 response leads to cell mediated immunity whereas Th2 shifts the response to a humoral response (203). The adaptive immune response is divided into two arms: Humoral mediated by B lymphocytes and cell-mediated mediated by T lymphocytes. B lymphocytes produce antibodies, the antibodies reduce free virus in fluid phase whereas T lymphocytes decrease the number of infected cells (199). Species have similarities and differences with regards to adaptive immune response. The porcine adaptive immune response has some differences to mouse and human host that may influence the outcome of a viral infection.

As with other species, porcine T cells migrate through secondary lymphoid structures such as tonsils, lymph nodes, spleen and Peyer's patches and can also be circulated in lung, liver and the small intestine (204). However, the porcine T cells leave the lymph node to the blood via high endothelial venules (HEV) as opposed to via efferent lymph ducts as seen in humans (204, 205). The porcine lymph nodes are structurally different from other species because the cortex and follicles are found in the central region while paracortex and medulla are located in the periphery (206). The cortical tissues consist of lymphoid follicles and diffuse lymphoid tissue. The lymphoid follicles are formed by a germinal center, consisting mainly of B and CD4+ lymphocytes and the diffuse lymphoid tissue is considered as a T- dependent zone. T cells found in the porcine lymph nodes are CD4+CD8-, CD4-CD8+ with very few γδ T cells (207, 208). In experimental infection of piglets with NiV, lesions in the lymph nodes were characterized by lymphoid depletion in cortical tissues where a large population of T cells reside; indicating NiV infection has an effect on lymphocyte population (136, 137). Furthermore in pigs, the porcine CD4-CD8+hi are usually grouped with CD4-CD8lo group and there is twice as many CD4-CD8+ T cells as to CD4+CD8- T cells in peripheral blood unlike in humans and mice where the ratio is reversed (209, 210). Both CD4+ and CD8+ T cells population increase with age whereas the γδ T cells decline with age (206, 209). This type of difference in the T cell population may influence the outcome of NiV infection if one subpopulation is effected by NiV infection in the porcine host. This knowledge offers the possibility to investigate specific interactions of porcine T lymphocytes with NiV and may offer why the porcine immune response is suspected to be modulated due to the identification of bacteria normally associated with immune comprised pigs (137).

1. 13 Vaccines and treatments for NiV infection

A vaccine program for both human and swine would be the best form of limiting infection. The development of effective therapies for NiV infections can be divided into main areas: those that could be used as post exposure measures such as passive therapeutic or antiviral drugs and those that prevent infection such as vaccine. The primary goal of experimental NiV infections in pigs and small animal models is to discover an antiviral treatment and/or vaccination program to protect humans and livestock.

The first post exposure attempt was with the use of ribavirin. Ribavirin was shown to be partially effective in humans with acute NiV encephalitis (211). However, in studies with hamsters, ferrets and non human primates, ribavirin or a combination of chloroquine and ribavirin did not prevent NiV induced mortality (132, 212, 213). Alternatively, the use of monoclonal (m) antibody passive transfer was also used to treat NiV infection in animal models (129, 214). One particular human monoclonal antibody (m102.4) showed cross reactivity against NiV and exhibited strong virus neutralizing properties in ferrets (131, 215). Although, passive immunity can prove to be vital for post exposure to NiV, it is the prevention of NiV infection in humans and domestic animals that is the focus of most research work.

Indeed it has been demonstrated that experimental immunization of animals with live attenuated virus vector can elicit a protective cross-reactive neutralizing humoral response. In pigs, canary pox virus vaccine vector carrying genes encoding for NiV F or G induced neutralizing antibodies and prevented shedding during NiV challenge (138). The prevention of viral shedding is very important as NiV infected pigs can transmit the virus to humans (216). In addition, the canarypox virus vector induction of T-helper immune response against NiV (138) was indicated by IFN γ accenting the need for a functional adaptive immune response. Recently

an alternative to canary pox vaccine was also developed in pigs, Newcastle Disease virus (NDV) vectors expressing F or G also elicited antibody response against NiV infection (217). The advantage of NDV vectors is its greater ease to culture and grow to high titers in chicken eggs (217). Another vaccine vector shows promise of eliciting long term immunity even with pre-existing immunity to the vaccine vector. Testing in non human primates with two MeV vaccine vectors that expressed G showed that antibodies against NiV are induced and the animals are protected even though non human primates were seropostive for MeV (218). Still, more work needs to done with the MeV vaccine vectors as low number non human primates were used in the study (218). An ideal live attenuated vaccine is a single replication vector which was developed in mice; the rVSV vector expresses either NiV F or G and elicits high neutralizing antibodies titers (219). A new study shows that a single injection of rVSV vaccine vector can provide protection against both the Malaysia and Bangladesh NiV isolates in ferrets; an animal model which is recognized to recapitulates NiV infections in humans (220). Protection against both Malaysia and Bangladesh isolates by the same vector is important as the activation of host immune response genes proves to be different by the two isolates in a hamster model (221).

An alternative to live attenuated vaccine vectors is the use of recombinant purified soluble (s) G preparation. The sG subunit vaccine has proven to be ideal immuogens, as it retains important functional and antigenic properties such as binding to virus receptor, blocking virus mediated membrane fusion as well as eliciting a robust polyclonal antibody response (222). NiV sG preparation was evaluated as a subunit vaccine in a cat model. However, NiV sG subunit vaccine proved not to be completely effective as live virus was present in the brain of one cat, and viral RNA was present throughout the 21 day post challenge period in the brains of the remaining challenged animals (127). On the other hand, vaccination with HeV sG prevented NiV

infection in ferrets and non human primate models (223, 224). Vaccination with HeV sG can protect against NiV infection and the protection persists for at least 14 months in a ferret model (223). The main benefit of this vaccination protocol is that it can protect from acute NiV infection (223). For this reason the HeV sG vaccine was used in horses, and all vaccinated horses showed no clinical disease or virus shedding in the immunized horses as a result a licensed and commercial vaccine became available for HeV(225). Although, the subunit vaccine proves to provide protection against NiV, these vaccines require repeated injections of high doses of sG proteins mixed with adjuvants to confer protection therefore, a single injection vaccine would be more advantageous.

Although many advances were made in recent years, at the current time there are no vaccine strategies or treatments for NiV infections that are available to either humans or domestic animals. A better understanding of the immune response to NiV would help to design and establish vaccination programs that would be effective for all species.

1.14 Gap in knowledge

The role of innate immunity and the development of adaptive immune response in NiV infected porcine host are poorly understood. On the onset of this research, there was no published work on IFN signaling pathways or on IFN mediated antiviral state in NiV infected cells. The ability of NiV V protein to hinder the IFN response was shown in recombinant study not to be species specific (103). However, it was unknown if in NiV infected porcine cells, the NiV V and W proteins have similar antagonistic effects on IFN signaling pathway as observed in the recombinant studies (97, 100) or whether the antiviral response is completely hindered.

In addition, there were no reports or studies regarding whether NiV can modulate the adaptive immune response in humans, pigs or any animal models. In experimentally infected

pigs, the involvement of immune cells was proposed as viral RNA was detected in PBMC and *in vitro* work showed positive staining for NiV antigen in an unidentified subpopulation of lymphocytes and monocytes (137). There was also evidence of lymphocyte necrosis and lymphoid depletion in the lymph nodes, with confirmation of bacteria in the CSF of NiV infected pigs (134, 136, 137). Consequently, this research work aimed to evaluate aspects of porcine immunological response to NiV by first looking at IFN signaling pathways in NiV infected porcine cells and the involvement of immune cells *in vitro* and *in vivo*.

1.15 Rationale # 1

Previous studies have shown that almost all pigs recover from NiV infection in contrast to humans (5). The innate immune response is not only the first line of defense but it also plays an important role in controlling viral infections. Adequate activation of the innate immune system is critical to initiate generation of protective adaptive immunity and to facilitate complete viral clearance. Among the major groups of innate immune effectors are interferons (IFNs). Both IFN α/β and IFN γ bind to their respective IFN receptors to activate the STAT-1 signal transduction pathways leading to the expression of multiple antiviral and immune regulating genes. The IFN-signaling pathways leads to the induction of an antiviral state in cells targeted by virus, or to immune cell signaling and activation. Consequently, the interaction between virus replication and its control by the host cells and host immune response drives the outcome of an infection.

Differences in the activation of the antiviral state or subversion of STAT1 signal transduction pathway may exist between human and porcine cells infected by NiV contributing to more favourable outcome in NiV infection in pigs. Inhibition of the JAK-STAT pathway was characterized by recombinant system studies in non-human primate or human cell lines (96,

97,100). These studies proposed evasion of IFN α/β induced antiviral state by binding of viral proteins to STAT1 in NiV infected cells of human origin, but did not consider cells of porcine origin or immune cells. As STAT1 is a component also of the IFN γ signaling pathway, implicating that the virus may evade also immune cell signaling and activation. At the beginning of this thesis, it was unknown if immune cells are infected by NiV. Thus, the initial focus of the thesis was on porcine cells including immune type cells. Additionally, porcine cells may have an alternative strategy for inducing an antiviral response in which the IFN signal transduction pathway is not blocked, such as the p38 MAPK pathway (164, 226, 227). There is indication that NiV G binding to ephrin B could activate the MAPK signaling pathways (76). The MAPK signaling pathways have not been examined in NiV infected cells and may regulate the antiviral response in pigs. Overall, the understanding of IFN signaling pathways and induction of antiviral state would allow for greater insight into differences observed between the human and pig recovery from NiV infection.

1.15.1 Hypothesis #1

IFN induced signaling pathways are not completely inhibited by NiV in infected porcine cells enabling an antiviral state to be established.

Objectives of aim #1

1. To determine if NiV non-structural protein (V and W) efficently interact with the STAT1 proteins in NiV infected porcine cell types.
2. To determine if an antiviral state is activated in the selected human and porcine cell lines and if a difference exits between the cells during the course of NiV infection.

3. To determine if alternative pathway to JAK-STAT pathway can be activated; such as MAPK signaling pathways during the course of NiV replication in a cell type dependent manner.

1.16 Rationale # 2

Porcine lymphocytes expressing markers CD4 or CD8 alone or CD4 and CD8 together are important in viral clearance by secreting IFN-γ, and in turn also need functional activation of the STAT-1 signal transduction pathway. The subversion of STAT 1 signal transduction pathway was indicated in NiV infected porcine monocytic like cells. However, it is not known if NiV replicates in porcine immune cells *in vivo* thus affecting the adaptive immune response. First immune cells maybe infected, ince *in vitro* analysis of porcine PBMC on flow cytometry showed positive staining for NiV antigen in monocytes and subpopulation of lymphocytes (137). Furthermore, cell associated viremia may be the main mode of dissemination of NiV throughout the host, including swine (114,125,136). Additional hints about the involvement of immune cells come from NiV experimentally infected pigs where neutralizing antibodies develop later than in other porcine virus infections such as influenza (137, 139). It was also observed that despite the presence of neutralizing antibodies, virus RNA was still recovered (137). Last, the identification of bacteria normally associated with immune compromised pigs was identified (137). In pigs, there is twice as many CD4-CD8+ T cells as to CD4+CD8- T cells in peripheral blood unlike in humans where the ratio is reversed (209, 228). Hence, immune modulation may be more adversely affected if for example the CD8+ T cell population is compromised by NiV infection. For that reason, it is suspected that cell associated viremic spread of NiV in porcine host may be due the permissibility of individual subpopulations of PBMC to the virus, that has additional effects on the cells of immune system present in peripheral blood of the porcine host.

1.16.1 Hypothesis # 2

Nipah virus infects porcine immune cells and affects population frequency of PBMC.

Objectives of aims #2

1. To determine the permissiveness of porcine immune cells to Nipah virus *in vitro*.
2. To determine if a subpopulation frequency of PBMC is affected *in vivo* during the acute stage post infection (up to 7 dpi).

2.0 Materials and Methods

2.1 Viruses

Nipah virus was re-isolated from a pig experimentally infected with human isolate (kindly provided by T. Ksiazek and P. Rollin, CDC, Atlanta) at NCFAD and subsequently was used for pig inoculations. The *in vitro* work was done in parallel with both, the NCFAD swine isolate and the CDC human isolate (passage 5 in Vero 76 cells). Nipah virus was inactivated by gamma irradiation using 5 MRADs.

2.2 Preparation of viral stocks

Nipah virus stocks for were grown in Vero76 cells infected at a multiplicity of infection (MOI) of 0.1. For infection, virus was added to 5ml of DMEM with no supplements. After 1 hour of incubation, at 37^{o}C, 5% CO_2, 5ml of DMEM containing 4% FBS (2% final FBS concentration) was added to the T75 flask (Costar, Corning Inc. Corning, NY). These cells were then incubated for 2 days at 37^{o}C, 5% CO_2 when cytopathic effect (CPE) was observed. The virus was harvested by removing the supernatant and centrifuging at 2000 g for 20 mins. The clarified supernatant was aliquoted and frozen at -70^{o}C before virus titration by plaque assay.

2.3 Cell lines

ST cells (swine testis, fibroblast) and Vero 76 cells (African green monkey, kidney epithelial) were cultured in Dulbecco's Modified Eagle's Medium (DMEM) (Wisent, Inc., St. Bruno, QC, CA), supplemented with 10% fetal bovine serum (FBS) (Wisent). MRC5 cells (human lung, fibroblast) were cultured in Eagle's minimal essential medium (EMEM) supplemented with 10% FBS (Wisent) and 1% non-essential amino acid (Sigma-Aldrich). IPAM (immortalized porcine alveolar macrophage) cells 3D4/31 (232) were cultured in RPMI

1640 with L-glutamine (Wisent), 10% FBS, 1% non-essential amino acid (Sigma-Aldrich) and 100 IU penicillin/100 mg/ml streptomycin (Sigma-Aldrich) in a humidified incubator at 37° C, 5% CO_2.

For subculture, the culture medium was removed and replaced with 0.05% trypsin (Sigma-Aldrich) and left to incubate at 37° C, 5% CO_2 for approximately 1-10 min depending on the cell line. The cells were visualised using an inverted microscope to confirm cell detachment from the flask surface. The cells were resuspended in culture media (containing FBS) and diluted to desired concentration depending on the flask or plate size.

2.4 Virus plaque assay

NiV titers were determined on Vero76 cells, and on all individual porcine and human cell lines used in the experiments to assure that the MOI was equal. Confluent (100%) cells prepared in 12 well plates (Costar) were washed, and 400µl of serial diluted virus (10^{-1} to 10^{-7}) in DMEM were added to the wells in duplicates. Cell controls had only media and no virus added to a well of each plate. Inoculum was removed after one hour incubation and 1.5ml of overlay was added to the cells; DMEM was supplemented with 2% FBS and 1.75% carboxymethylcellulose (CMC) (Sigma-Aldrich, Ottawa, ON, CA). Cells were then incubated at 37°C, 5% CO_2 for 2 days. After incubation period, the overlay was removed then the cells were washed, and fixed for 30 min to 1 hour at room temperature by the addition of 10% PBS buffered formalin (Fisher Scientific, Ottawa, ON, CA), which contained 4% paraformaldehyde. The fixed cells were washed and stained with crystal violet (0.5% w/v crystal violet in 80% methanol in PBS). The titer of the virus was determined as plaque forming units per ml (PFU/ml).

2.5 Antibodies

See Appendix 6.1 for a list of primary and secondary antibodies used.

2.6 Immunofluorescence

2.6.1 Co-localization by confocal microscopy

Cells were seeded onto glass slides for IFAs. The ST and MRC5 cells were infected with NiV at a MOI of 0.1 while IPAM cells were infected at an MOI of 1. Mock inoculated controls were handled in a similar manner to infected cells.

After 24 or 48 hours post infection of cells, slides were fixed in 10% formalin containing 1% Triton X-100 for 1 hour at 37^{o}C. Slides were then immersed in 1:1 methanol: acetone for 10 minutes at -20^{o}C. Blocking buffer (1% normal goat serum in PBS) was added after removal of methanol: acetone and incubated for 30 minutes at room temperature or at 4^{o}C overnight. Proteins were labeled with respective primary antibodies: rabbit or mouse monoclonal STAT-1 (Santa Cruz Biotechnology, Santa Cruz, CA) (1:500), mouse monoclonal NiV-P58 (1:100) generated at NCFAD, rabbit polyclonal NiV- P, V, W (1:100) kindly provided by Dr. C. Kai, U. of Tokyo by diluting the antibodies in blocking buffer and adding antibodies directly to slides. Secondary antibodies anti- rabbit or anti-mouse conjugates with Alexa Fluor- 488 or 594 (Molecular Probes, Invitrogen, Burlington, ON, CA) were diluted in blocking buffer (1:1000) and added to the slides. Washing between primary and secondary antibodies was carried out using PBS-Tween (0.1%) three times for 10 minutes. Slides were counterstained with antifade (Molecular Probes) and sealed with coverslips and visualized using an Olympus Fluoview FV300/500/1000c confocal microscope.

2.7 Cell viability by trypan blue exclusion

The Neubauer haemocytometer slide was used to determine the number of cells in a defined volume. The number of live (clear) and dead (blue) cells was determined by counting the

four corners of the grid and cell yield was calculated. Percent viable cells = [(number of live cells – number of dead cells)/ total number of cells] X 100

2.8 Cell toxicity and viability assay

Potential toxic effects of inhibitors were assayed using the LIVE/DEAD ® Cell Vitality Assay kit (Invitrogen). This kit distinguishes metabolically active cells from injured cells and dead cells. The assay is based on the reduction of C12-resazurin to red-fluorescent C12-resorufin in metabolically active cells and the uptake of the cell-impermeant, green-fluorescent nucleic acid stain, SYTOX® Green dye, in cells with compromised plasma membranes (usually late apoptotic and necrotic cells). DMSO 0.01% (vol/vol) or inhibitor was added to each of the media for their respective cell lines (ST, MRC5, and IPAM). After incubation with DMSO or inhibitor for 6, 12, 24, 48, 72 hr at 37°C 5% (vol/vol) CO_2, the cells were washed with D-PBS. The cells were detached as described in section 2.3. Once the cells were detached, respective media was used to dilute the cells to 1 X 10^6 cell/mL for each concentration of inhibitor and time point. A working solution of AM consisting of 2µl of 50 µM calecein and 4 µl of the 2 mM ethidium homodimer-1 stock was added to each milliliter of cells. The cells were mixed gently by tapping after addition of AM followed by an incubation period of 20 min at room temperature, protected from light. Within 1-2 hours after the incubation period, the cells were analyzed by FC500 flow cytometry (Beckman Coulter). The cells were gated to exclude debris. The population was separated into two groups: live cells and dead cells.

2.9 Inhibition of p38 MAPK and ERK signaling pathways

Confluent cell monolayer in 6 well plates (Corning Inc.) was washed with PBS. Inhibitor were diluted in respective media (supplemented with 5% FBS) to the final concentration of 25µM or 50µM of SB202190 p38 MAPK inhibitor (Calbiochem, New England Biolabs Ltd.

Pickering, ON, CA) or 1, 10, 20 µM of FR180204 ERK1/2 kinase inhibitor (Sigma). Control for DMSO was included in each plate. The DMSO was diluted to the same concentration as final concentration of the inhibitors. The inhibitors and DMSO control were incubated at 37°C with 5% (vol/vol) CO_2 for 1 hour. Prior to NiV inoculation, the cells were washed with PBS and then the cells were inoculated with NiV. After one hour adsorption period, the inoculum was replaced with media with inhibitor or DMSO at the indicated concentrations for the remainder of the infection. At different time points (15 mins, 30 mins, 1 hr and 3, 6, 12, 24 and 48 hrs), the culture supernatant and cell lysate was collected. The virus concentration was measured as described in section 2.4 and quantified as pfu/ml. To quantify the viral proteins, whole cell lysates were analyzed by western blot as in section 2.9 and densities of NiV-P (1:1000) were observed in terms of relative density to ß-actin (1:1000) (Cell Signaling) described in section 2.11.

2.10 Whole cell lysate preparations

Confluent cell monolayers in 6 well plates (Corning Inc.) were washed with PBS and either mock infected or infected with NiV. MRC5, ST and IPAM cell lines were inoculated with NiV at an MOI of 1. For all the cell lines after a one hour post-adsorption the inoculum was removed and replaced with respective media. Mock inoculated cell lines served as negative control. As a positive control for eIF2α phosphorylation, 10 nM thiapsigargin (Calbiochem) was added to respective media and incubated 1 hour at 37°C with 5% (vol/vol) CO_2.

Whole-cell lysate extracts from the cell lines at various time points after NiV or mock inoculation were prepared as follows: the media was removed from the cell cultures; the cells were washed with 1X PBS; washed cells were lysed by adding 100 µl of 1% SDS (Gibco) sample buffer containing HALT proteinase and phosphatase inhibitor (Fisher Scientific) per well. Immediately the cells were scraped off the plate and the extracts were transferred to a tube;

mixed thoroughly by vortex and centrifuged at 1,300 g for 5 min at 4°C. Each sample was heated at 95-100°C for 8 minutes; cooled on ice and stored at -70°C. After removal from BSL 4 and prior to protein quantification, the samples were heated for an additional 2 min at 95-100°C; cooled and microcentrifuged for 5 minutes. The total protein concentrations in the whole cell lysates were determined using a Pierce BCA protein assay kit (Fisher Scientific).

2.11 Total protein BCA microassay

The protein concentration of samples was measured using the bicinchoninic acid protein (BCA) assay according to the manufacturer's instructions (Pierce). Briefly, BSA standards were prepared by diluting samples of working range of 1500, 1000, 750, 500, 250, 125, 25 µg/mL and a blank. A 96 well plate was loaded with: 25 µl of each protein lysate sample diluted to 1/10 concentration, 25 µl of each BSA standard and 25 blank per well. All of the samples were added to separate wells in triplicate and 200 µl BCA reagent (50: 1 dilution of BCA reagents A: B) was added to each well. A 96 well plate was incubated at 37°C for 30 min, cooled to room temperature (RT) and the absorbance was read at a wavelength of 560nm. The protein concentration of unknown samples was determined from the BSA standard curve.

2.12 Western blots

To each gel used for western blots both SeaBlue Protein ladder (Invitrogen) and biotinylated protein ladder with anti- biotin, HRP linked antibody ladder (Cell Signaling) were loaded at recommended concentrations. The whole-cell lysate extracts prepared as described above were diluted in a loading sample buffer 62.5 mM Tris-HCl (pH 6.8 at 25°C), 2% w/v SDS, 10% glycerol,0.01% w/v bromophenol blue and 1.25 M dithiothreitol (Cell Signaling). Equal amount of total protein (12 µg) of each extract was resolved by electrophoresis in a NuPAGE 4-

12% 1.0 mm Bis-Tris gel (Invitrogen) and ran with MOPS SDS buffer (Invitrogen) at 150V. Gels were transferred using the iBlot7 Transfer Stack, Regular (Nitrocellulose) on the iBlot Gel Transfer Device (Invitrogen). The recommended P3 program (20 V for 7 min) was used for all transfers. The membranes were blocked for 2 hrs at room temperature in blocking buffer TBST (20 mM Tris-HCl [pH 7.4], 150 mM NaCl, 0.1% Tween 20) containing 5% w/v skim milk (Fisher Scientific) to prevent non-specific binding and then incubated with specific primary monoclonal antibodies (Cell Signaling) rabbit raised against total eIF2α (1:1000) and phosphorylated eIF2α (1:1000), total ERK (1:1000) and phosphorylated ERK (1:1000), total p38 (1:1000) and phosphorylated p38 (1:1000), mouse monoclonal or rabbit polyclonal NiV- P (1:1000), mouse monoclonal N (1:1000) diluted in 5% w/v BSA, 1X TBS, 0.1% Tween-20 at 4°C with gentle shaking, overnight. The membranes were washed three times with TBST buffer and then incubated for 1 hr at room temperature with HRP-conjugated secondary antibodies diluted in blocking buffer (1:5000) (affinity purified Ab peroxidase labeled goat anti rabbit IgG (H&L)(KPL, Mandel Scientific, Guelph, ON, CA). Protein bands were detected using enhanced chemiluminescence (ECL) reagents (Amersham Biosciences, GE healthcare Life Sciences, Baire d'Urfe, QC, CA) according to the instructions of the manufacturer. When reprobing was required, membranes were stripped in Re-Blot plus mild solution (Millipore, Cedarlane, Burlington, ON, CA) as per manufacture instructions. The ratios of phosphorylated (p-eIF2α)/ total eIF2α, (p-ERK) / total ERK, (p-p38)/ total p38 were compared by densitometry of corresponding bands using a computer densitometer with the Wright Cell Imaging Facility (WCIF) version of the ImageJ software package (http://www.uhnresearch.ca/facilities/wcif/imagej/).

2.13 Peripheral blood mononuclear cells (PBMC)

For the *in vitro* studies, PBMC were harvested into cell preparation tubes (CPT) (Becton Dickinson, Oakville, ON, CA) from six pigs (Landrace cross): four pigs in the age group of 10-15 weeks, and two pigs at 40 weeks old. The CPT tubes were centrifuged at 1800 g for 20 minutes. After centrifugation, the PBMC were collected into a 50 ml conical tube. The 50 ml conical tubes were filled with PBS and mixed gently by inversion. The cells were pelleted by centrifugation at 300 g for 15 min. The supernatant was discarded and the conical tube was filled again with PBS and centrifuged at 300 g for 10 min. The PBMC were resuspended in RPMI 10 % FBS, 10 mM HEPES (Winsent) and 100 IU penicillin/100 mg/ml streptomycin (Wisent).

2.14 PBMC lymphocyte separation

Monocytes were allowed to adhere overnight at 37 °C in a 5% CO_2 incubator. The non-adherent cells were removed by light washing with PBS and centrifuged at 300 g for 10 min to pellet the cells. Non-adherent cells were used for positive selection of T, NK and B cells on the basis of CD6+, CD16+, and CD21+ expression, respectively (Fig. 8A). Cells were labeled with mouse monoclonal anti-human CD21+ (1:100) (IgG1, AbD SeroTec, Raleigh, NC), mouse monoclonal anti- porcine CD16+ (1:100) (IgG1,AbD SeroTec) and CD6+ (1:100) (IgG2a,AbD Sero Tec) antibodies and separated using paramagnetic microbeads coupled with rat anti-mouse IgG2a/b or goat anti-mouse IgG1 (Miltenyi Biotech, Auburn, CA). The PMBC were diluted to approximately 10^8 cells/ml in MACS buffer (phosphate buffered saline, 1% bovine serum albumin (BSA), 0.09% sodium azide), 20 µl of the respective paramagnetic beads were added and incubated on ice for 1 hour. During the incubation period, 3 ml of MACS buffer was added 3 times to the LS columns (Miltenyi Biotech) and allowed to flow by drop wise in 15 mL in order

equilibrate the column before adding the sample with the paramagnetic beads. After the 1 hour incubation period, cells were filtered by pre-separation filter (Miltenyi Biotech) and loaded onto a ferric LS column in a magnetic field such that labeled cells were retained and unlabelled cells were eluted. The enriched cells were obtained by removing the magnet and eluted with MACS buffer at a high flow rate. After elution, the enriched cells were washed twice with 5% FBS RPMI media by centrifugation at 300 g for 10 min, then plated onto 12 or 6 well plates. Before plating the enriched cells, cell viability of the enriched cells was determined by trypan blue exclusion assay. The percent purity of recovered cells was determined by staining the cells with secondary goat anti mouse Alexa 488 IgG_1 (H&L) antibodies and analyzed by flow cytometry (Molecular Probes, Invitrogen, Burlington, ON, CA).

2.15 NiV infection of enriched lymphocytes or PBMC

The enriched lymphocytes input cell number was 10^5 cells/well and PBMC input cell number was 10^6 cells/well. The cells were infected with NiV at 0.1 or 1.0 MOI for 1 hr at 37°C, 5% CO_2. After 1 hr, cells were washed twice by centrifugation at 300 g for 10 min. Following the second wash, cells were resuspended in the RPMI 2.5% FBS, plated onto 6 or 12 well plates in 2.5 ml or 500 µl volumes, and incubated for 48 hrs at 37°C, 5% CO_2. The washes after the adsorption period, supernatants and cells were collected for plaque titration.

Activation of enriched CD6+ cells was performed one hour prior to infection with ionomycin 430 ng/ml (Sigma-Aldrich) and phorbol 12-myristate 13-acetate (PMA) 7 ng/ml (Sigma-Aldrich) in RPMI media. PBMC were activated with concanavalin A (ConA) 5µg/ml (Sigma-Aldrich) overnight before infection with NiV. After the adsorption period, the inoculum was replaced with RPMI supplemented with 2.5% FBS with ConA (PBMC) or ionomycin and

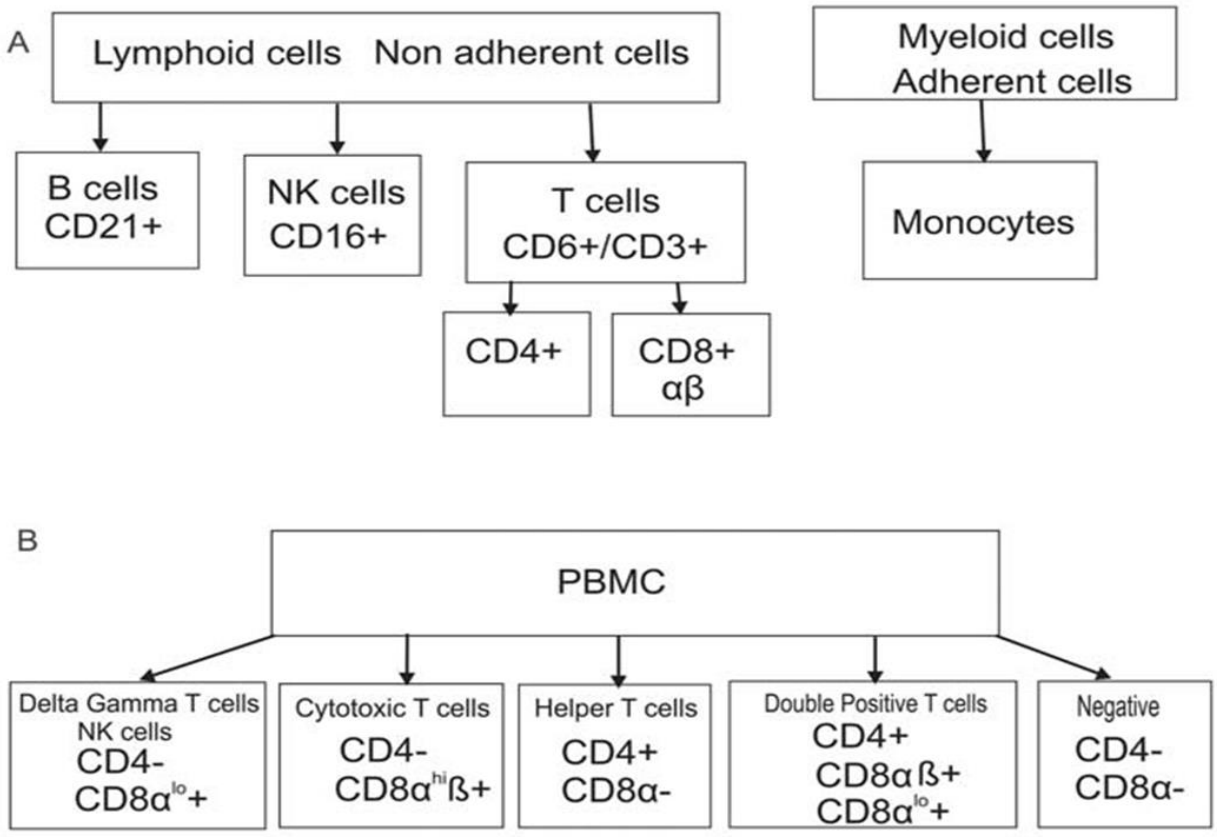

Figure 8 Flow chart of sorting and staining of PBMC. Sorting of cell subpopulations from peripheral blood mononuclear cells (PBMC) by magnetic beads coated with antibodies against selected markers (Fig. 8A), and staining of PBMC for CD4 and CD8 markers for analysis by flow cytometry (Fig. 8B). (hi) indicates high density expression of a specific marker, and (lo) indicates low density expression.

PMA (T cells). Supernatant and cells were harvested at 24 hrs and 48 hrs and frozen at -70°C. Supernatant and lyzed cells were plaque titrated on Vero76 cells.

2.16 Intracellular staining for NiV antigen

CD6+ enriched T cells or PMBC, respectively, were stained for CD8+ or CD4+ markers prior to fixation as described in the above section. The cells were fixed with 100 µl of BD Cytofix/Cytoperm solution (BD Pharmigen) for 30 min at 4°C, washed twice with BD Perm/Wash buffer, followed by addition of either 1:50 diluted mouse monoclonal anti-N antibody or 1:100 diluted guinea-pig polyclonal NiV antiserum. After incubation on ice for 30 min, secondary antibody was added. Both anti- mouse Alexa 488 IgG and anti-guinea pig Alexa IgG 594 were diluted 1:1000 and incubated with the cells in dark at 4°C for 30 min, washed twice with BD Perm/Wash. The cells were fixed in 4% formaldehyde for 24 hrs in order to remove them from the BSL4, and resuspended in 500 µl of MACS buffer for flow cytometry analysis. All samples were analyzed on a two laser FC500 flow cytometer (Beckman Coulter).

2.17 RNA extraction

PMBC or enriched lymphocytes were pelleted by centrifugation at 300 g for 10 min in a 1.5 mL centrifuge tube. The pelleted cells were stored at -70^{o}C until all the samples for each experiment were collected in order to dunk out the cells out of the BSL4 at the same time. Prior to removing the cells out of BSL4, 750 µl of TriPure Isolation Reagent (Roche Diagnostics Corporation, Indianapolis, IN) was added. This reagent is very effective at inhibiting RNase activity, which is highly beneficial, considering RNA, is generally unstable and can degrade readily. The cells were lyzed by pipetting the cells in the TriPure solution and then removed out of BSL4. As soon as possible, 250 µl of chloroform was added to each sample. The samples were shaken vigorously by hand for 15 seconds followed by an incubation period at RT for 20

min. In order to separate the solution into three phases, the samples were centrifuged at 12,000 g for 15 min at 4°C. The resulting mixture separates into three phases: 1) an upper aqueous phase containing RNA, 2) an interphase containing DNA and 3) an organic phase containing proteins. After centrifugation, the colourless upper aqueous phase was collected into a new 1.5 mL tube. To the aqueous phase, 500 µl of isopropanol was added. Invert the tube several times and incubated for 10 min at RT to precipitate the RNA. After the incubation, the tubes were centrifuged at 12,000 g for 10 min at 4°C and the supernatants were discarded. To the RNA pellet, 500 µl of 75% ethanol was added. The RNA pellet was washed in the 75% ethanol followed by centrifugation at 7500 g for 5 min at 4°C. The supernatant was discarded and the RNA pellet was air dried for 5 min. The RNA pellet was resuspended in RNase free water (Ambion) and frozen at -70°C or used for reverse transcription immediately.

2.18 Ephrin B2 RT-PCR

Total cellular RNA was isolated by TriPure Isolation Reagent (Roche Diagnostics Corp.) as described in the previous section. The extracted RNA was incubated for 10 min at 65°C prior to DNAse treatment. Following the incubation 1µl of Turbo DNA Free DNAse (Ambion, Austin, TX) was added and gently mixed in a final total volume of 50 µl. The mixture was incubated at 37°C for 30 min then 5µl of DNAse inactivation reagent was added. The inactivation reagent was incubated for 5 min at room temperature with occasional flicking of the tube. After inactivation the RNA was centrifuged at 10,000 g for 5 min and the supernatant was collected and placed in a new tube. The DNase treated RNA concentration was determined using 260/280 nm light absorbance ratio (N-D spectrometer Nano Drop Technologies). Reverse transcription was performed using Superscript II kit (Invitrogen). A total of 6 µl mRNA was added to each RT reaction and incubated for 45 min at 50°C followed by 72°C for 15 min. Two microliters of

cDNA were added to Hotstart PCR mix (Qiagen, Mississauga, ON, CA) which included 10 µM of forward and reverse Ephrin B2 primers. A total 25 µl reaction was incubated for 15 min at 95°C followed by 35 cycles of (95°C-30 sec, 55°C- 45 sec, 72°C-30 sec) and extension period of 10 min for 72°C. PCR fragments were run on 1.5 % agarose gels with a 1kp ladder (Invitrogen). Forward (ACCAGGCATAATGAGCCAAC) and reverse (CCTCAGCGGATGATAATGT Ephrin B2 primers were designed based on published porcine sequence (Accession NM0001114286 and EF682141.1) by using Primer 3 Input 4.0 software.

2.19 Optimization of real time RT-PCR for mRNA cytokine expression

2.19.1 Design of control plasmid for semi-quantification RT-PCR

Primers included the entire sequence of the selected cytokine and housekeeping gene (Section 2.17.3) and were designed to be used for real time mRNA cytokine expression RT-PCR described in the section below. RNA was extracted from IPAM cells induced with ionomycin and PMA. Prior to DNAse treatment, RNA was incubated at 65°C for 10 minutes then Turbo DNA Free DNAse (Ambion) was added as described in section (2.16). The RNA concentration was determined using 260/280 nm light absorbance ratio (N-D spectrometer Nano Drop Technologies). Reverse transcription was performed using Superscript II kit (Invitrogen). A total of 6 µl mRNA was added to each RT reaction and incubated for 45 min at 50°C followed by 72°C for 15 min. Two microliters of cDNA were added to Hotstart PCR mix (Qiagen) which included 100 µM of forward and reverse cytokine cloning primers. A total 25 µl reaction was incubated for 15 min at 95°C followed by 35 cycles of (95°C -30 sec, 60°C -45 sec, 72°C-1 min) and extension period of 10 min for 72°C. PCR fragments were run on 1.5 % agarose gels with a 1kp ladder (Invitrogen).

The PCR fragments were excised from the gel and cleaned by Wizard SV gel (Promega). For each 1 µg of agarose gel, 1µl of membrane bind solution was added. This mixture was added to the column and the column was placed in 1.5 ml tube. Incubated for 1 min then spun at full speed for 1 minute. Next, 750 µl of membrane wash was added and spun at full speed for 1 min, followed by 500 µl of membrane wash and spun for 5 minutes. A new tube was placed under the column and 50 µl of RNAse water (Ambion) was added to the column, incubated for 1 min and spun at full speed for 1 min in a microcentrifuge (Beckman). The eluted cleaned PCR fragments were cloned into pGEM T easy vector system (Promega).

2.19.2 Cloning of PCR fragments

The ligation mixture was set up by adding in 10 µl of 2X rapid ligation buffer, 50 ng vector, T4 DNA ligase 3 Units/µl and 3:1 insert: vector ratio and incubated O/N at 4^{o}C. Ligation mix (a total of 5µl) was transformed into competent JM 109 *E.coli* cells (Promega) by heat shocking the cells at 42^{o}C for 45-50 seconds and cooled on ice for 2 minutes. To each tube, 950 µl of RT super optimal broth (SOC) media was added and incubated at 37^{o}C with shaking for 1.5 hour. The 100 µl of the transformed cells were plated on agar plates (ampicillin/IPTG/X-gal) and incubated over night at 37^{o}C. The white colonies were selected and DNA was isolated following protocols from QIAGEN mini prep kit (Qiagen). The ligation products were screened for the correct inserts by EcoRI (NEB) restriction analysis. The digested DNA was separated on a 1% agarose gel. After restriction enzyme digest screening, the suspected positive clones were sequenced by the Sequence Core at NFCAD and the results were analyzed by Chromas and Vector NTI sequence analysis programs. All the cytokine plasmid controls (IFN α, IFN γ, TNF α, IL-8) sequences were 100% homologous to literature sources (233, 234). The housekeeping plasmid controls were 100% homologous to porcine cyclophilin and porcine HPRT

((hypoxanthine-guanine phosphoribosytransferase) sequences obtained from BLAST search database.

2.19.3 Optimization of real time RT-PCR conditions

The plasmids were diluted to the following concentration: 0.01, 0.1, 1 and 10 ng/µl. The real time PCR was performed using Taqman 3100 and Quantitech SYBR green PCR kit (Qiagen). Two ml of plasmid were added to a total volume of 25 µl. Primers used for amplification were the following: cyclophilin (TAACCCCACCGTCTTCTT/ TGCCATCCAACCACTCAG), IL-8 (TTCTGCAGCTCTCTGTGAGGC/ GGTGGAAAGGTGTGGAATGC) (233), TNF α (CCCCCAGAAGGAAGAGTTTC/CGGGCTTATCTGAGGTTTGA) (233), INF α (TCAGCTGCAATGCCATCTG/AGGGAGAGATTCTCCTCATTTGTG) (234), INF γ (TGGTAGCTCTGGGAAACTGAATG/ GGCTTTGCGCTGGATCTG) (234). Real time PCR reaction had the following conditions: 95^{o}C for 15 min, followed by varying cycles of 35 – 41 (95^{o}C - 15 sec, 50 - 55^{o}C- 30 sec, 72^{o}C- 30 sec). Dissociation curve and controls were added to each reaction. All the primer sets were tested at 100, 200, 300 nM for the each set of PCR conditions.

2.20 Real-time semi-quantitative RT-PCR for mRNA cytokine expression

Total cellular RNA was extracted from enriched lymphocytes by TriPure isolation reagent (Roche Diagnostics) method. Reverse transcription was performed using random hexamer primers, and employing Quantitect RT kit (Qiagen). Ten microliters of 100 ng/µl samples were added to each RT reaction. After DNase treatment at 42^{o}C for 4 min, RNA was reversing transcribed at 42^{o}C for 20 min, and the reaction was terminated by 2 min incubation at 72^{o}C. The real time PCR was performed on Taqman 3100 using Quantitech SYBR green PCR

kit (Qiagen). Two microlitres of cDNA were added to a total volume of 25 µl. Real time PCR reaction had the following conditions for all primer sets (300 nM): 95^{o}C for 15 min, followed by 41 cycles of (95^{o}C- 15 sec, 55^{o}C-30 sec, 72^{o}C-30 sec). Primers used for amplification are in section 2.17.3. Dissociation curves, negative controls and plasmid controls were added to each reaction. The real time RT-PCR reactions were performed in duplicates. A relative expression ratio of cytokine gene was calculated $2^{-\Delta\Delta Ct}$ according to Livak and Schmittgen (235), and using cyclophilin mRNA as reference.

2.21 Detection of NiV genomic RNA

All cultures (PBMC, enriched T cells, enriched B cells, enriched NK cells, IPAM and Vero 76 cells) used in the *in vitro* study for NiV inoculation were verified for NiV infection by NiV N-gene RT-PCR. In the *in vivo* study, detection of NiV RNA was from a 100 µl of approximately 10^{6} cell/ml of PBMC from control and inoculated pigs. Total cellular RNA was isolated by TriPure isolation reagent (Roche Diagnostics) as per manufacturer's protocol. The RNA concentration and integrity was determined prior to the RT reaction. The first strand cDNA synthesis reaction was catalyzed by Superscript II reverse transcriptase (Invitrogen) with random hexamer primers. A total of 5 µl of RNA (200 ng/µl) was added to each RT reaction and incubated for 42 min at 50°C followed by 72°C for 15 min prior to amplification of target cDNA. RNase H was added to each reaction. Ten percent of cDNA synthesized in the first strand reaction was amplified on Corbett Research RotorGene RG-3000 real time system (Montreal Biotech Inc, Dorval, QC). The PCR reactions were performed with Quantitect RT-PCR kit (Qiagen), using same probe and the primers as for the NiV N-gene RT-PCR (136, 138). Detection of cyclophilin mRNA was used for each sample tested as described in our protocol for mRNA cytokine expression to allow for sample comparison.

2.22 Titration of antibodies for flow cytometry analysis

PBMC were diluted to 10^6 cell/ml and added 1:100, 1:250, 1:500 of antibodies against porcine CD4 and CD8. The stained cells were incubated for ½ hour at 4°C. The cells were washed twice with MACS buffer and ran on the flow cytometry.

2.23 Inoculation of piglets with NiV

In the *in vivo* studies, PBMC were harvested from piglets (Landrace cross) of 4 - 6 weeks of age. The piglets were housed in BSL4 animal facility, the animal use protocol approved by the Institutional Animal Care Committee (CSCHAH), complied with the Guidelines of the CACC. Sampling and inoculation of animals were done under inhalation anesthesia with Isoflurane under BSL4 conditions by personnel from the Animal Care Unit at at NCFAD. The nine piglets were infected intranasally with $2.5x10^5$ PFU of NiV per animal and the blood was collected from the cranial vena cava into CPT tubes. The CPT tubes were transferred for further analysis under BSL4 conditions.

2.24 Flow cytometry analysis of *in vivo* infected PBMC

The PBMC for the cell analysis were collected prior to the inoculation, and on days 2 - 7 post inoculation. The blood from four control pigs was collected at the corresponding time points. The blood was collected in CPT tubes and PBMC were prepared as described in section 2.13 with the following exception: instead of PBS, the cells were washed in cold MACS buffer and remained on ice until the antibodies were added to each sample.

For phenotyping lymphocytes in PBMC by flow cytometry, both single and double staining was employed to define different subpopulation. The following monoclonal antibodies were used: anti-CD4 (1/100) (FITC or PE conjugated, IgG2bk, BD Pharmingen), anti-CD8 (1/100) (PE conjugated IgG2ak, BD Pharmingen), and anti-CD3 (1/100) (FITC IgG2ak, BD

Pharmingen). Irrelevant isotype-matched antibodies were used as background controls. The lymphocytes were resuspended in MACS buffer and first filtered by pre-separation filter (Miltenyi Biotech) followed by incubation with a mixture of two antibodies directed against the surface molecule of interest. All incubations were done at 4^{o}C for 30 min and washed twice with MACS buffer at 600 g for 5 min at 4^{o}C. After the final wash, all samples were kept on ice until 4% paraformaldehyde was added. Analysis was on a two laser FC500 Flow Cytometer (Beckman Coulter). The data was analyzed using CXP software (Beckman Coulter).

Lymphocytes were first gated from PBMC by size (FSC) and granularity (SSC), and were further gated to distinguish lymphocytes. The number of events collected for analysis was 10,000.

2.5 Statistical Analysis

Data analysis was performed using Graph Pad In Stat version 3.0 (GraphPad software, San Diego, CA). Student t-test was used for comparison between means of groups. Differences were considered as significant at P value < 0.05.

3.0 Results

To compare the ability of porcine and human cells to establish an antiviral state against NiV, first porcine and human cell lines were selected. These cells needed a same type to support the growth of NiV and to be able to enter an antiviral state. Initially, the SPJL cell line was selected (St. Jude porcine lung epithelial) as oronasal epithelium provides the first line of defence. The cell line was able to support NiV growth and was used to determine the co-localization NiV P/V/W proteins with STAT1. However, SJPL cells are more genomically similar to monkey cells and not of pig origin (236). In order to substitute the SPJL cell line, the swine testis fibroblast (ST) cell line was selected. The ST cell line supports NiV growth and was readily available. Human lung fibroblasts (MRC5) cell lines were used to complement the porcine fibroblast cell line, although the cell lines were of different origin, both cell lines are fibroblasts and fulfill the criteria of supports NiV growth and have the capability to enter an antiviral state. In addition, human fibroblasts require an intact p38 MAPK pathway for the induction of IFN signaling pathway (237), hence fibroblast cell lines would function well as a replacement.

Nipah antigen was detected in monocytes (140) and monocytic cells are vital innate immune cells in pigs to provide early immune surveillance and bridge adaptive antiviral immunity (238) . The immortalized porcine alveolar macrophage cell line (IPAM) was selected for this study to represent monocytic like cells of the innate immunity. The use of IPAM cell line is more advantageous as there is no need to collect porcine blood to acquire monocytes as well as the cell line is a well characterized (232) and shows to support NiV growth (137).

3.1 Localization of STAT-1 and NiV antigen in NiV infected and uninfected IPAM cells

It was previously demonstrated that NiV- P,V,W protein was detected in the cytoplasm of porcine testis fibroblast (ST) and human lung fibroblast (MRC5) cell lines by binding to the common N-terminal shared by all the three proteins (Fig. 3B) (239). To confirm these findings, a similar assay was performed using antibodies specifically against NiV V and W binding to the unique C terminal of each protein (Fig. 3B) (Dr. C. Kai, U. of Tokyo). Analysis of nuclei fractions (those with membrane and those without membranes) and cytoplasmic fractions from MRC5 and ST cells confirmed that NiV V and W proteins were only detected in the cytoplasm of human and porcine NiV infected fibroblast cell lines (MRC5, ST) (data not shown). It was also observed by Goolia (239) and confirmed by this study that STAT1 in porcine cell line (ST) is present in the cytoplasm and nucleus of both IFN induced and NiV infected cells. The human cell line (MRC5) showed similar results in the NiV infected cells where both the nucleus and the cytoplasm had STAT1 (data not shown).

The immortalized porcine alveolar macrophage cell line (IPAM) was used to determine if NiV infection and IFN response may differ in an immune type cell line. Figure 9 shows the results from IFN α induced (b) and NiV infected (c) IPAM cells 24 hrs post infection at an MOI of 1. As with porcine fibroblast cell line (ST), STAT1 was observed in the cytoplasm and nucleus in both IFN induced and NiV infected cells. NiV P antigen (Fig. 9D) can be observed in the cytoplasm of NiV infected IPAM cells at 24 hpi and the single cell figure of NiV infected IPAM (Fig. 9E) demonstrates that STAT1 and NiV V antigen co-localized in the cytoplasm. Co-localization of NiV V, W, and P with STAT1 was also observed by Goolia (241) thesis work in NiV infected ST and MRC5 fibroblast cell lines. Therefore there appears to be no observed

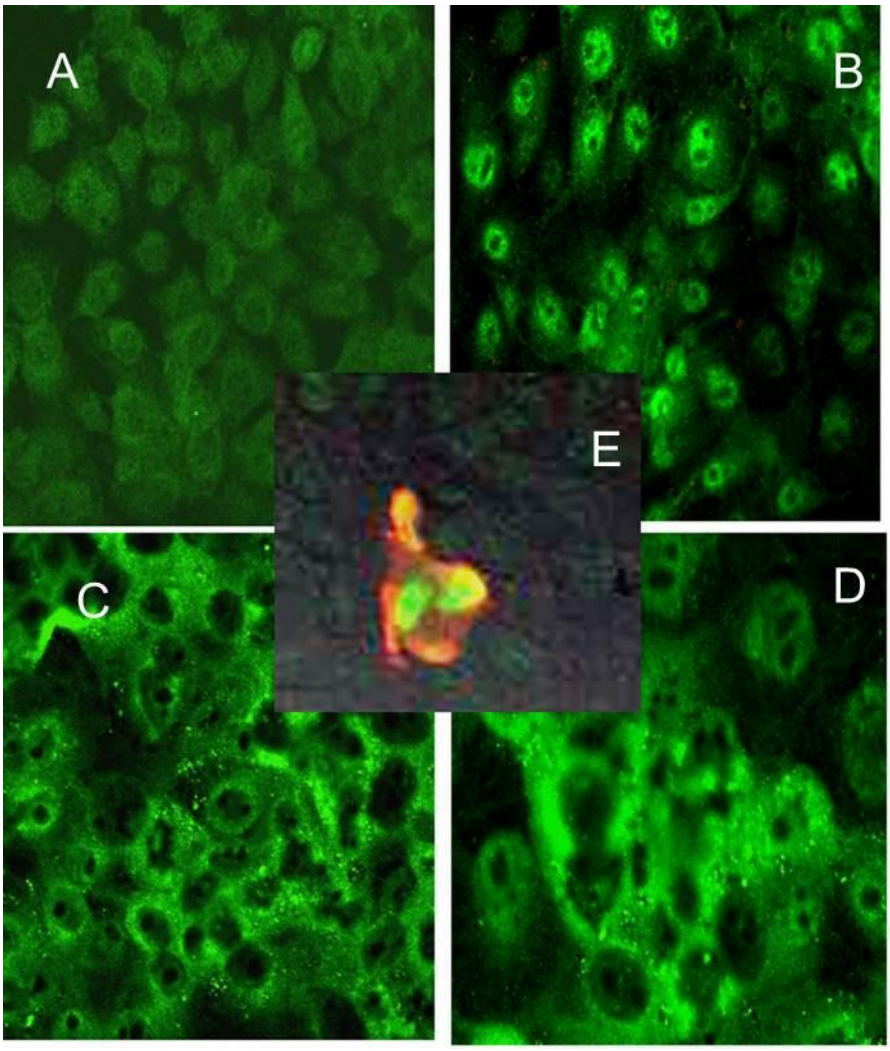

Figure 9 Localization of STAT1 in uninfected IPAM and infected IPAM cells with NiV at MOI of 1. Infections were carried out at MOI of 1.0. Cells were grown to confluence and STAT1 was detected with rabbit anti STAT1 polyclonal antibody (1:200) (**A**) for uninfected, (**B**) IFN induced for 24 hours (**C**) NiV infected for 24 hours and (**D**) infected for 24hrs stained with NiV-P58 mAB. (**E**) shows the co-localization of STAT1 and rabbit polyclonal NiV -V antibody in NIV infected IPAM for 24hrs. Goat anti-mouse Alexa Fluor 594 (red- detecting NiV P/V/W proteins or NiV-V protein) and goat anti-rabbit Alexa Fluor 488 (green- detecting STAT1) were used. Co-localization of NiV proteins with STAT1 is visualized by yellow. All slides were prepared in duplicates and experiments were repeated twice. Magnifications: IPAM (a,b) 20X (c,d,e) 40X

differences between NiV infected cell types (ST fibroblast and IPAM monocytic-like) cell lines in the localization of STAT1 and co-localization NiV P/V/W proteins with STAT1.

3.2 Phosphorylation of eIF2α in human and porcine cell lines inoculated with NiV

As cells can use alternative pathways to the JAK-STAT pathway to activate an antiviral state, we wanted to determine if there is a difference in the intracellular status of an antiviral state in NiV infected human and porcine cells, even though, the JAK-STAT pathway was likely to be blocked, as previously reported by Rodriguez *et al.* (100, 102) and Shaw *et al.* (97) and as suggested by the results presented here. The intracellular activation of an antiviral state in NiV infected cell lines was detected by western blot using phospho-specific antibodies against eIF2α (Fig. 10). The phosphorylation of eIF2α not only halts the translation of viral proteins but may also lead to apoptosis which makes this kinase another important check point against viral invasion and antiviral defence (152, 153).

Swine testis fibroblasts (ST), human lung fibroblasts (MRC5) and immortalized porcine alveolar macrophage cell line (IPAM) were inoculated with NiV at an MOI of 1 and whole cell lysates were prepared at 6, 8, 12, 24, and 48 hrs post inoculation. The status of eIF2α phosphorylation was assessed in cells inoculated with live NiV and gamma irradiated NiV, mock infected or treated with thapsigargin. Incubation with thapsigargin for one hour served as a positive control for eIF2α phosphorylation. This drug treatment induced phosphorylation of eIF2α in all the cell lines used in this study. To determine if virus attachment induced the phosphorylation of eIF2α, each cell line was inoculated with gamma irradiated NiV at an MOI of 1. Fig. 10A shows a graph which represents the fold in change in the levels of eIF2α phosphorylation to total eIF2α starting from 6 to 48 hrs post inoculation. In NiV infected MRC5 cells, the levels of eIF2α phosphorylation were observed from 12 hpi followed by a subsequent

increase at 24 to 48 hpi when compared to the mock infected cells (Fig.10B). Whereas the swine testis fibroblast (ST) levels of eIF2α phosphorylation were detected as early as 6 hpi until 48 hpi. As with the fibroblasts, levels of eIF2α phosphorylation were observed in NiV inoculated, mock and chemical induced IPAM cells. In NiV infected IPAM cells, phosphorylation levels of eIF2α increased significantly ($p< 0.05$) after 8 hpi and peaked at 48 hrs post inoculation (Fig. 10A/B).

To determine if virus attachment to the cells would induce phosphorylation of eIF2α, each cell line was inoculated with gamma irradiated NiV at an MOI of 1. Such inactivated virus fails to express viral proteins but retains the capability for receptor binding (240). In both MRC5 and ST cells inoculated with gamma irradiated NiV, the phosphorylation levels of eIF2α were comparable to the mock infected cells at all the different time points (Fig. 11).

In the selected cell lines, an antiviral state was detected by the phosphorylation of eIF2α in NiV infected cells. Hence, an alternative pathway other than the JAK-STAT may be functional in NiV infected cells. The p38 MAPK signaling pathway was proposed to have the ability to lead to an antiviral state in virus infected cells. In addition, NiV G binding to ephrin B may allow indirect initiating of the ERK pathway (76). Hence, the both p38 and ERK pathways of MAPK pathways may be important for mounting the first line of defense against viral infections.

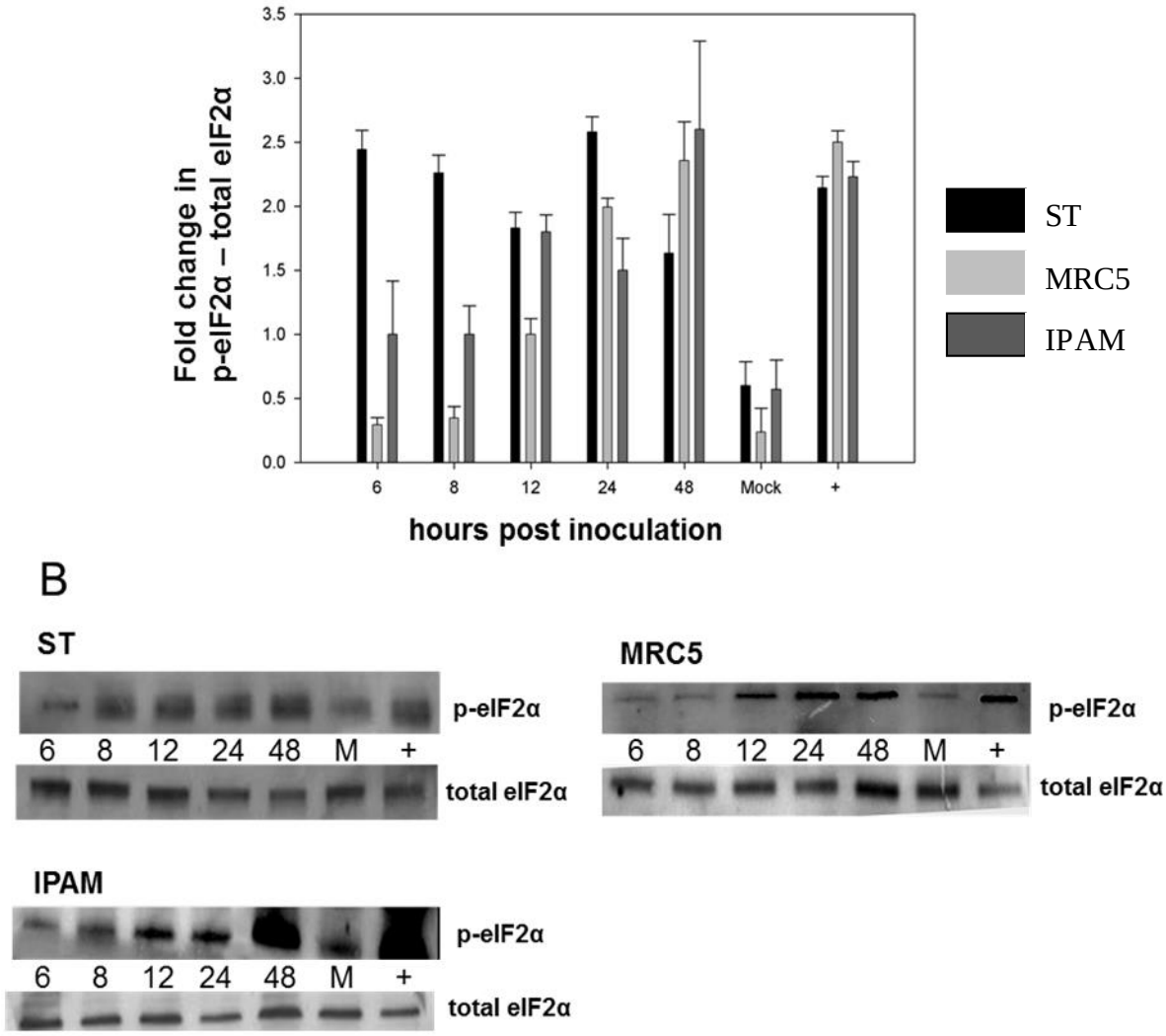

Figure 10 Detection of phosphorylation of eIF2α in human and porcine cell lines inoculated with NiV. (A) Plot of fold changes in ratios of phosphorylated eIF2α (p-eIF2α) to total eIF2α compared by densitometry of corresponding bands using a computer densitometer. **The bars are black for ST, light grey for MRC5 and dark grey for IPAM cells.** Both the human and porcine cell lines were mock inoculated (M) or infected with NiV (MOI of 1). Thiapsigargin incubated for 1 hour in each cell type was used as a positive control (+) for detection of eIF2α phosphorylation. (B) Whole cell lysates were prepared at the indicated times post inoculation and analyzed by western blot using antibodies specific for the phosphorylated (p) -eIF2α , and then reprobed with total eIF2α to verify equal protein loading. The data are shown as the mean and standard deviation of duplicates from three independent experiments and one of three experiments are shown as a representatives.

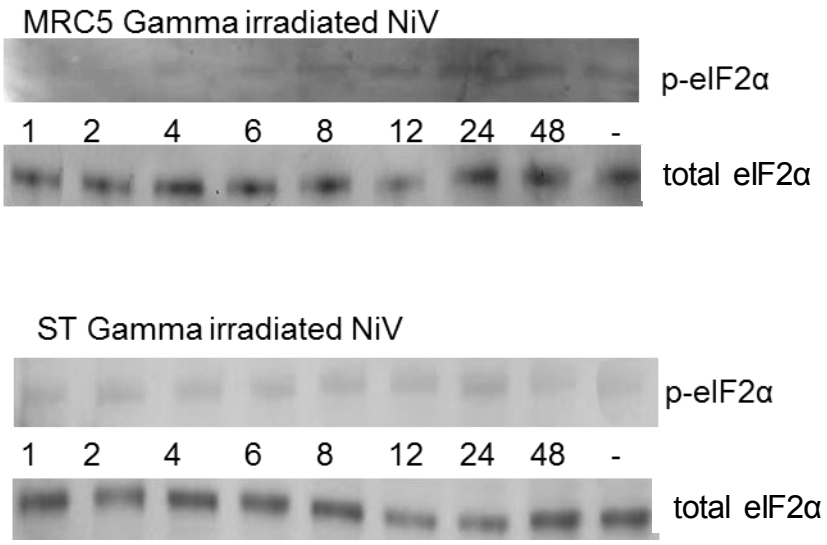

Figure 11 Detection of phosphorylation of eIF2α in human and porcine cell lines inoculated with gamma-irradiated NiV. Both the human and porcine cell lines were mock inoculated (M) or inoculated with gamma-irradiated NiV (MOI of 1). Whole cell lysates were prepared for the indicated times post inoculation and subjected to western blot analysis with the specific p-eIF2α and total eIF2α. The blots were stripped of phosphorylated antibodies to verify equal protein loading with total eIF2α. One of two experiments are shown as a representatives.

3.3 Activation of p38 MAPK signaling pathway in human and porcine cell lines inoculated with NiV

As mentioned earlier, MAPK signaling pathways are also activated by IFNs binding to IFNAR (164,165,166). In particular, the p38 pathway mediates the regulation of transcription of ISG genes which are important for antiviral response (226, 227, 241, 242). We began to detect p38 phosphorylation at 1 hour post adsorption followed by 3, 6, 12, 24, and 48 hours for both porcine and human cell lines. In Fig. 12A, the graph shows that the human MRC5 cell lines become phosphorylated as early as 1 hour post adsorption until 6 hpi at which point there was a significant decrease of 0.5 units ($p < 0.05$) in p38 MAPK phosphorylation. After 12 hpi, there was a gradual increase followed by a continuous and sustained phosphorylation of p38 MAPK until the last time point (48 hpi). In NiV infected IPAM cell lines, the phosphorylation of p38 MAPK was activated early post inoculation at 1 and 3 hpi but not in ST cells. After the initial phosphorylation in IPAM a significant decrease was observed until 12 hpi. After 12 hpi a spike in the phosphorylation of p38 MAPK was detected at 24 and 48 hpi in both ST and IPAM cell lines. The phosphorylation levels of p38 MAPK were significantly more intense in IPAM cells compared to ST cells. There is a significant ($p < 0.05$) difference between ST and IPAM porcine cell lines inoculated with NiV. At the last time points, a sustained phosphorylation of p38 MAPK was evident in both human and porcine cell lines.

3.4 The effects of p38 MAPK inhibitor on NiV viral titers and NiV-P protein production in human and porcine cell lines

Since the p38 MAPK pathway is activated in NiV infected cell lines and is potentially used as a compensatory pathway for the establishment of an antiviral. It was also of interest to

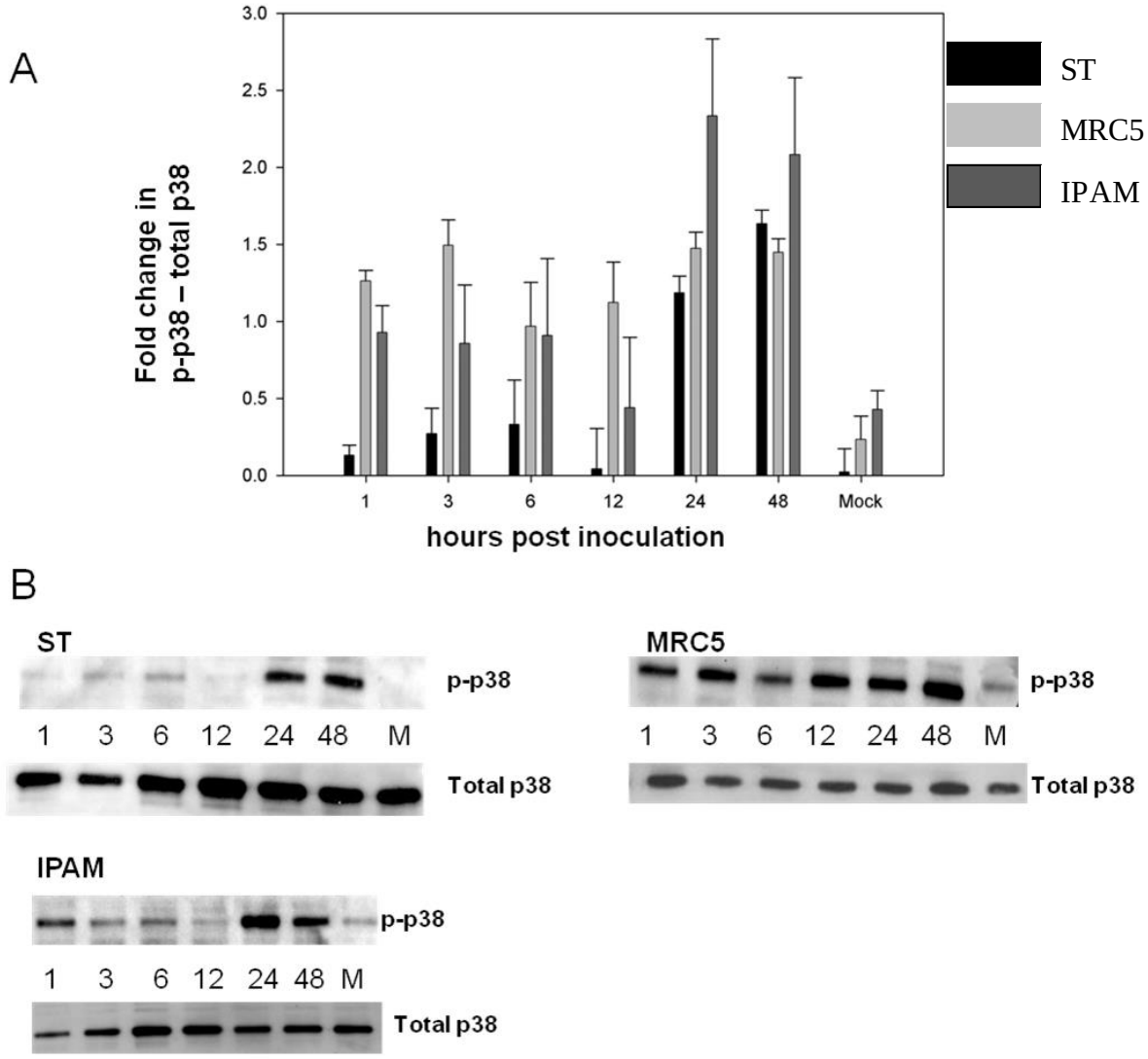

Figure 12 Detection of phosphorylation of p38α in human cell line and porcine cell lines inoculated with NiV. (**A**) Plot of the fold changes in ratios of phosphorylated p38α (p-p38α):total p38α compared by densitometry of corresponding bands using a computer densitometer. **The bars are black for ST, light grey for MRC5, and dark grey for IPAM cell lines.** Both the human and porcine cell lines were mock inoculated (M) or infected with NiV (MOI of 1). (**B**) Whole cell lysates were prepared at the indicated times post inoculation and analyzed by western blot using antibodies for the phosphorylated p-p38α and then reprobed with antibody specific for total p38α. The data are shown as the mean and standard deviation of duplicates from three independent experiments and one of three experiments is shown as a representative.

determine if this pathway is required for NiV replication. For this study, the SB202190 (Sigma) p38 MAP kinase inhibitor was used. It is a highly selective and cell permeable inhibitor with no effects on JNK, ERK or other multiple related kinases at concentrations of up to 100 µM (243). It should be noted that all the concentrations of SB202190 used in this study showed no evidence of cell death in either human or porcine cell lines (data not shown) suggesting SB202190 did not inhibit virus replication by host cell death.

To determine the effect of p38 inhibitor, we first examined the expression of viral proteins in NiV inoculated cell lines. All the cell lines were incubated with the two different concentrations of p38 inhibitor (25 and 50 µM) for 1 hour prior to NiV inoculation. The p38 inhibitor was removed during the 1 hour adsorption period with NiV and fresh media with p38 inhibitor was added and remained on the cells for the duration of the incubation period. Six hours post infection, the cell lysates were collected and western blots were performed using a NiV- P58 antibody. There was no evidence of NiV-P expression at 6 hpi in these cell lines, hence western blots show as an example results starting from 12 hpi from one independent experiment. From the western blots it was evident that the intracellular expression NiV-P was reduced in a dose dependent manner in both human and porcine cell lines (Fig. 13 B, D, F). In addition, we tested the expression of NiV nucleocapsid (N) protein and the same pattern of reduction in N protein were observed in a dose dependent manner (data not shown). The NiV-P expression in porcine cell lines appeared to be more affected by the p38 inhibitor compared to the human cell line. Next, viral titers were determined by plaque assays from collected supernatants at 12, 24 and 48 hpi. As shown in Fig. 13 (A, C, E) the presence of p38 inhibitor reduced viral progeny release in a dose dependent manner in both human and porcine cell lines. Compared to the NiV infected controls, once again the porcine cell lines had a greater reduction

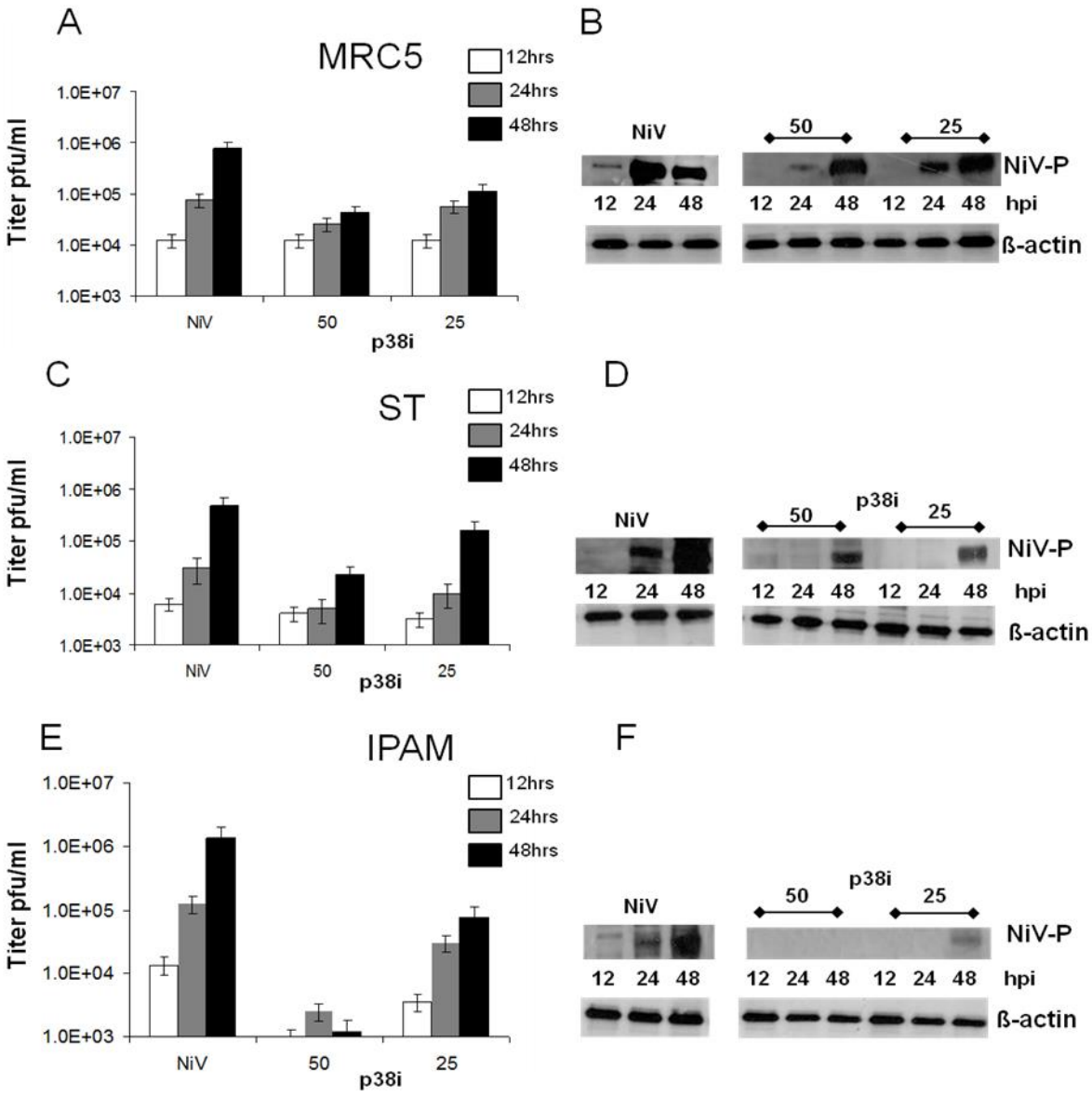

Figure 13 The effects of p38 MAP kinase inhibitor on NiV replication in human and porcine cell lines. Cells were infected with NiV (MOI =1) in the presence of the indicated concentration of SB212190 or in the absence of inhibitor. Left panel: The bar graphs A,C,E represent virus titers in collected supernatants at 12 (white column), 24 (grey column) and 48 hrs (black column) post infection, determined by plaque assay (PFU/ml) from two independent experiments for each respective cell line. Right panel: Western blots analysis of whole lysates from MRC5 (**B**), ST (**D**), IPAM (**F**) cells harvested at the indicated time points. The membranes were first probed with NiV-P antibody, stripped and reprobed with antibody against ß-actin. The western blots represent two independent experiments and one of the experiments is shown as a representative.

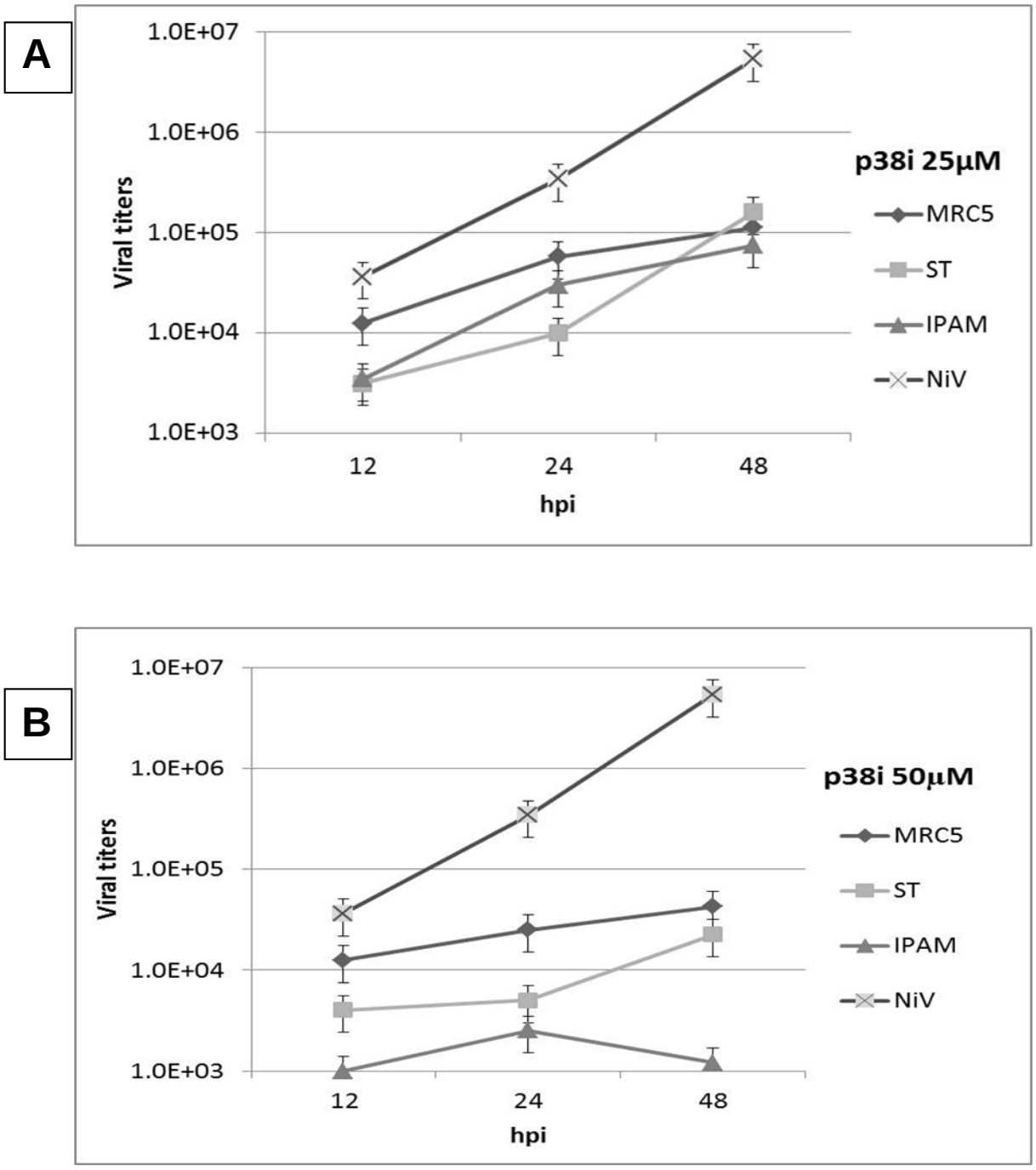

Figure 14 The comparison of viral titers in porcine and human cell lines infected with NiV in the presence of p38 MAPK inhibitor at (A) 25 µM and (B) 50 µM concentrations. The line graphs represent collected supernatant at 12, 24, 48 hrs post inoculation. The data shown for MRC5, ST, and IPAM cells are the mean progeny virus by plaque assay with the addition of p38 MAPK inhibitor. The line designated as NiV represents the average progeny virus from all the selected cell lines determined by plaque assay without the addition of p38 MAPK inhibitor.

of NiV viral progeny compared to human cell line, especially in IPAM cells.

A comparison figure (Fig. 14) of viral titers (PFU/ml) in each selected cell line demonstrated how the concentration of p38 MAPK inhibitor affected each cell line compared to an average NiV replication in the cell lines used in this study. Taken together, these results indicate that p38 MAPK pathway may play an important role in NiV replication, especially in immune cells.

3.5 Activation of ERK 1/2 signaling pathway in human and porcine cell lines inoculated with NiV

To determine the role of MAPK signaling pathways in NiV replication, we also examined the kinetics of ERK activation. The ERK pathway can be activated by ligands binding to cellular receptors; virus binding to its cellular receptor may also begin the signaling cascade depending on the nature of the cellular receptor. Nipah virions specifically bind to host cell surfaces through cellular receptor Ephrin B2 or B3 (70, 71, 72, 75) which may lead to activation of ERK pathway. Human and porcine cell lines were inoculated with NiV and cell lysates were harvested at 15 mins, 30 mins, and at 1, 3, 6, 12, 24 and 48 hpi. The phosphorylation of ERK 1/2 was determined by western blots with antibodies against phosphorylated-ERK 1/2. As shown in Fig. 15, ERK 1/2 was phosphorylated upon exposure to the virus in human fibroblasts (MRC5) and porcine monocytic like cells (IPAM) cell lines with the first peak detected at 15 and 30 minutes. The ERK 1/2 activity returned to baseline at 1 hpi for both cell lines and returned to significantly ($p<0.05$) elevated levels of phosphorylation at 12 hpi for MRC5 and at 24 hpi for IPAM cell lines. Compared to MRC5 and IPAM cells, the porcine fibroblast (ST) cells inoculated with NiV

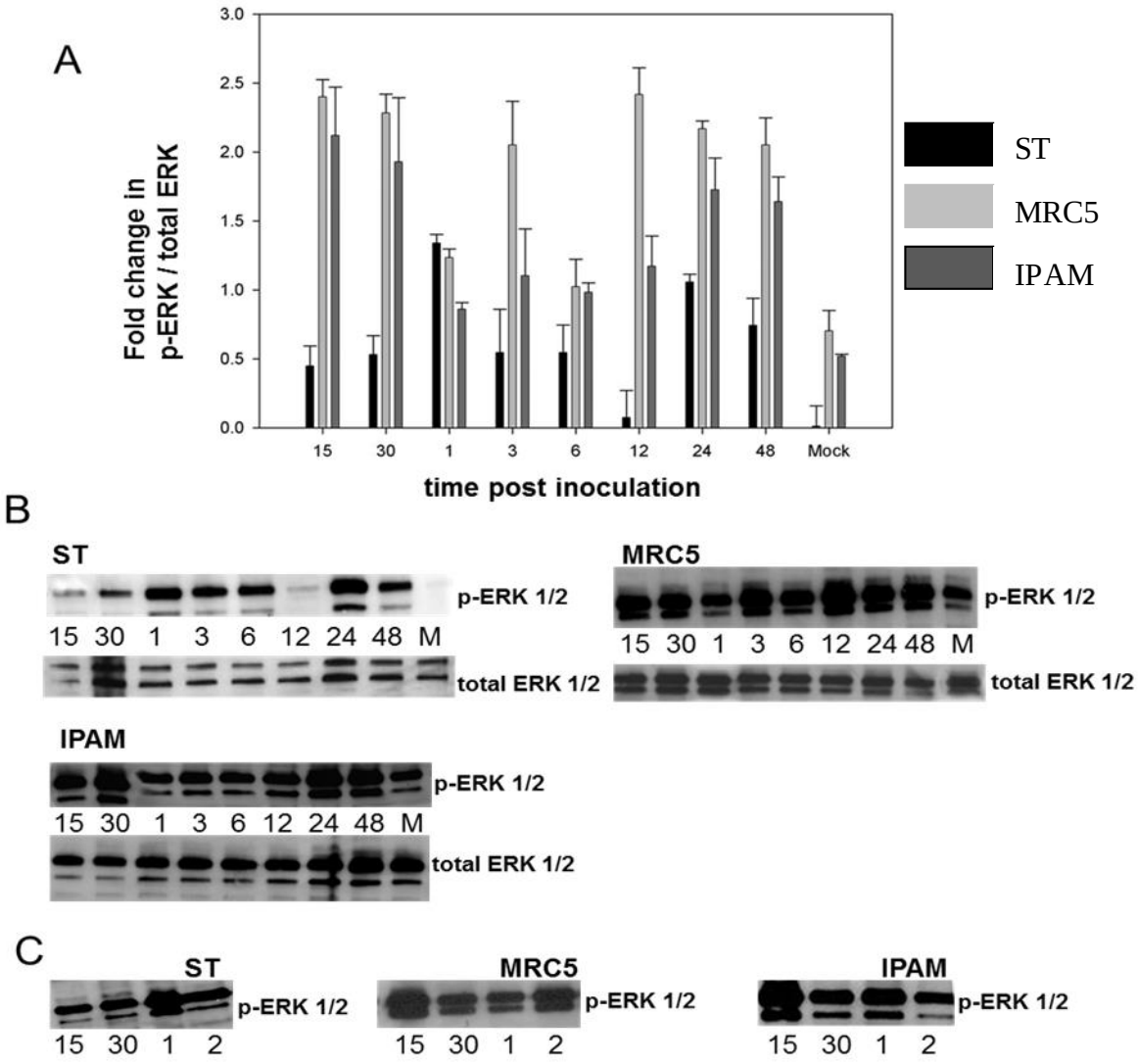

Figure 15 Detection of phosphorylation of ERK 1/2 in human cell line and porcine cell lines inoculated with NiV. (**A**) Plot of fold changes in ratios of phosphorylated p-ERK1/2:total ERK1/2 compared by densitometry of corresponding bands using a computer densitometer. **The bars are black for ST, light grey for MRC5, and dark grey for IPAM cell line.** Both the human and porcine cell lines were mock inoculated (M) or infected with NiV (MOI of 1). **(B**) Whole cell lysates were prepared for the indicated times post inoculation and analyzed by western blot using antibodies against p-ERK 1/2 then stripped and reprobed with antibody specific for total ERK 1/2 . The data are shown as the mean and standard deviation of duplicates from three independent experiments and one of the three experiments is shown as a representative. (**C**) Whole cell lysates were prepared from gamma irradiated NiV inoculated cell lines for the indicated times and subjected to western blot analysis with the specific p-ERK 1/2.

required an hour before the activated form of ERK1/2 was significantly ($p<0.05$) phosphorylated (Fig. 15A). A gradual decrease was detected after 6 hpi followed by a second wave of phosphorylation at 24 hpi compared to mock infected cell lines. The phosphorylation of ERK 1/2 did increase significantly ($p<0.05$) at 24 and 48 hpi compared to the mock control. We also tested whether ERK 1/2 phosphorylation increased over time in mock inoculated cell lines. No significant increases of ERK 1/2 phosphorylation were observed over time in the mock inoculated controls (data not shown). However, it should be noted that there was a higher basal of ERK 1/2 phosphorylation in IPAM and MRC5 cell lines compared to ST cell lines.

To further elucidate the mechanism of NiV mediated ERK 1/2 activation, we used gamma irradiated virus. Fig. 15C shows ERK 1/2 phosphorylation was detected upon inoculation with gamma irradiated NiV in all cell lines although ERK 1/2 phosphorylation returned to basal level within an hour or less depending on the cell line. The phosphorylation of ERK 1/2 did not increase over time with gamma irradiated NiV in all the cell lines. In agreement with live, inoculation with gamma irradiated NiV was delayed in ST cell line. In ST cells an increase of ERK phosphorylation was detected at 1 hpi as opposed to 15 min in IPAM and MRC5 cell lines (Fig.15C).

3.6 The effects of ERK inhibitor on NiV viral titers and NiV-P protein production in porcine and human cell lines

To determine the potential role of ERK activation in viral replication, we selected FR180204, a direct inhibitor of the ERK pathway and not upstream cellular kinases such MEK1, since recent studies have revealed that MEK inhibition can lead to the blocking of cellular responses via substrates other than ERK (244). This ERK inhibitor (FR180204) suppresses ERK

1/2 kinase mediated cellular responses with 30 fold greater selectivity against p38α and more than 100 fold greater against other kinases (MEK1, MKK4, Src and IKK α) (245).

All the cell lines were incubated with different concentrations of FR180204 inhibitor for one hour prior to inoculation with NiV. The inhibitor was not present during adsorption of the virus but was added post adsorption and remained in the media for subsequent incubation periods. Cell lysates and supernatants were collected at 6, 12, 24 and 48 hpi. Western blots were performed on the cell lysates using NiV - P58 antibody that recognizes the viral phosphoprotein. As with p38 experiments, there was no evidence of NiV-P expression at 6 hpi in these cell lines, and western blots signals were detected starting from 12 hpi. In the western blots, the expression of NiV-P protein was significantly reduced by ERK inhibitor at 20 μM (Fig. 16) or higher doses (data not shown). There was no difference in NiV-P production in MRC5, ST or IPAM cells with 1 and 10 μM concentrations. ST cells inoculated with NiV were more sensitive to the addition of the inhibitor at greater than 20 μM, with cells dying at 24 hpi compared to ST cells inoculated only with NiV (48 hpi). It should be noted that all the concentrations of ERK inhibitor used throughout this study did not induce cell death in either human or porcine cell lines without NiV inoculation (data not shown). As indicated in Figure 16, the viral titers in the collected supernatants were determined at each time point. In the presence of 10 μM concentration of the ERK inhibitor, there was no reduction of viral progeny release observed, and only at 20 μM concentration was a difference observed. In ST and IPAM cells there was a log reduction in viral titers at 24 hpi and almost a 2 log viral titers reduction for MRC5 at 24 hrs post infection. However, after 48 hpi, both MRC5 (Fig.17) and IPAM cells viral titers increased significantly (Fig.17) but remained lower than the viral titers for NiV infection without the inhibitor. The ST cells were the most significantly ($p<0.05$) affected by ERK inhibitor at 20 μM (Fig.17).

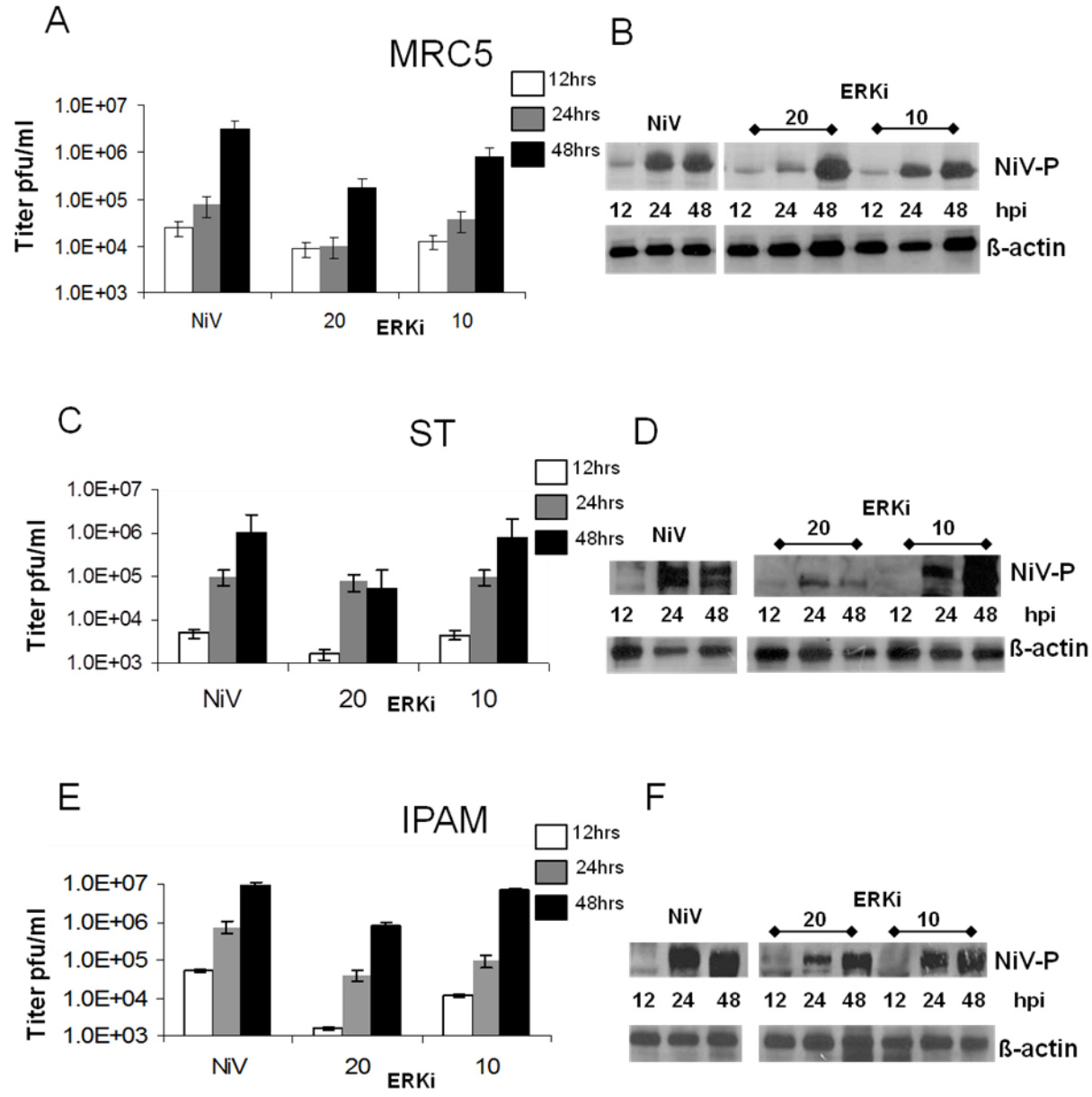

Figure 16 The effects of ERK inhibitor on NiV replication in human and porcine cell lines. Cells were infected with NiV (MOI =1) in the presence of the indicated concentration of FR180204 or in the absence of inhibitor. Left panel: The bar graphs A,C,E represent virus titers in collected supernatants at 12 (white column), 24 (grey column) and 48 hrs (black column) post infection, determined by plaque assay (PFU/ml) from two independent experiments for each respective cell line. Right panel: Western blots analysis of whole lysates from MRC5 (**B**), ST (**D**), IPAM (**F**)cells harvested at the indicated time points. The membranes were first probed with NiV-P antibody, stripped and reprobed with antibody against ß-actin. The western blots represent two independent experiments and one of the experiments is shown as a representative.

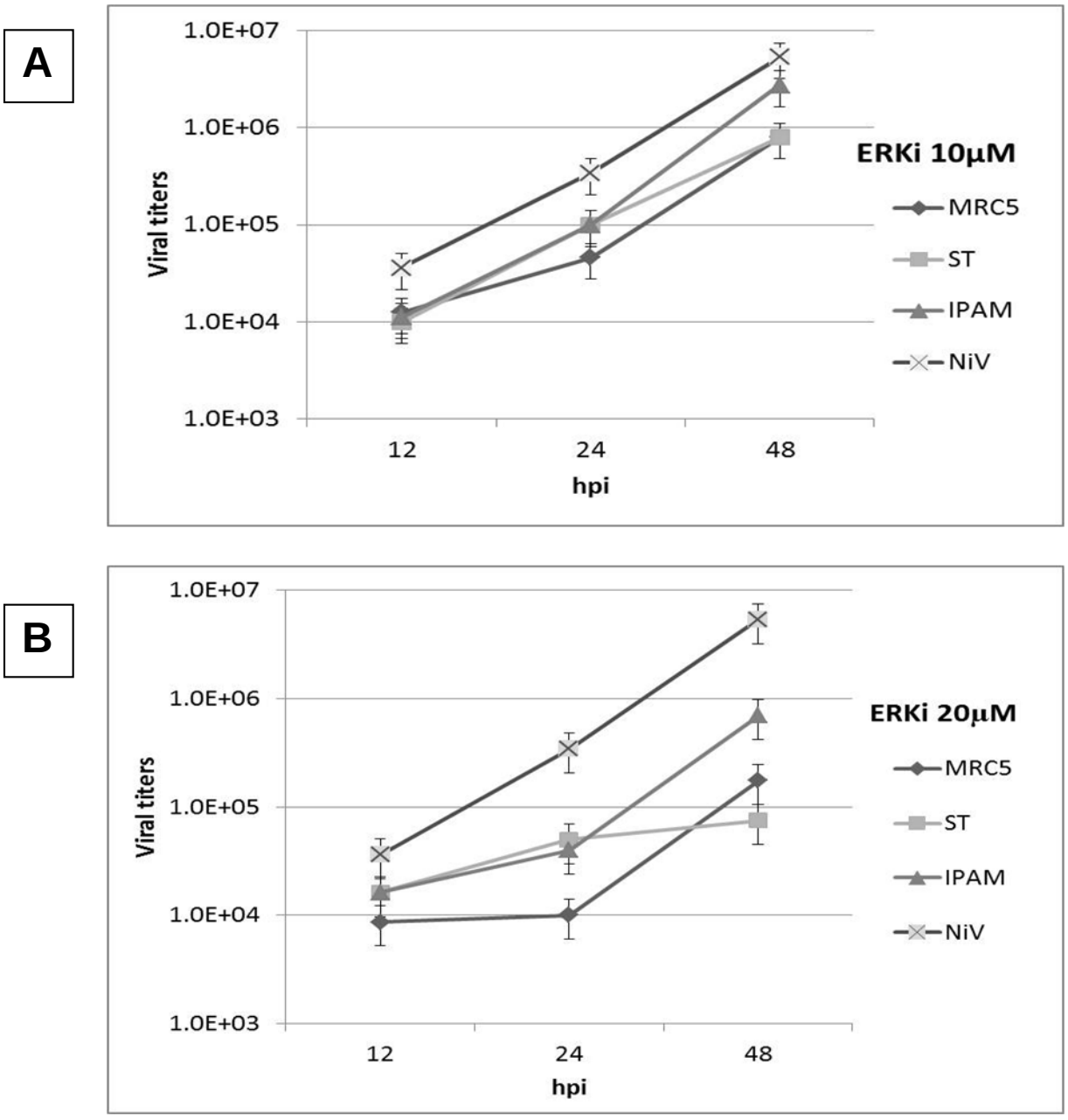

Figure 17 The comparison of viral titers in NiV porcine and human cell lines infected in the presence of ERK inhibitor at (A) 10 and µM (B) 20 µM concentrations. The line graphs represent collected supernatant at 12, 24, 48 hrs post inoculation. The data shown for MRC5, ST, and IPAM cells are the mean progeny virus by plaque assay with the addition of ERK 1/2 inhibitor. The line designated as NiV represents the average progeny virus from all the selected cell lines determined by plaque assay without the addition of ERK inhibitor.

The results indicated that the inhibition of ERK 1/2 kinase at the selected concentrations decreased the viral titers in a cell type dependent manner as summarized in Fig 17.

3.7 NiV infection of porcine PBMC subpopulations *in vitro*

The subversion of STAT 1 signal transduction pathway was investitaged in NiV infected porcine monocytic like cells. However, it is not known if NiV replicates in porcine immune cells *in vivo* thus affecting the adaptive immune response. First indication that immune cells are likely infected was observed by *in vitro* analysis of porcine PBMC on flow cytometry that showed positive staining for NiV antigen in monocytes and subpopulation of lymphocytes (137). In addition, viremia was implicated as a mode of dissemination of NiV throughout the host, including swine (114, 125, 136). There was also previous reported evidence of lymphocyte necrosis and lymphoid depletion in the lymph nodes, with confirmation of bacteria in the CSF of NiV infected pigs (125, 135, 137) indicating NiV infection has an effect on porcine immune cells. In order to determine the role of cells in the viremic spread of the virus, and permissiveness of porcine immune cells to Nipah virus, the work was initiated using porcine PBMC. In young pigs there is a higher frequency of NK cells (246), hence this lymphocyte population along with B and T cells may prove to be important in NiV infected piglets in regards to immune modulation. Monocytes were also included in this study as it was previously shown with positive staining that NiV antigen was present in this cell type (137, 247).With regard to porcine T lymphocytes with cytolytic activities, two subsets within the CD4-CD8+ T-cell subpopulation could be defined by the expression of CD6 differentiation antigens: CD6- cells which showed spontaneous cytolytic activity and CD6+ MHC I-restricted cytolytic T lymphocytes including virus-specific cytolytic T lymphocytes (247); therefore the CD6+ surface marker was selected to distinguish these two phenotypes. Due to constraints of working in BSL4

containment, selection and combinations of markers/antibodies had to be limited to maximum triple staining when internal staining for viral antigen was employed, and to only double staining for the cell surface markers.

PBMC from non-infected pigs were separated into subpopulations prior to inoculation. After adhering the monocytes to a cell culture plate, the non-adherent cells were sorted using magnetic beads coated with antibodies against CD16 (NK cells), CD6 (T lymphocytes), or CD21 (B lymphocytes) (Fig. 8A). The purity of NK, T, and B cells was verified by flow cytometry using the above markers. The T cells had the highest purity (90-95%), followed by NK cells (85%), whereas purity of B cells was the lowest in the range of 75-85%. Sorted cells were inoculated with NiV in non-stimulated state, and after stimulation with PMA combined with ionomycin to approximate activated immune system post infection.

Replication of NiV in the individual subsets of cells was determined by detection of infectious virus particles in supernatant harvested from monocytes, NK and T lymphocytes. The MOI in these experiments was based on NiV infectivity in Vero 76 cells to ascertain that the same concentration of infectious particles was used for inoculation of all cell preparations. The titer of the same NiV stock can be very different when titrated on Vero 76 cells and on immortalized alveolar macrophages (IPAM): 4×10^6 and 5×10^4 pfu/ml, respectively. Consequently, it was expected that actual MOI can be as low as 0.001 (for example on monocytes).

At 48 hrs, the highest virus yield was detected in supernatants harvested from monocytes (Fig. 18A). Both the NK and CD6+ T lymphocytes had similar viral titers at approximately 2000 PFU/ml after 48 hpi (Fig. 18A). Very low level of infectivity was recovered from the B

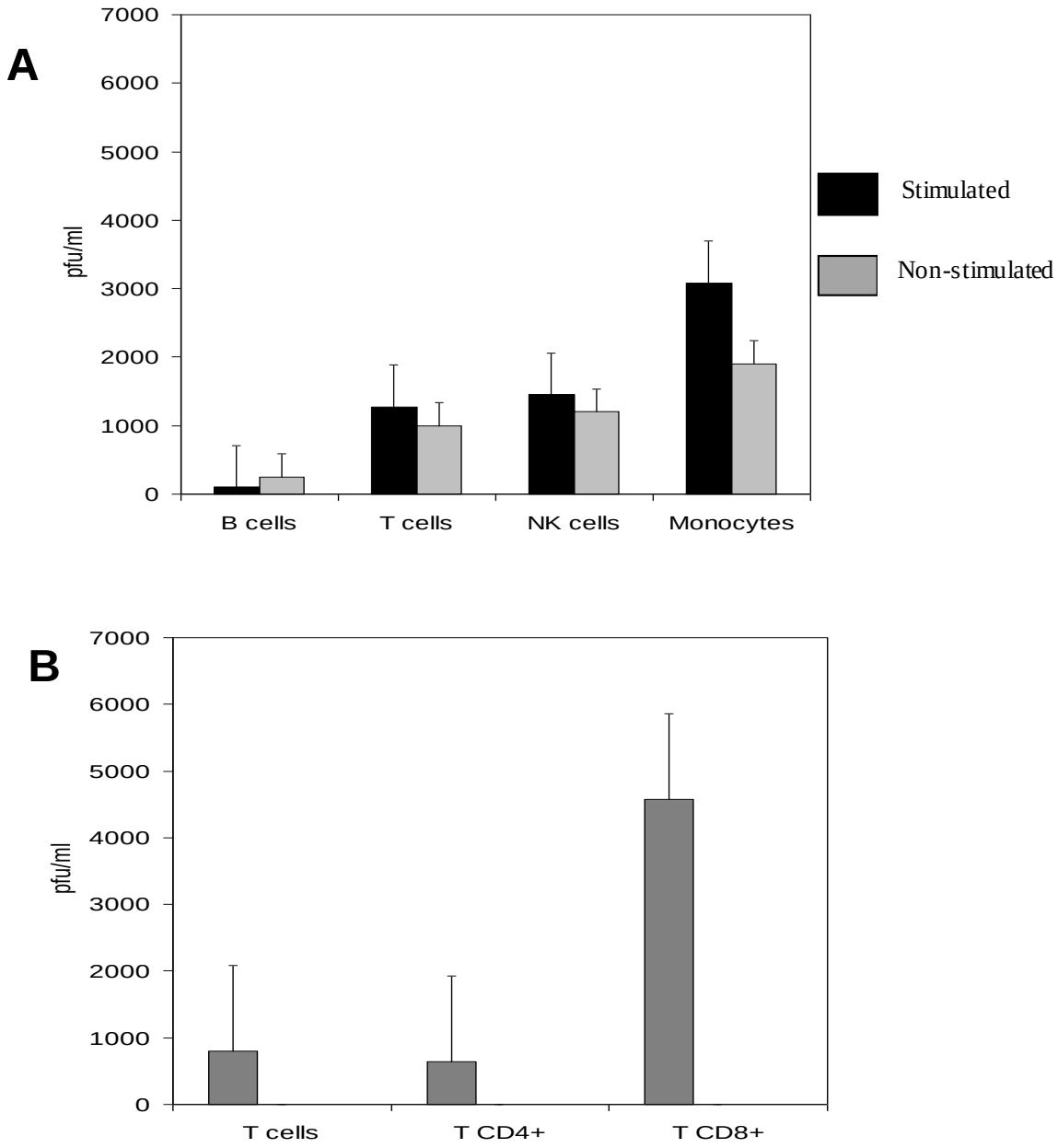

Figure 18 Replication of NiV in the individual subpopulations of PBMC. Sorted cells were inoculated with NiV in three independent experiments. Total of 10^5 cells per subpopulation were inoculated with 10^4 PFU of NiV in a 1 ml volume. The infectivity in cell supernatants was determined by plaque titration on Vero 76 cells. (**A)** Comparison of virus yield from stimulated and non-stimulated PBMC subpopulations at 48 hrs post inoculation. Black filled columns represent mean of pfu/ml in supernatant collected from non-stimulated cells, the grey filled columns represent mean of pfu/ml in supernatant collected from stimulated lymphocytes or monocytes. (**B)** NiV yield in supernatants of sorted T lymphocytes (CD6+ T cells, CD3+CD4+ T cells and CD3+CD8+ T cells) at 24 hpi.

cells. Stimulation of these sorted cells (Fig. 18A) did not significantly ($p<0.05$) change the virus yield obtained in their supernatants, and was not used in follow up experiments.

Next, each individual subpopulation of T lymphocytes was sorted by surface markers CD4 and CD8 to determine if NiV can replicate in a specific subpopulation of T lymphocytes. Initially, the CD6 marker was tested, but it appears that there was interference in binding between the anti-CD6 and the anti-CD4 or anti-CD8 antibodies. The PBMC were alternatively sorted using CD3 marker and CD4 or CD8 markers, as this increased the purity of the T cell preparations in the double antibody sorting with the resulting purity around 95%. At 24 hrs post inoculation, the highest infectivity was recovered from supernatants of the CD3+CD8+ sorted T lymphocytes (Fig. 18B). Lower yield of virus was recovered from the CD6+ T lymphocytes and the CD4+ T lymphocyte.

Interestingly, no infectivity was recovered from monocyte supernatants at 24 hrs post inoculation (Fig. 19A). The finding was supported by detection of NiV genomic RNA at different time points post inoculation. The amount of genomic RNA dropped at 24 hrs, and then significantly increased at 48 hrs post infection (Fig. 19B), while genomic RNA of gamma-irradiated NiV was gradually decreasing below detectable level by 48 hrs post exposure. Due to phagocytic nature of monocytes, most of the virions were likely digested or processed for antigen presentation, and only small number of infectious virions was able to initiate productive infection in these cells.

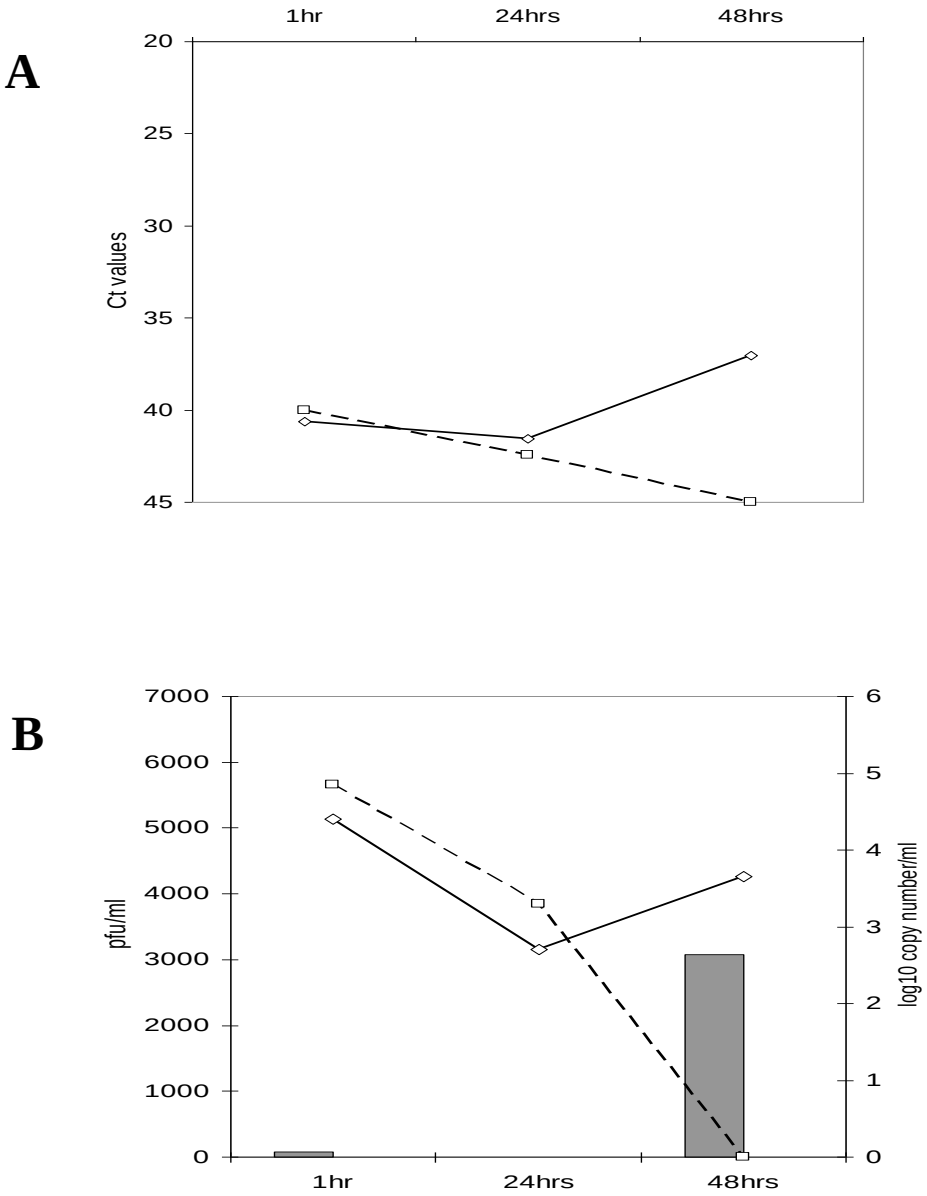

Figure 19 Replication of NiV in porcine monocytes. (A) Presence of genomic RNA at indicated time points post inoculation in cell lysates from monocytes inoculated with live NiV (solid line) or with gamma-irradiated NiV (dashed line). **(B)** Detection of infectivity in supernatant harvested from monocytes at 24 and 48 hpi with NiV (gray columns), and detection of viral RNA in cells inoculated with live virus (solid black line) or with gamma-irradiated NiV (black dashed line).

3.8 Detection of ephrin B2 mRNA in sorted PBMC

In the absence of an effective antibody specific for porcine ephrin B2 one of the NiV receptors, the detection of mRNA of ephrin B2 in sorted PBMC was used to assess whether virus replication could be blocked at the level of virus attachment. In uninfected and untreated, all T lymphocytes expressed ephrin B2 mRNA, whether they were permissive to NiV or not (Table 1). On the other hand, monocytes and NK lymphocytes were permissive to NiV infection in uninfected and untreated cells without expressing the mRNA of ephrin B2, and started to express the mRNA upon NiV infection. While stimulation of the B lymphocytes with NiV leads to ephrin B2 expression, it did not render the cells permissive to NiV.

3.9 Intracellular staining of NiV antigen in T lymphocytes

Infection of T cells with NiV was confirmed by internal positive staining for the NiV-N protein in the CD6+ sorted T cells as analyzed by flow cytometry, and in the CD3+CD8+ sorted cells by positive staining for the non-structural C protein (Fig. 20). It was observed that efficient replication of MeV (a member of *Paramyxoviridae*) in peripheral blood mononuclear cells requires the expression of the non-structural C protein (248); hence it was also hypothesized with NiV. As well the NiV C mRNA needs to transcribed by viral polymerase and translated during NiV replication cycle (Fig. 3B). NiV N antigen was detected in approximately 30% of CD6+ T cells at 48 hrs post inoculation at 0.1 MOI (Fig. 20C). NiV C protein was detected in about 10% of the CD3+CD8+ T lymphocytes at 24 hrs post inoculation (Fig. 20B), and reached 30% at 48 hrs (Fig. 20D). NiV C protein was not detected in NiV infected CD3+CD4+ T lymphocytes at 24 hrs post inoculation (Fig. 20A). The results cannot be directly correlated as viral polymerase begins all RNA synthesis at the 3' end of the genome and transcribes the gene

Table 1

Detection of porcine ephrin B2 mRNA in NiV infected and uninfected monocytes and enriched lymphocytes cells 48 hrs post inoculation.

Cell subsets	Untreated Uninfected cells	NiV infected cells
Monocytes	-	+
CD6+ T cells	+	+
CD8+ T cells	+	+
CD4+ T cells	+	+
CD21+ B cells	-	+
CD16+ NK cells	-	+

(+) indicates mRNA of ephrin B2 was detected **(-)** indicates mRNA of ephrin B2 was undetectable

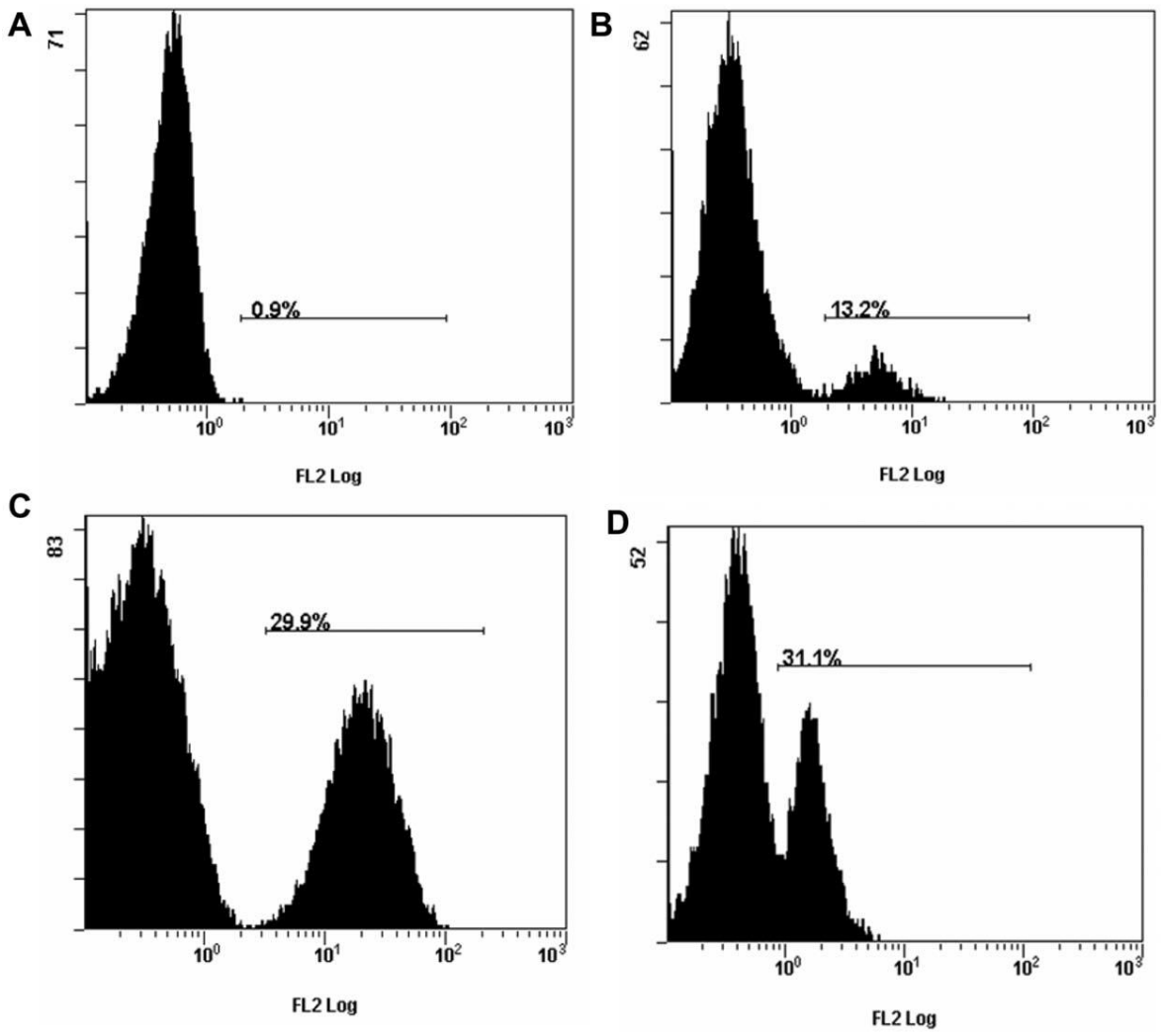

Figure 20 Intracellular staining for NiV nucleocapsid N or non-structural C protein in T cells. The cells were sorted based on the presence of CD4, CD6 or CD3CD8 markers, and infected with NiV at 0.1 MOI. Representative flow cytometry histograms were selected from three independent experiments. (**A)** Lack of intracellular staining for NiV non-structural C protein in CD4+ T cells at 24 hrs post inoculation. (**B)** Intracellular staining for NiV C protein in CD3+CD8+ T cells at 24 hrs post inoculation. At 48 hrs post inoculation/infection about 30% of the CD3+CD8+ stained internally for the NiV C protein (**D**), confirmed by about 30% of CD6+ T cells stained internally for the NiV nucleocapsid N protein (**C**).

into mRNA sequentially thereby producing a large amount of N protein (40) compared to the C protein which is downstream and initiates at P gene ORF (52). Therefore, NiV infected cells produce substantially lower amount of C protein compared to the N protein, making the detection less sensitive (94). We were able to narrow the infection of the CD6+ lymphocytes to CD4-CD8+ T lymphocytes by using triple staining for NiV antigen, CD8 marker, and CD4 marker (Fig. 21). At 24 hpi, the CD6+CD8+ stained for NiV antigen at 50% (Fig. 21A) compared to only 3% of CD6+CD4+ cells (Fig. 21B). And of the 50% of the CD6+CD8+ that stained for NiV antigen about 90% were positive for NiV antigen (Fig. 21C). The dot plots from flow cytometry analysis further indicated that CD4+CD8- cells, and CD4-CD8- cells appeared to be non-permissive to NiV infection.

It should be noted that numerous controls were used for this flow cytometry analysis to eliminate any false positive results. The controls included: isotypes for each surface marker with or without NiV antiserum, isotypes for each surface markers only with secondary antibody, and non-infected sorted CD6+ T cells were also stained with the same procedures as with the NiV infected CD6+ T cells. The non-infected CD6+ T stained with NiV polyclonal guinea pig antiserum and CD4/CD8 surface markers were negative for NiV antigen.

3.10 Real time RT-PCR mRNA cytokine expression

Based on cell culture images, NiV infection appeared to activate the T lymphocytes. Generally, formation of the cell clusters is considered to be a phenotypic characteristic of

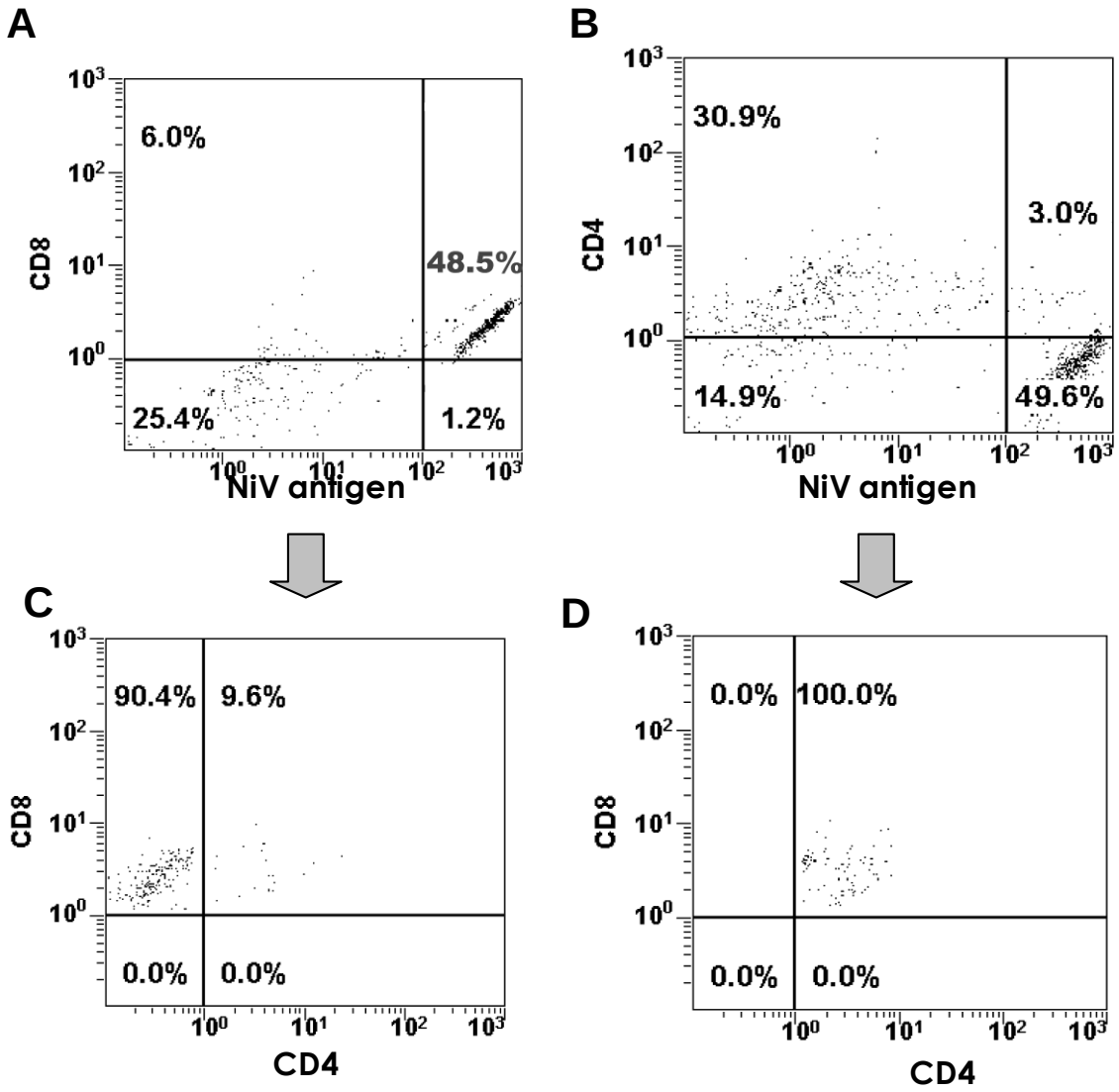

Figure 21 NiV infected CD6+ T cells triple stained for CD4 and CD8 markers, and NiV antigen. Dot plot of flow cytometry analysis of NiV infected CD6+ T cells, triple stained with monoclonal antibodies against CD4 and CD8 markers, and NiV polyclonal guinea pig antiserum 24 hrs post infection. T cells gated for CD8+ and NiV antigen (**A**). T cells gated for CD4+ and NiV staining (**B**). Analysis of cells positively stained for CD8+ and NiV antigen (**C**). Analysis of cells positively stained for CD4+ and NiV antigen (**D**).

activation (Fig. 22 A-D). To confirm the observation, changes in levels of selected cytokines were determined by semi-quantitative real-time RT-PCR in CD6+ cells. IFN γ was selected for this study since in pigs active T lymphocytes secrete IFN γ and IFN γ is important in viral clearance in pigs (249, 250). Both IL-8 and TNF α were selected because they are potent chemotactic factors expressed by activated T cells (251) and would offer explanation as to why there is a formation of the cell clusters. In addition, both IL-8 and TNF α might play a role in the recruitment of target cells to the sites of viral replication in the lymph nodes. Furthermore, TNFα provides signals involved in the cellular control of programmed cell death potentially affecting bystander cells (252). In addition, it would be of interest to also evaluate IFN α (antiviral cytokine) in activated porcine T lymphocytes as other several porcine viruses stimulate lower IFN α production leading to inadequate stimulation of antiviral immune responses (253). Hence, the relative levels of mRNA expression of IL-8, TNF α, IFN α and IFN γ were selected and are summarized in Figure 22E.

The optimization results for mRNA cytokine expression RT-PCR are summarized in the appendix 6.2. NiV infected cells slightly (less than one-fold) upregulated expression of IFN γ and IL-8 in non-stimulated cells. Significant upregulation of IL-8 expression was however observed in stimulated cells infected with NiV (6 fold). Upregulation of IFN γ and TNF α greater than one-fold was observed in stimulated, NiV infected cells. On the other hand, infection of lymphocytes with NiV appeared to down-regulate IFN α mRNA, both in non-stimulated and stimulated cells, when compared to the constitutive expression levels of IFN α in non-stimulated T lymphocytes or PMA/ionomycin activated T cells, respectively.

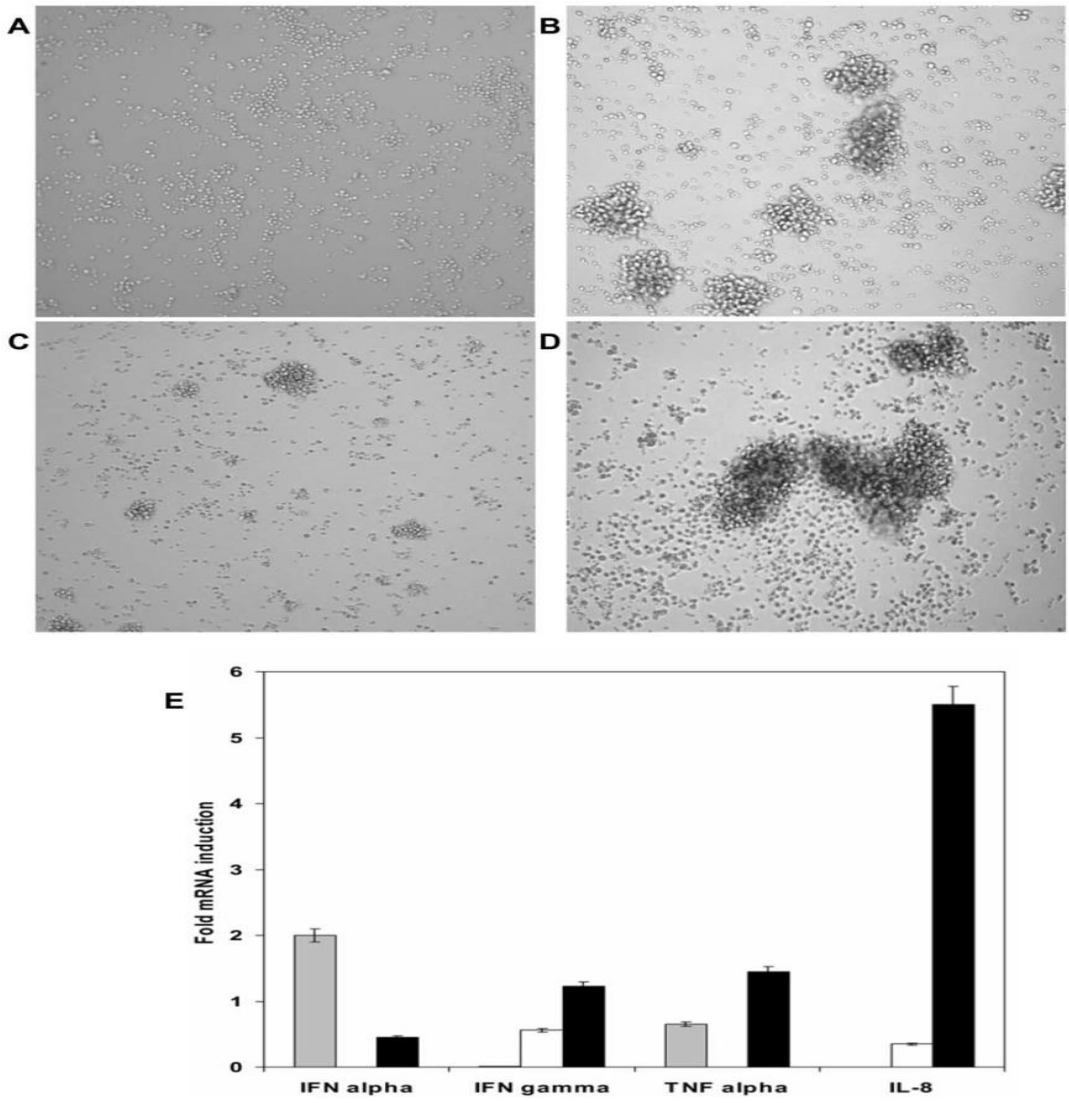

Figure 22 Stimulation of T cells with PMA/ionomycin and/or NiV infection. Figs. **22A-22D** illustrate changes in cell appearance of the CD6+ T cells after 18 hrs post infection with NiV at 0.1 MOI. Formation of cell clusters in NiV infected cells suggests that the infection stimulates T lymphocytes. Appearance of non-stimulated T cells (Fig.22A) in comparison to NiV infected T cells (**B**) and the PMA/ionomycin stimulated cells (**C**). NiV infected PMA/ionomycin activated T cells (**D**). **E** Cytokine RNA profiles were determined 48 hrs post incubation/ infection by quantitative RT-PCR. Gray columns represent ratio of PMA/ionomycin activated cells and non-stimulated T cells; white columns represent ratio of NiV infected cells compare to non-stimulated cells; black columns represent ratio of infected PMA/ionomycin activated cells compared to PMA/ionomycin activated T cells.

3.11 Effect of NiV infection *in vitro* on PBMC

Effect of NiV infection on lymphocyte population frequencies was studied in the context of PBMC to approximate the *in vivo* situation, allowing for interaction (cell cross-talk) of several cell populations. We were able to follow up the lymphocyte staining for CD4 or CD8 marker (Fig. 8B). The mock infected PBMC controls were examined for percent change of CD4 and CD8 subpopulations at both 24 hrs (Fig. 23 A/B) and 48 hrs; there was no significant changes in these populations compared to NiV infected PBMC. In the infected cells at 24 hrs post infection, the number of CD8+ cells decreased from about 40% to 30% and down to 20% at 48 hrs post infection, with notable reduction of the CD8+hi cytolytic T cells (Fig. 23 A-C). Almost no change in percentage of the CD4+ population was observed at 24 hrs post inoculation (Fig. 23E), while an apparent decrease in CD4+ was observed at 48 hrs post infection (Fig. 23F). The drop in CD4+ cells could be attributed to the decrease in CD4+CD8+ cells (mostly memory helper T cells); however the significant drop at 48 hrs due to bystander cell death of the CD4+CD8- cells cannot be excluded, considering the *in vivo* data below.

3.12 Effect of NiV infection *in vivo* on PBMC

Low levels of NiV RNA were detected in PBMC from 2 to 7 days post inoculation by real-time RT-PCR targeting the N gene, corresponding with previously published data on low level NiV detection in serum, PBMC or whole blood in swine (125, 136, 137). Although it was difficult to detect the virus in peripheral blood of NiV infected piglets by flow cytometry, and total white blood cell count was considered to be within the normal range (data not shown), an effect on population frequencies of lymphocytes was observed using double staining for CD4 and CD8 surface markers. Since, CD4+ T lymphocytes aid in the development of the humoral

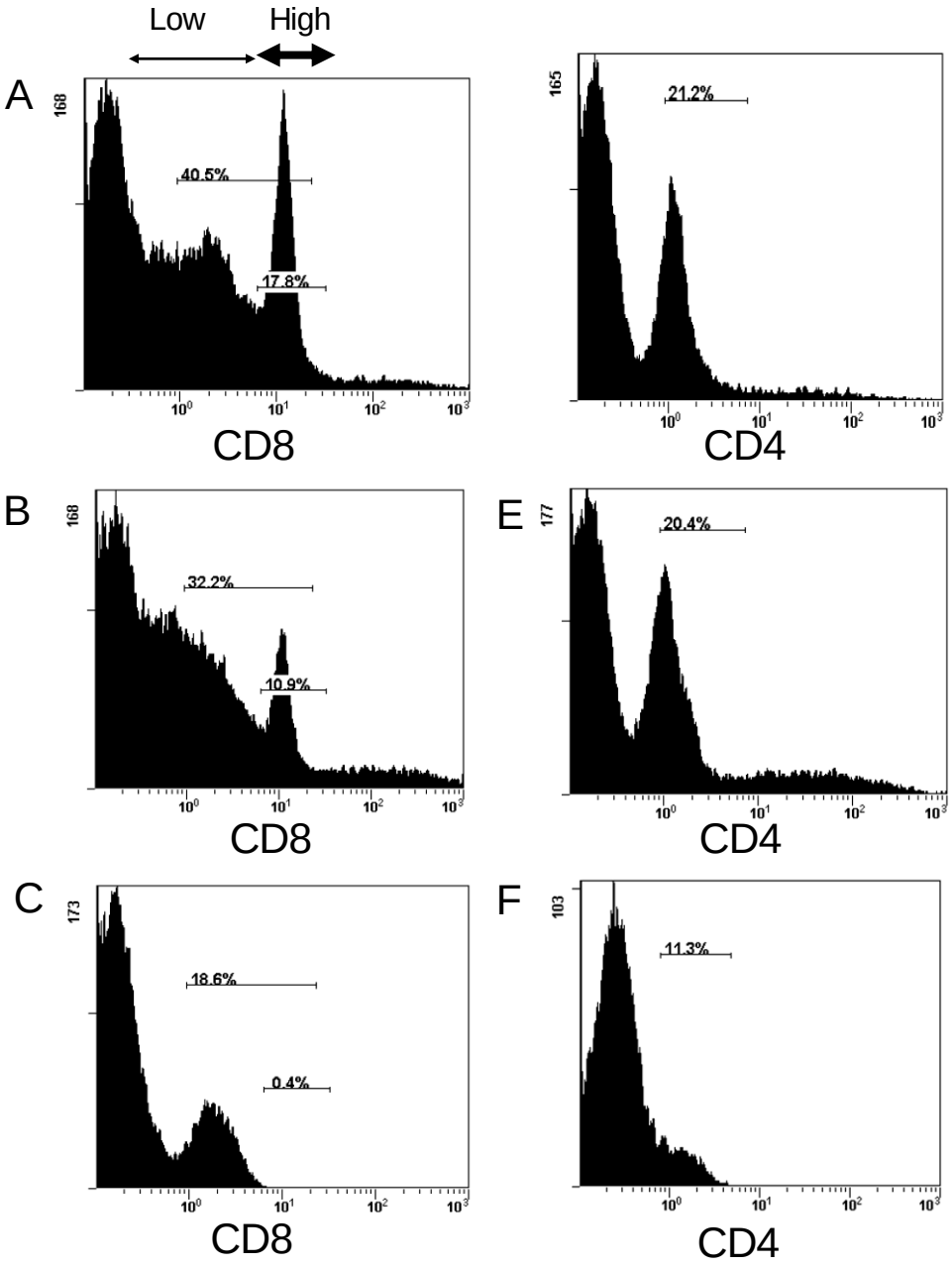

Figure 23 Changes in population frequencies of CD8+ and CD4+ cells following NiV *in vitro* inoculation of PBMC. (A) PBMC control after 24 hrs incubation stained for CD8 marker. Thin arrow on top of the figure indicates CD8 $\alpha\beta^{lo}$ T cells. The highest intensity peak corresponds to CD8 $\alpha\beta^{hi}$ T cells (cytolytic T cells) indicated by the bold arrow. (**B)** NiV infected PBMC stained for CD8 marker at 24 hrs post inoculation. (**C)** At 48 hrs post inoculation, the peak corresponding with CD8 $\alpha\beta^{hi}$ T cells was absent, and the proportion of CD8+ cells decreased from 40% to about 20%. Fig. 23D PBMC control stained for the CD4 marker after 24 hrs post incubation. (**E)** Cells inoculated with NiV stained at 24 hrs post inoculation for CD4 marker. (**F)** Decrease in CD4+ cells from 20% in the control uninfected PBMC to about 10% at 48 hrs post inoculation with NiV.

response, the observation of this subpopulation would of great importance in a rapid production of virus-specific antibodies necessary for full protective anti-NiV response. In this work it was identified that NiV infects CD8+ subpopulation therefore it necessary to evaluate this cell population in NiV infected in pigs. The effect on population frequencies of lymphocytes was observed using double staining for CD4 and CD8 surface markers.

At two days post inoculation a significant drop ($p>0.05$) in CD4-CD8+ lymphocytes was observed in PBMC collected from all 6 infected pigs compared to 4 control animals (Fig. 24A). At the same time point, the CD4+CD8- population circulating in peripheral blood increased significantly ($p>0.05$) when evaluating all infected piglets versus negative control pigs (Fig. 24 B). At 4 dpi, both subpopulations returned close to basal levels. The population frequency of double positive (CD4+CD8+) T cells showed a low gradual decrease following the inoculation with NiV but it was not statistically significant ($p< 0.05$) compared to control animals and the pre-infection status (Fig. 24C).

Interesting trends appeared in population frequencies for piglets which had to be euthanized during the first week post inoculation compared to piglets which survived past 7 dpi, and were euthanized at 28 dpi (end of the study). In piglets requiring early euthanasia, the CD4-CD8+ T cells dropped again at day 6/7, in contrast to the survivors, where the CD4-CD8+ T cells returned to pre-infection levels (Fig. 25A). Dramatic differences in population frequency trend between survivors and non-survivors were observed for the CD4+CD8- lymphocytes. While there was a significant increase of CD4+CD8- T helper cells in survivors at 2 dpi, returning to normal by 7 dpi, piglets which had to be euthanized had no upregulation of CD4+CD8- T cells, and the population frequency continued to decrease until the end point at 7 dpi (Fig. 25B).

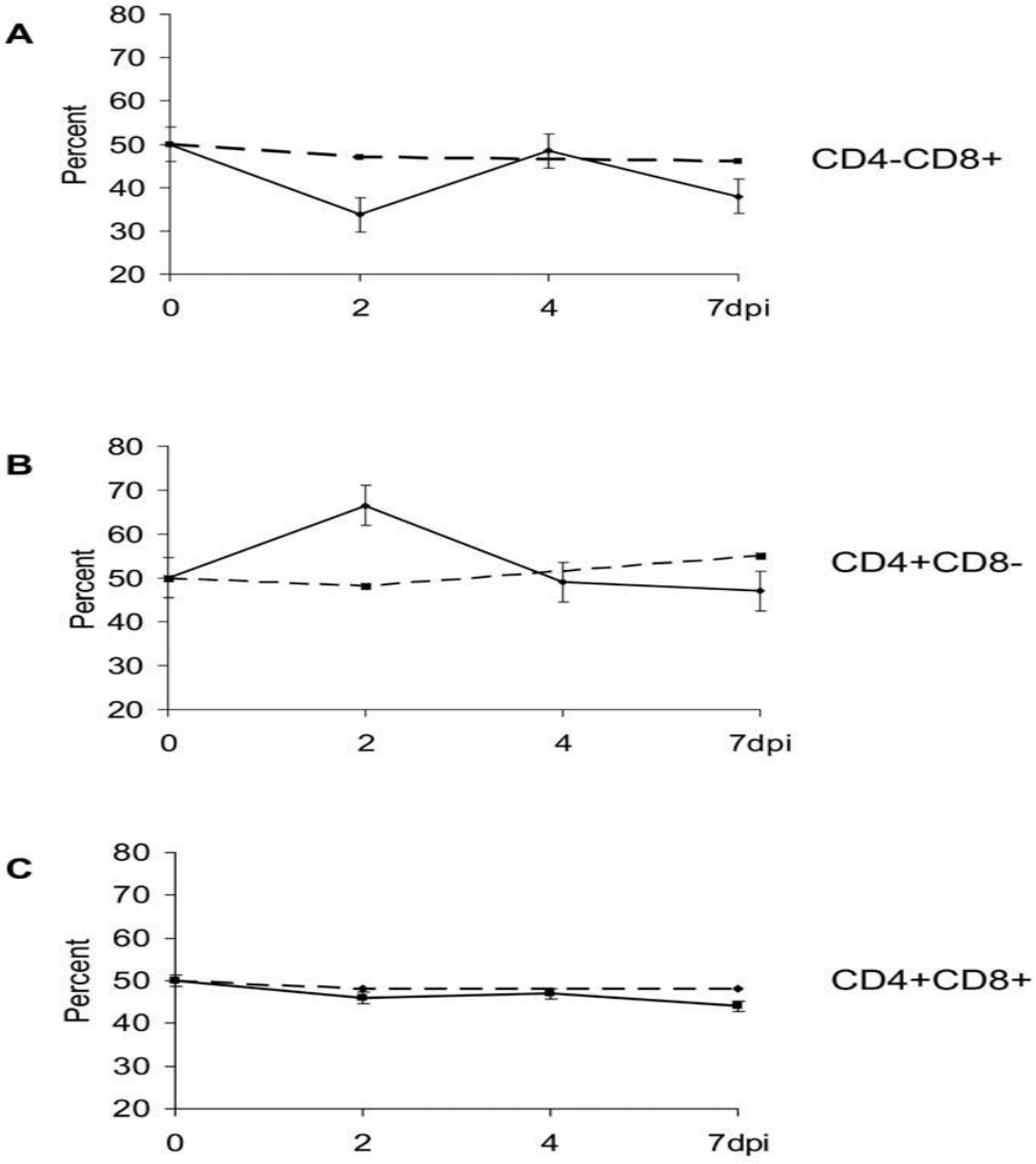

Figure 24 T cell subpopulation frequencies in NiV infected pigs during the acute phase of the infection. Changes in CD4CD8 cell subpopulation frequencies in PBMC of pigs infected with NiV based on flow cytometry analysis. The values obtained at 0 dpi were arbitrarily set at 50%. The data (mean and standard error) are based on six infected (solid line) and 4 control (dashed line) animals. Notably, significant changes with opposite trends were observed for CD4-CD8+ T cells (**A**), and CD4+CD8- T cells (**B**). The changes in CD4+CD8+ T cell frequency, although statistically significant, were only minor, perhaps with slight decline toward the 7 dpi in the infected piglets compared to the controls **(C).**

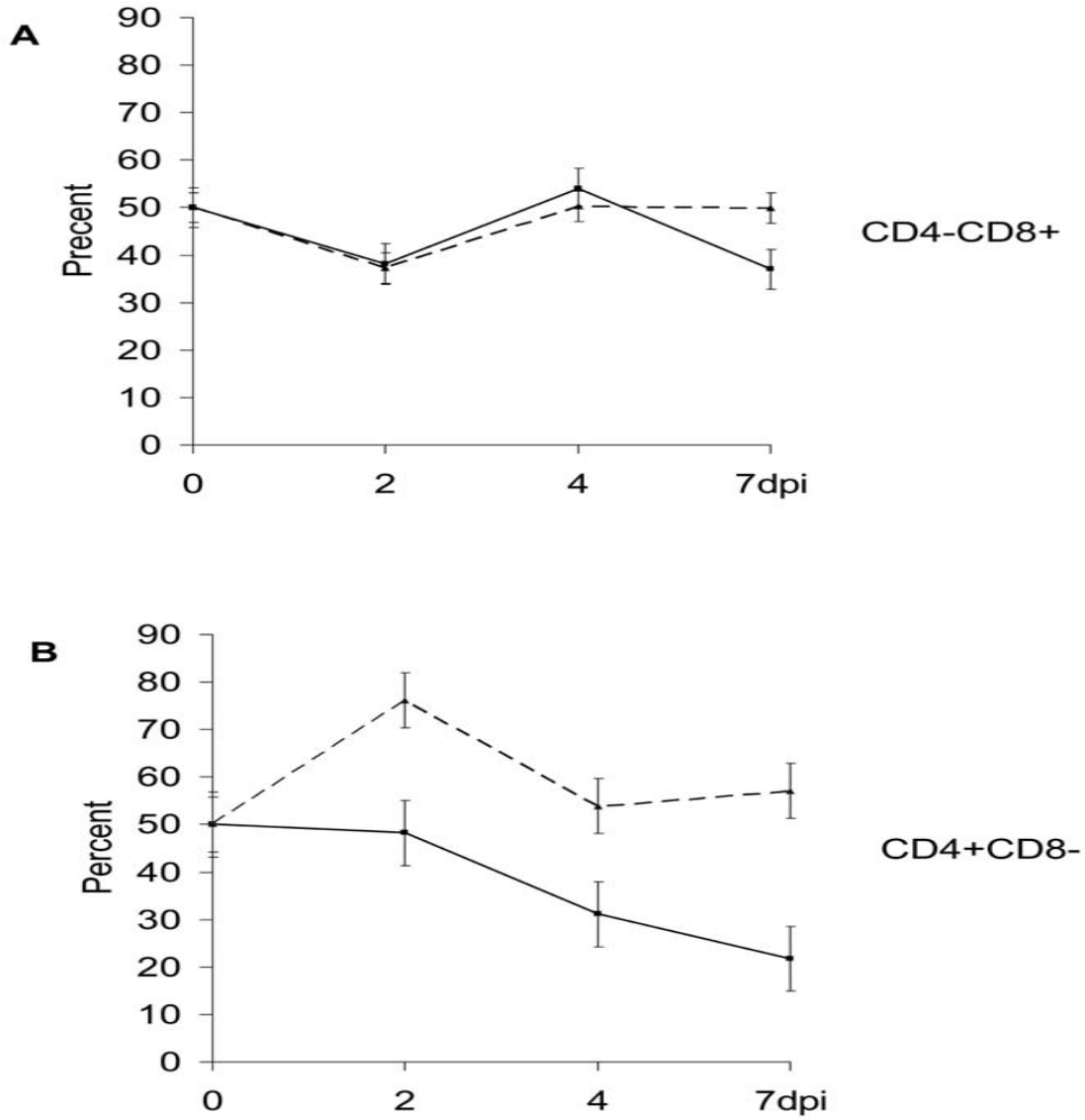

Figure 25 Comparison of T cell subpopulations between pigs that died during acute infection versus survivors. The differences in CD4+ and CD8+ cell subpopulations during the acute infection with NiV up to 7 dpi. Values, based on flow cytometry analysis, were arbitrarily set as 50% at 0 dpi. The solid line represents piglets that died at 7 dpi, the dashed line represents the survivors. Standard Error is represented as error bars for 2 pigs per each group/mean value. Survivors had significantly higher values for the CD4-CD8+ (**A**) at 7 dpi compare to the piglets which died at that day. Marked difference was observed for the CD4+CD8- T lymphocytes (**B**). The down-trend starting almost immediately post infection for this cell subpopulation in pigs that died due to NiV infection was especially pronounced. In contrast, there was an up-regulation of CD4+CD8- T helper cells at 2 dpi in the survivors.

4.0 Discussion

In pigs, the mode of transmission is suspected to be airborne or due to direct exposure to NiV infected pigs given that NiV is shed in oronasal secretions (5, 134,137). The virus can enter through the nostrils and mouth into the oral-nasal cavities (136). The oronasal cavities are lined with mucosal surfaces composed of epithelium with loose lymphocytes and monocytic like cells. This area is rich in infiltrating lymphocytes in the form of isolated lymphatic nodules (submandibular) and tonsil (254). The experimental work presented here showed that NiV can productively infect porcine monocytes, NK cells and CD4-CD8+ T lymphocytes. The lymphocytes and monocytes present in the oronasal cavity would initiate replication at this port of virus entry.

NiV enters permissible cells either via macropinocytosis (111) or fusion with the plasma membrane (82, 92, 112) following viral attachment to host cellular receptors. We showed that the MAPK signaling pathways are involved in viral entry depending on the cell type and mode of entry. The rapid activation of ERK pathway in IPAM is associated with macropinocytosis (111) whereas a slow activation of the ERK pathway in swine fibroblasts is associated with membrane fusion (256). In addition, the early and strong activation of the p38 pathway in IPAM would be correlated more to rearrangement and could be needed for macropinocytosis (255), unlike the lack of phosphorylation of p38 in swine fibroblasts.

Once NiV has entered the cell, viral proteins are generated, in turn initiating and/or hindering innate intracellular signaling cascades to promote viral replication. In NiV infected porcine cell lines; the STAT signaling pathways were likely hindered by NiV non-structural proteins but not completely inactivating the antiviral immune response, as the p38 MAPK pathway was activated and found to be required for viral replication. Following replication and

assembly of new virions, the virus will egress from the cells. In the oral-nasal cavity, initial replication in immune cells leads to infection of the epithelial cell layers. NiV replication and egress from the infected epithelium leads to disruption of the basement membrane allowing for transmigration of NiV to the lymphatic vascular system (65). NiV infected lymphocytes and monocytes situated in the porcine oronasal cavity along with the newly replicated virus would be taken up by the local lymphatic vascular system. In the lymphatic system, NiV and NiV infected immune cells can migrate through lymph nodes where they encounter more immune cells as well enter the bloodstream via lymphatic vessels allowing for viremic spread of NiV in the porcine host. By entering the bloodstream NiV escapes from local innate immune defenses in tissues. In addition, direct infection of CD4-CD8+ T cells likely contributes to viral pathogenesis. We observed a decrease in CD4-CD8+ cell population frequency in NiV infected pigs at 2 dpi. The CD4- CD8+ T cells are characterized in pigs as cytotoxic T cells and their decrease would affect the clearance of virus infected cells (246). As the p38 MAPK activation is needed for NiV replication in cells, the activation of this pathway would induce rapid apoptosis of CD8+ T cells (257) and pro-inflammatory cytokines production (181-184). In NiV infected T cells, cytokines such as TNF α and IL-8 were upregulated. IL-8 and TNF α are potent chemotactic factors expressed by activated T cells as a result may recruit more target cells to the sites of infection. Furthermore, TNF α provides signals involved in the cellular control of programmed cell death potentially affecting bystander cells such as the CD4+CD8- T cells which are not infected by NiV. In piglets which succumbed to NiV infection, there was a dramatic decrease in the CD4+CD8- T cell subset which can also hamper the development of humoral immunity. Figure 26A shows a schematic diagram of NiV dissemination from initial site of virus entry in the porcine host and Fig. 26B shows the effect on the T cell subpopulations in NiV infected pigs.

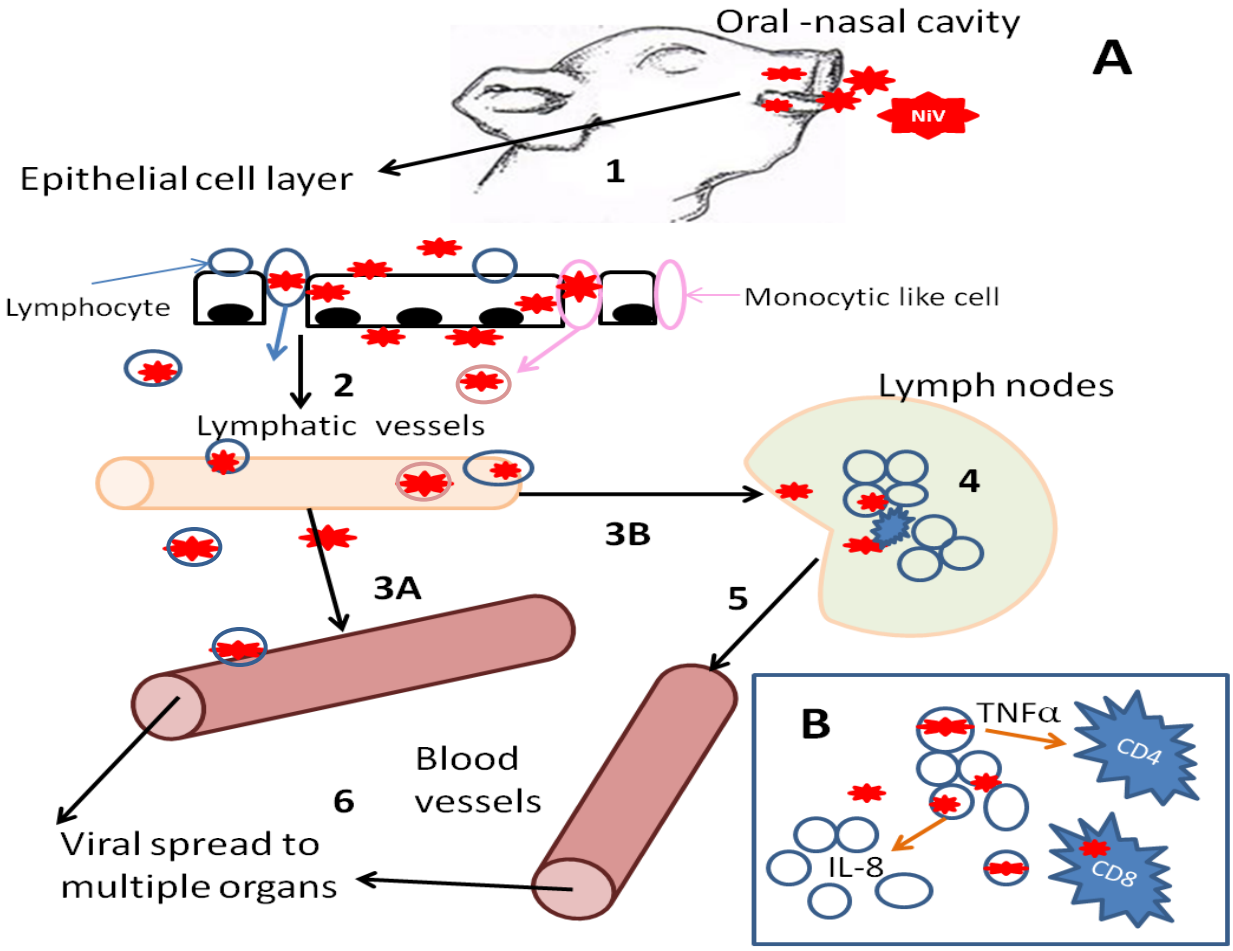

Figure 26A The dissemination of NiV in porcine host (1) Nipah virus enters the oronasal cavity via nostrils and mouth **(2)** Initial replication begins in lymphocytes and monocytic like cells leading to infection of the epithelium and disruption of the basement membrane allowing for the transmigration of NiV and NiV infected lymphocytes to enter the lymphatic vessels **(3A)** Lymphatic capillaries are considerably more permeable than circulatory system capillaries, facilitating virus entry. As the lymphatic vessels ultimately join with the venous system, virus particles in lymph have free access to the bloodstream. (**3B**) In the lymphatic system, NiV and NiV infected immune cells pass through lymph nodes. (**4**) In lymph node, NiV and NiV infected lymphocytes encounter more immune cells. **(5)** The infected lymphocytes also migrate away from the local lymph node to distant parts of the circulatory system. (**6**) Once in the blood, NiV can access almost every tissue and organ in the hosts. **B. NiV effect on T cell populations in porcine blood and lymph nodes.** The need for p38 MAPK activation in NiV infected T cells induces apoptosis of CD8+ T cells and pro-inflammatory cytokines production. NiV infected T cells upregulate TNF α and IL-8. IL-8 is chemotactic factor that can recruit more target cells to the sites of infection. TNF α provides signals involved in the cellular control of apoptosis potentially affecting bystander cells such as the CD4+ T cells which are not infected by NiV. The blue stars represents apoptosis of lymphocytes.

Hence, in this thesis work, there is indication that NiV modulates the porcine host immune response by multiple pathways, consequently delaying the development of antibodies and clearance of virus infected cells to facilitate NiV pathogenesis by not protecting susceptible tissues in the host and allowing for the progression of the infection.

4.1 Innate Immune Response

The first hypothesis in this thesis was that IFN induced signaling pathways are not completely inhibited by NiV in infected porcine cells compared to human cells, and an antiviral state can be more readily established.

There was no published work on IFN signaling pathways or on IFN mediated antiviral state in NiV infected cells at the onset of the thesis research. Hence, the first objective was to determine whether a difference exists in NiV non-structural proteins (V and W) ability to interact with the STAT1 proteins (part of the JAK-STAT pathway) between selected human and porcine cell types. The approach was via co-localization studies using confocal microscopy, and employing antibodies with previously confirmed specificity. In addition to the fibroblast cell lines, the porcine monocytic-like cell line (IPAM) was included in this work to better understand the role of the innate antiviral response in immune cells. The IPAM cell line is an excellent *in vitro* system to directly examine the host-virus interactions at the cellular level, since there is no influence of other host immune cells.

The results were similar in NiV infected IPAM (Fig. 9) and the fibroblast cell lines from both species, showing that the co-localization of NiV accessory proteins with STAT1 in these selected cells lines was only in the cytoplasm. These findings are in agreement with another live NiV infection study reporting intracellular co-localization of NiV W proteins with STAT1 only

in the cytoplasm of human endothelial cells unlike in M17 neuronal cells where NiV W also localized to the nucleus (95).

This set of data (Fig. 9) indicated that NiV may successfully block/evade the establishment of antiviral state via the STAT-1 signaling pathway in the infected cells. There was however no difference observed between cells of porcine and human origin in NiV ability to interact with the STAT1 proteins.

Although, co-localization of NiV V and W proteins with the STAT1 was confirmed in IPAM, MRC5 and ST cells, it was still unknown if a binding of the V and W proteins to STAT1 leads to a complete block of the STAT-1 signaling pathway and to a block of activation of antiviral state, or an alternative IFN signaling pathway may compensate for this block in the selected cells. Second objective was then to determine if an antiviral state is activated in porcine versus human cells during the course of NiV infection.

Phosphorylation of eIF2α was chosen as a read out system. The increased levels of eIF2α phosphorylation would indicate an activated antiviral state in NiV infected cells, as this elongation factor is phosphorylated by protein kinase R (PKR), a well-characterized and powerful antiviral molecule activated by IFN. Increase in phosphorylation of eIF2α results in a block of protein expression and apoptosis (192, 258). Hence, the phosphorylation levels of eIF2α are an important check point in antiviral defence for host antiviral response (193,197).

An increase in phosphorylation of eIF2α was detected in all three examined cell lines infected with NiV but not in cells treated with gamma-irradiated NiV, indicating that viral replication is required for the phosphorylation of eIF2α (Fig. 10). In porcine fibroblast (ST) cells, the increased levels of eIF2α phosphorylation were detected at 6 hpi, whereas the human fibroblast cell line (MRC5) showed significant eIF2α phosphorylation after 8 hpi. Both IPAM

and MRC5 cells inoculated with NiV had a longer lag time before increased eIF2α phosphorylation than the porcine fibroblasts (ST) (Fig. 10). Although, we observed differences in the onset of phosphorylation, high levels of eIF2α phosphorylation were detected in both human and porcine cells at the last time points collected (Fig. 10). This set of data suggested that NiV activates an antiviral state in ST, MRC5 and IPAM cells. Virtue *et al.*, (190) made a similar observation by detecting the upregulation of interferon signaling genes (ISG 54 and ISG 56) in HEp-2 cells indicating that the IFN signaling was not effectively blocked in the NiV infected cells, and the activation of an antiviral state was cell-type dependent. There was no further examination of the block of NiV replication in Virtue (190) study.

In summary both set of data would indicate that the activation of antiviral state is cell type specific and may not be related to the species. The detected increase in eIF2α phosphorylation indicated that the block of STAT1 shuttling through NiV V and W proteins was either incomplete, and/or alternative IFN signaling pathway was activated to establish the antiviral state.

The third objective under the Hypothesis #1 was to investigate activation of an alternative IFN-signaling pathway. Two IFN signaling pathways, the JAK-STAT and the mitogen activated protein kinase (MAPK) signaling pathways play an essential role in the innate immune response to viral infection (259, 260). Accordingly, both the p38 MAP kinase and STAT factors are critical for regulation of IFN mediated gene transcription and cellular antiviral responses generated by IFN α/ß (261). The p38 MAP kinase pathway is essential for type I dependent gene transcription, but it does not interfere with modification of serine/tyrosine phosphorylation or nuclear translocation of STATS (242). The p38 MAPK pathway compensates for block in STATs or cooperates with the JAK-STAT signaling pathway, resulting in an antiviral state as

well (226, 227, 242). In addition, there was an indication that this pathway may be functional from cytokine induction studies. IL-8 transcription was not hindered in NiV infected porcine T cells (data presented in the thesis). Since the p38 MAPK pathway regulates the transcription of IL-8 (262) this suggests that this pathway is functional during NiV infections.

To determine whether the p38 MAPK IFN-signaling pathway is activated in NiV infected cells, the changes in phosphorylation levels of p38 MAPK were determined in NiV infected MRC5, ST and IPAM cells at set time points.

In NiV inoculated IPAM and ST cells, the time-profile of p38 MAPK phosphorylation was similar, with activation early post inoculation (Fig. 12), then a decrease at 12 hpi followed by a dramatic (double) increase at 24 hpi. Although in ST cells the phosphorylation was less pronounced during all the time points (Fig. 12).

As indicated in Figure 12 the overall trend of p38 MAPK phosphorylation in MRC5 cells is higher at earlier time points but shows similarity in phosphorylation to ST cells at the final time points. A sustained phosphorylation of p38 MAPK was evident in both human and porcine cell lines at the 24 and 48 hpi, the levels of p38 MAPK phosphorylation peaked in both human and porcine cells and remained high at 48 hpi (Fig.12). In MRC5 and IPAM cells the activation of the p38 MAPK pathway preceded the phosphorylation of eIF2α (Fig. 11), implying that this pathway may be involved in establishment of transient antiviral state. The situation in ST cells appeared to be more complicated with the eIF2α being constitutively expressed.

In summary, these findings provide evidence that the p38 MAPK pathway is functional in NiV infected MRC5, ST and IPAM cells, and is potentially an alternative pathway to the JAK-STAT pathway to establish an antiviral state in NiV infected cells. Inoculation with gamma-irradiated NiV did not result in significant levels of p38 MAPK phosphorylation in any of the

cell lines examined, suggesting that virus replication is required for activation of this pathway.

To confirm that the activation of p38 MAPK pathway leads to an antiviral state, we hypothesized, that blocking this pathway would lead to an increase in virus yield/replication of NiV. The importance of the activation of p38 MAPK in NiV replication was addressed through the use of p38 MAPK inhibitor (SB202190). As illustrated in Fig. 14, the inhibition of p38 MAPK signaling pathway surprisingly resulted in a significant and clear reduction of viral protein expressions and viral titers. The NiV-P expression and infectious titers in porcine cell lines and especially in IPAM cells appeared to be more affected by the p38 inhibitor compared to the human MRC5 cells (Fig.14). The presence of p38 inhibitor reduced viral progeny in a dose dependent manner.

Taken together, these results indicate that although NiV replication activated the p38 pathway usually involved in development of antiviral state, and the phosphorylation of eIF2α as a read-out for antiviral state, NiV replication was not inhibited. In contrary, the p38 MAPK pathway activation was required for virus replication.

This has been observed for some other viruses such as HIV, RSV, Hepatitis B or influenza; although in influenza infected cells the eIF2α phosphorylation is blocked (170, 263-265).

The block of NiV replication due to inhibition of p38 MAPK pathway may occur on several levels: at virus entry, at phosphorylation of viral proteins, or at fusion protein maturation. The block at the level of phosphorylation processing of viral proteins can occur with the phosphorylation of the N protein as phosphorylation of NiV-N plays an important role in virus transcription and replication (59) as well as P and V can be phosphorylated by cellular kinases (62, 266).

As p38 MAPK kinase influences the regulation of the Rab5 (267, 268), an enzyme shown to be activated in early endosomal compartments (90). The p38 MAPK may be also involved at the level of proteolytic activation of the F protein which requires endocytic trafficking from the plasma membrane and recycling the mature F protein back to the plasma membrane for virion assembly (83).

At virus entry, p38 MAPK may be required for internalization by the activation of effectors necessary for endosomal processing (such as macropinocytosis or endocytosis). Different kinetics of phosphorylation of p38 MAPK in MRC5, ST and IPAM cells suggested a cell type dependent activation of this pathway. In macrophages and DCs, p38 MAPK is needed for functional macropinocytosis by regulating small GTPase (Rab5) (255, 269) which may explain why IPAM cells were the most affected cell line. The significant early activation of p38 MAPK at 1 hpi for IPAM and MRC5 correlates to the ERK data (see below) where more intense phosphorylation suggests a trigger of stress response possibly due to rearrangement of cytoskeleton (267). The involvement of the p38 MAPK pathway has been observed with enveloped viruses like influenza and RSV, also a paramyxovirus, to facilitate endocytic- like uptake and entry (170). The low p38 phosphorylation in the ST cells compared to the IPAM and MRC5 cells may therefore indicate a different mode of entry. Experiments directly addressing virus entry and mechanisms of internalization would be however required to elucidate a specific mode of entry into respective cell lines.

To further elucidate the importance of MAPK signaling pathway, the ERK pathway was examined as it could be associated with virus replication along with p38 MAPK (170, 176, 270). Activation of the ERK 1/2 pathway was also of interest because of the receptor specificity of NiV for ephrin B2 and B3. Stimulation from Eph to ephrin is known as reverse signaling and

was demonstrated to be accompanied with activation of ERK signaling (76,111). Nipah virus G protein binds to the same region of ephrin B2 and B3 that mediates high affinity to EphB receptors (75) and the binding of the virus to ephrins may result in similar effect: activation of the ERK pathway connected with macropinocytosis and internalization of NiV as proposed by Pernet *et al.* (111) and different kinetics of ERK phosphorylation associated with viral fusion to the cell membrane (256). Alternatively, in other cell lines increased levels of ERK phosphorylation may also indicate NiV involvement with endocytosis (271).

Based on indications from studies of p38 MAPK activation in NiV infected cells, we hypothesized that the phosphorylation of ERK will be accordingly different in different cell types, reflecting the type of entry.

Both human fibroblasts (MRC5) and porcine monocytic-like cells (IPAM) exhibited a robust phosphorylation of ERK 1/2 within 15 minutes of live NiV or gamma-irradiated NiV inoculation (Fig.15C). The rapid activation of ERK pathway may indicate macropinocytosis or endocytosis as a mode of NiV entry into MRC5 and IPAM cells. This would be in agreement with study by Pernet *et al.* (111) who indicated that attachment of NiV G to ephrin B results in phosphorylation of specific tyrosine kinases leading to viral entry via macropinocytosis in CHO-K1 cells.

A delay in ERK phosphorylation was observed in ST cells either infected with NiV or treated with gamma-irradiated NiV (Fig. 15C). The different profile of ERK phosphorylation in ST cells compared to IPAM and MRC5 cells could be due to differences in receptor numbers (272) and/or mode of the entry (256). Sharma *et al.* (256) study suggests that membrane fusion is a slow process where the levels of ERK phosphorylation peak after one hour post stimulation with low levels of ERK activation as observed with NiV infected ST cells (Fig. 15). It appears

that despite using the same receptor, NiV is internalized into ST cells by direct cell membrane fusion, proposed by Tamin *et al.*, Aguilar *et al.*, Bossart *et al.* (82, 92,112).

In NiV infected cells two phases in ERK 1/2 phosphorylation were observed. The "early" one described above which declined after initial activation, and increased again after 12 hpi, only in cell lines inoculated with live NiV (Fig. 15C). As NiV replication cycle takes approximately 8-12 hours, this may further support the notion that the ERK pathway is activated as a result of virus entry into the cells. It cannot be excluded that this late and sustained phosphorylation of ERK 1/2 may also depend on viral gene expression and may be induced by exposure to a viral protein, similar to reports with HIV-1 and RSV (178, 273).

The next step of the study was to determine if inhibition of the ERK pathway inhibited NiV replication. There was no difference NiV-P expression in MRC5, ST or IPAM cells with concentrations of 1 and 10 μM. Differences in the reduction of virus replication were observed only with the concentration of the inhibitor at 20 μM (Fig.17). Our results are comparable with results reported for other paramyxoviruses (MeV and RSV) where only at a high dose of ERK inhibitor (UO126) had a significant effect at the efficiency of viral replication (178, 177). The UO126 inhibitor blocks the pathway upstream of ERK 1/2 kinase via MEK-1 and does not directly affect the ERK 1/2 kinase, while inhibitor (FR180204) in this thesis work directly affects ERK 1/2 kinase (245). Differences of viral production were observed in a cell type dependent manner (Fig. 17). It would be interesting to examine other cell types for example brain microvascular endothelia, where ERK activation is important for HIV entry by macropinocytosis (270) or neurons. Additional experiments directly addressing virus entry and mechanisms of internalization would be required to further elucidate a specific mode of entry into respective cell lines.

In summary, data presented in this thesis prove the first part of the hypothesis: IFN induced signaling pathways are not completely inhibited by NiV in infected porcine cells and an antiviral state based on gene activation and eIF2α phosphorylation can be established. Second part of our original hypothesis that there will be difference in this respect between human and porcine cells however did not hold true, as no differences was linked to species of origin. Although there was an evidence for the p38 MAPK pathway, one of the IFN signaling pathways, being activated and the antiviral state being induced, reduction in NiV replication and virus yield were not observed. Interestingly, the p38 pathway was indispensable for NiV replication in both porcine and human cell lines selected for this thesis work. Thus the established antiviral state was not found to be effective in NiV infected cells, and the cells under study (MRC5, IPAM, ST) were not able to control or suppress NiV replication.

The modulation of the host antiviral system is a fine balance between negative and positive regulation of signaling pathways potentially exerted by NiV replication leading to a successful host infection. This part of the thesis work showed that multiple signaling pathways need to be explored to better understand the pathogenesis of NiV infection in a cell dependent manner. In addition, this part of the thesis work provide a potential new antiviral therapy with the use of p38 MAPK inhibitor as opposed to the ribravirin therapy which was shown to be unsuccessful in other some small animal models of NiV infection (128, 213) and humans (211).

4.2. Cell Mediated Immune Response

The innate and adaptive immunity are linked by induction of cellular pathways to produce IFNs and cytokines that have an immediate impact on the host immune response (199). Porcine lymphocytes expressing markers CD4 or CD8 alone and CD4 and CD8 together are important in viral clearance by secreting IFN-γ (249, 250), and in turn also need functional

activation of the STAT-1 signal transduction pathway. The subversion of STAT- 1 signal transduction pathway was indicated in NiV infected porcine monocytic like cells. However, there were no reports or studies regarding whether NiV can modulate the adaptive immune response in humans, pigs or any animal models. There was some evidence that there is an involvement of immune cells in experimentally infected pigs by the detection of viral RNA in PBMC, and in the *in vitro* studies by detection of NiV antigen in an unidentified subpopulation of lymphocytes and monocytes (137). There was also evidence of lymphocyte necrosis and lymphoid depletion in the lymph nodes, with bacteria considered to be associated with immune-compromised state detected in the cerebrospinal fluid of NiV infected pigs (134, 136, 137).

Second part of the research for this thesis was therefore driven by Hypothesis # 2: that NiV infects porcine immune cells, and consequently affects cellular immune response, both at the immune cell signaling and population frequencies of PBMC levels. The two main objectives of this part of the thesis work was to (A) determine the permissiveness of porcine cells to NiV *in vitro* and (B) determine if a subpopulation of frequency of PMBC is affected *in vivo*.

This hypothesis was examined first through the objective A: determining the permissiveness of porcine immune cells to Nipah virus *in vitro,* and the effect of the infection on upregulation of selected cytokines.

The permissiveness of immune cells to NiV was evaluated in monocytes, NK cells, B cells and T cells purified from pig peripheral blood. Monocytes and NK cells are essential in the activation and amplification of the adaptive T cell response (200) and if these cells are permissive to NiV, which would lead to modulation of a cell, mediated response.

T lymphocytes infection by NiV may impact virus clearance via CD8+ T cells and via the magnitude of Th1 or Th2 response by CD4+ T cells (200). NiV infection of B lymphocytes may influence their proliferation or immunoglobin secretion (153, 188).

Due to constraints of working in BSL4 containment, selection, number of cell markers and combinations of markers/antibodies were limited to only two cell surface markers; and one internal staining: of NiV nucleocapsid protein or non-structural protein C. Viral replication was also determined by infectivity recovered from collected supernatant.

The experimental work presented here confirmed that NiV can productively infect porcine peripheral blood monocytes (Fig. 18). Increased levels of NiV genomic RNA were detected in infected monocytes at 48hrs post infection (Fig. 19). Interestingly the amount of genomic RNA decreased in the infected monocytes at 24 hpi (Fig. 19), before increasing to the levels higher than one hour post inoculation. Correspondingly, no infectivity was detected in the supernatants harvested from the cells at 24 hpi, and relatively high virus yield was obtained at 48 hrs post infection (Fig. 19). The dynamics of NiV replication in monocytes would indicate that majority of the virus is phagocytized for antigen processing and presentation, and only small proportion of the virus is internalized in an alternative way allowing for replication.

From the non-adherent cells, only cells carrying CD8+ marker were permissive to NiV: the NK cells (also carrying the CD8+ marker) (Fig. 18) and the CD8+ subset of T lymphocytes (Figs. 20 and 21). The purified B cells and the CD4+ CD8- subpopulations of T cells were not permissive to NiV (Figs. 20 and 21). The low level viremia detected in NiV infected pigs somewhat reflects the distribution of the type of cells in the swine host, where monocytes and NK cells altogether represent between 5 - 15% of PBMC, and the majority of CD8+ cells home into the lymph nodes via lymphatic system (246). The low level of viremia detected in peripheral

blood is not exceptional for paramyxoviruses, and was observed e.g. for measles virus in humans (229). The permissiveness of lymphocytes and monocytes to NiV infection appears to be species specific. Recently Mathieu *et al.* (119) reported that although leukocytes likely contribute to viremia in humans and hamsters, NiV does not replicate in them, and the cells serve merely as mechanic transporters. Only in human dendritic cells was a low level of virus replication detected (119), and a human monocytic cell line (THP-1) was also found permissive to NiV replication although virus replication was at a slower rate (274).

Infection of the individual subsets of immune cells, thus confirmed the hypothesis of cell associated viremia during NiV infection in the swine host (125, 136). Furthermore, the identification of CD3+CD6+CD8+ T lymphocytes as cells productively infected by NiV helps to elucidate the importance of peripheral immune blood cells in the viremic spread of NiV.

Interestingly in all host species (114, 125, 134, 136, 275), NiV has a preference for a small blood and lymphatic vessels in brain and lung. The CD6 marker is a strong ligand for the activated leukocyte cell adhesion molecule (ALCAM - CD166) expressed on the microvascular endothelial cells of the blood-air barrier in lung (276) and blood brain barrier (277). Consequently, dissemination of NiV within the host by the CD3+**CD6+**CD8+ cells would be preferentially targeted to small blood vessels leading to vasculitis, a characteristic of NiV infection in different hosts and may require further investigation in pigs.

The infection of different subpopulations of PBMC did not appear to be entirely dependent on pre-existing expression of ephrin B2, a primary receptor for NiV (71, 72). Resting monocytes and NK cells did not have detectable levels of ephrin B2 mRNA (Table 1), but upregulated the ephrin B2 mRNA following NiV inoculation. Based on literature, monocytes express the alternative ephrin B3 receptor for NiV (69), sufficient for the initial infection.

Mechanism of the initial infection of NK cells with NiV is not clear at this moment, as there are no reports on ephrin B3 expression (or lack of thereof) in NK cells. However, since the NK cells preparation contained up to 15% of other cells presumably permissive to and activated by NiV, the rapidly released pro-inflammatory cytokines (253) could possibly stimulate ephrin B2 expression on the NK cells, and render them permissive to NiV. While all CD6+ T lymphocytes expressed ephrin B2 (Table 1), only the ones expressing CD8 marker were permissive to NiV. Further investigation of this phenomenon could lead to elucidation of the role of CD8 marker in the permissiveness of porcine immune cells to NiV or identification of important cellular factors involved in block of NiV replication in the CD6+ cells lacking the CD8 marker.

The effect of NiV replication on IFN and cytokine production was considered. Depending on the cell type infected by NiV, inhibition of IFN and cytokine production in these immune cells would influence the outcome of a functional cell mediated response. We have focused on IFN α and γ, IL-8 and TNF α in T lymphocytes. Both IL-8 and TNFα were upregulated in the infected T lymphocytes (Fig. 22), indicating that in the T cells NiV infection similarly to the IPAM, MRC5 and ST cells, activated the p38 MAPK pathway. Some of the implications of the upregulation are discussed along with viremia and virus tropism for endothelial cells of small blood vessels (recruitment of additional immune cells) and in connection with possible apoptosis in CD4+ T cells (next section). Since both type I and II IFNs enhance antigen presentation on CD4+ T cells and affect the magnitude of the response in addition B lymphocytes are impacted by IFN by directly inducing proliferation, immunoglobulin (Ig) secretion and isotype switching (153, 188) as also evidenced by antibody development in the animals (137).

Very interestingly, induction of IFN α was downregulated in the infected activated CD6+ T cells (Fig. 22). This indicates that NiV can likely evade the IFN system at the level of induction in these cells, and it would be of interest for future to investigate the actual mechanism behind it. While *in vitro* production of type I IFN was demonstrated in NiV infected endothelial cells, the infection downregulated production of type I IFN in several other cell lines of human origin, including neuronal M17 cells (95, 190). Recent studies demonstrate that NiV C protein can inhibit IFN α induction in pDC (110) and in NiV infected human DC, IFN α is not induced (278). Therefore both pDC and DC can also have significant impact on immune response activation and regulation, and contribute to disease progression (260).

The second objective under Hypothesis # 2 was to determine if a subpopulation frequencies of peripheral T lymphocytes in the PBMC are affected *in vivo* during the acute stage post infection (up to 7 dpi) with NiV, as this can also further affect and modulate cell mediated immune response.

Flow cytometry was the primary tool in the studies of changes in population frequencies of T cells in the PBMC. Again the number of antibodies/markers was limited due to constraints posed by the BSL4/CL4 requirements (e.g. 24 hrs fixation of cells with 1% paraformaldehyde in order to remove the cells from the CL4 laboratory).

Infection of immune cells can modulate the immune response by down regulation of specific cell populations due to virus replication followed by cell death or due to release of cytokines with subsequent bystander death of susceptible cells. To participate in an adaptive immune response, T cells need to proliferate and differentiate into CD4+ helper (Th) cells and CD8+ cytotoxic cells from their naïve states after encountering antigen. In the context of *in vitro* infected PBMC, the CD8+ ^{hi} T cells were the most affected subset of cells already at 24 hrs post

inoculation with almost complete elimination of this population at 48 hrs post infection (Fig.23), consistent with these cells being permissive to NiV. The needed for p38 MAPK activation in NiV infected cells could have also induced rapid apoptosis of CD8+ T cells *in vitro* as these cell types are sensitive to hyperactivation of p38 (257). CD4- CD8+^{hi} T cells were characterized in pigs as cytotoxic T cells and their decrease would have an effect on clearance of virus infected cells (246). We have observed decrease in CD4-CD8+ cell population frequency also *in vivo* at 2 dpi (Fig. 24), however it remains to be determined whether those were NK cells, γδ T cells or cytotoxic T cells to offer any comments on the *in vivo* significance. The reduction in the number of CD4-CD8+ may be due to NiV activation of the p38 MAPK as observed in our *in vitro* work, potentially leading to apoptosis as observed in infected cells by Merritt *et al.* (257). In addition, p38 MAPK regulates the upregulation of pro-inflammatory cytokines (TNF α or IL-8) (279, 280), as observed with NiV infected T cells (Fig. 22B). The activation of p38 MAPK pathway leading to production of TNF α and IL-8 observed by other viruses and could be utilized in NiV infections (181, 281-283).

A decrease in CD4+CD8- T helper cells, observed *in vitro* (Fig. 23), would influence development of humoral immunity. Interestingly, the work with *in vivo* NiV infected PBMC confirmed there was a dramatic decrease in population frequency of CD4+CD8- T cells in piglets which succumbed to NiV infection (Fig. 25), while values for surviving piglets indicated that the CD4+CD8- T cell subset expanded following the infection (Fig. 25), corresponding with functional humoral response and protection. In surviving animals, the production of antibodies is not considered impaired, but may be somewhat delayed compared to development of antibodies against for example swine influenza (137, 139). It remains to be determined whether drop in CD4+CD8- T cell population can be used to predict the outcome of NiV infection in pigs.

In conclusion this part of the thesis has proven the hypothesis that NiV does infect a specific population of immune cells and affects the population frequency of PMBC in pigs to be true. Though, additional work is warranted to understand the role of NK cells, monocytes and plasmacytoid dendritic cells in the pathogenesis and development or modulation of immune response to NiV, which decides the outcome of the NiV infection or the secondary bacterial infections. In summary, it appears that the focus of further studies has to shift to innate immune response, as the critical aspect in the development of adaptive immune response.

4.3 Conclusion

The work presented in this thesis provides new insight into NiV evasion of IFN system in infected cells, although further work is required to elucidate this aspect of virus-host interaction. We propose that NiV blocks IFN α induction in T lymphocytes and importantly very likely also in other immune cells, from which the dendritic cells may be of critical importance. Next, the virus then interferes with the JAK-STAT signaling pathway, although the p38 MAPK pathway is activated. However antiviral state in the infected cells does not appear to be functional. In contrary, the p38 MAPK signaling pathway was determined to be important to NiV replication, especially in porcine monocytic-like cells. NiV replication may lead to hyperactivation of this pathway in the infected cells leading to an imbalance of inflammatory response and contributing to NiV pathogenesis. On the other hand, cells pre-treated with IFN α will successfully enter antiviral state against NiV (Boczkowska *et al.*, manuscript submitted). This may explain why ribavirin treatment of NiV patients was not effective (211), and the use of interferon treatments may be more successful with NiV infections. Currently, p38 MAPK inhibitors are being exploited as therapeutics for human neurological, gastrointestinal and cardiovascular diseases (284). Hence, these findings may provide a new format for development of new antiviral

therapeutics without species specificity, although with caution as the p38 MAPK pathway affects the production of pro- inflammatory cytokines to stimulate the innate immune response, and in turn induce the adaptive response. Targeted delivery to the infected cells may thus be required.

The second part of the thesis proved that specific porcine immune cells (CD8+, monocytes, NK cells) are permissive to NiV, and NiV infection has an effect on the subpopulation frequencies of T cells subsets in PMBC in the infected pigs. The data revealed that subpopulation frequencies are affected during the acute stage of NiV infection, potentially influencing a functional humoral response and protection. A significant drop in CD4+CD8- T cell population frequency observed in pigs which did not survive the NiV infection may be further examined to determine if this subpopulation can be used to predict the outcome of NiV infection in pigs. It also supports vaccine studies that the development of humoral immunity requires the aid of the T helper cells to induce rapid and protective antibody response to NiV (137, 138, 217).

Thus in the porcine host, aspects of innate and adaptive immune response are affected and contribute to NiV pathogenesis. This knowledge will benefit researchers when considering innovative strategies during design of effective vaccines and antiviral therapeutics.

5.0 References

1. **Wang, L., B. H. Harcourt, M. Yu, A. Tamin, P. A. Rota, W. J. Bellini, and B. T. Eaton.** 2001. Molecular biology of Hendra and Nipah viruses. Microbes Infect. **3:**279-287.

2. **Chua, K. B.** 2003. Nipah virus outbreak in Malaysia. J. Clin. Virol. **26:**265-275.

3. **Hossain, M. J., E. S. Gurley, J. M. Montgomery, M. Bell, D. S. Carroll, V. P. Hsu, P. Formenty, A. Croisier, E. Bertherat, M. A. Faiz, A. K. Azad, R. Islam, M. A. Molla, T. G. Ksiazek, P. A. Rota, J. A. Comer, P. E. Rollin, S. P. Luby, and R. F. Breiman.** 2008. Clinical presentation of nipah virus infection in Bangladesh. Clin. Infect. Dis. **46:**977-984. doi: 10.1086/529147.

4. **Chua, K. B., W. J. Bellini, P. A. Rota, B. H. Harcourt, A. Tamin, S. K. Lam, T. G. Ksiazek, P. E. Rollin, S. R. Zaki, W. Shieh, C. S. Goldsmith, D. J. Gubler, J. T. Roehrig, B. Eaton, A. R. Gould, J. Olson, H. Field, P. Daniels, A. E. Ling, C. J. Peters, L. J. Anderson, and B. W. Mahy.** 2000. Nipah virus: a recently emergent deadly paramyxovirus. Science. **288:**1432-1435.

5. **Mohd Nor, M. N., C. H. Gan, and B. L. Ong.** 2000. Nipah virus infection of pigs in peninsular Malaysia. Rev. Sci. Tech. **19:**160-165.

6. **Luby, S. P., E. S. Gurley, and M. J. Hossain.** 2009. Transmission of human infection with Nipah virus. Clin. Infect. Dis. **49:**1743-1748. doi: 10.1086/647951.

7. **Homaira, N., M. Rahman, M. J. Hossain, J. H. Epstein, R. Sultana, M. S. Khan, G. Podder, K. Nahar, B. Ahmed, E. S. Gurley, P. Daszak, W. I. Lipkin, P. E. Rollin, J. A. Comer, T. G. Ksiazek, and S. P. Luby.** 2010. Nipah virus outbreak with person-to-person transmission in a district of Bangladesh, 2007. Epidemiol. Infect. **138:**1630-1636. doi: 10.1017/S0950268810000695.

8. **Sazzad, H. M., M. J. Hossain, E. S. Gurley, K. M. Ameen, S. Parveen, M. S. Islam, L. I. Faruque, G. Podder, S. S. Banu, M. K. Lo, P. E. Rollin, P. A. Rota, P. Daszak, M. Rahman, and S. P. Luby.** 2013. Nipah virus infection outbreak with nosocomial and corpse-to-human transmission, Bangladesh. Emerg. Infect. Dis. **19:**210-217. doi: 10.3201/eid1902.120971; 10.3201/eid1902.120971.

9. **Field, H., P. Young, J. M. Yob, J. Mills, L. Hall, and J. Mackenzie.** 2001. The natural history of Hendra and Nipah viruses. Microbes Infect. **3:**307-314.

10. **Lam, S. K., and K. B. Chua.** 2002. Nipah virus encephalitis outbreak in Malaysia. Clin. Infect. Dis. **34 Suppl 2:**S48-51. doi: 10.1086/338818.

11. **Chua, K. B., K. J. Goh, K. T. Wong, A. Kamarulzaman, P. S. Tan, T. G. Ksiazek, S. R. Zaki, G. Paul, S. K. Lam, and C. T. Tan.** 1999. Fatal encephalitis due to Nipah virus among pig-farmers in Malaysia. Lancet. **354:**1257-1259. doi: 10.1016/S0140-6736(99)04299-3.

12. **Paton, N. I., Y. S. Leo, S. R. Zaki, A. P. Auchus, K. E. Lee, A. E. Ling, S. K. Chew, B. Ang, P. E. Rollin, T. Umapathi, I. Sng, C. C. Lee, E. Lim, and T. G. Ksiazek.** 1999. Outbreak of Nipah-virus infection among abattoir workers in Singapore. Lancet. **354:**1253-1256. doi: 10.1016/S0140-6736(99)04379-2.

13. **Goh, K. J., C. T. Tan, N. K. Chew, P. S. Tan, A. Kamarulzaman, S. A. Sarji, K. T. Wong, B. J. Abdullah, K. B. Chua, and S. K. Lam.** 2000. Clinical features of Nipah virus encephalitis among pig farmers in Malaysia. N. Engl. J. Med. **342:**1229-1235. doi: 10.1056/NEJM200004273421701.

14. **Chadha, M. S., J. A. Comer, L. Lowe, P. A. Rota, P. E. Rollin, W. J. Bellini, T. G. Ksiazek, and A. Mishra.** 2006. Nipah virus-associated encephalitis outbreak, Siliguri, India. Emerg. Infect. Dis. **12:**235-240.

15. **Harit, A. K., R. L. Ichhpujani, S. Gupta, K. S. Gill, S. Lal, N. K. Ganguly, and S. P. Agarwal.** 2006. Nipah/Hendra virus outbreak in Siliguri, West Bengal, India in 2001. Indian J. Med. Res. **123:**553-560.

16. **Luby, S. P., M. J. Hossain, E. S. Gurley, B. N. Ahmed, S. Banu, S. U. Khan, N. Homaira, P. A. Rota, P. E. Rollin, J. A. Comer, E. Kenah, T. G. Ksiazek, and M. Rahman.** 2009. Recurrent zoonotic transmission of Nipah virus into humans, Bangladesh, 2001-2007. Emerg. Infect. Dis. **15:**1229-1235. doi: 10.3201/eid1508.081237;10.3201/eid1508.081237.

17. **Arankalle, V. A., B. T. Bandyopadhyay, A. Y. Ramdasi, R. Jadi, D. R. Patil, M. Rahman, M. Majumdar, P. S. Banerjee, A. K. Hati, R. P. Goswami, D. K. Neogi, and A. C. Mishra.** 2011. Genomic characterization of Nipah virus, West Bengal, India. Emerg. Infect. Dis. **17:**907-909. doi: 10.3201/eid1705.100968;10.3201/eid1705.100968.

18. **Gurley, E. S., J. M. Montgomery, M. J. Hossain, M. Bell, A. K. Azad, M. R. Islam, M. A. Molla, D. S. Carroll, T. G. Ksiazek, P. A. Rota, L. Lowe, J. A. Comer, P. Rollin, M. Czub, A. Grolla, H. Feldmann, S. P. Luby, J. L. Woodward, and R. F. Breiman.** 2007. Person-to-person transmission of Nipah virus in a Bangladeshi community. Emerg. Infect. Dis. **13:**1031-1037. doi: 10.3201/eid1307.061128;10.3201/eid1307.061128.

19. **Broder, C. C.** 2013. Passive immunization and active vaccination against Hendra and Nipah viruses. Dev. Biol. (Basel). **135:**125-138. doi: 10.1159/000171017;10.1159/000171017.

20. **Luby, S. P., and E. S. Gurley.** 2012. Epidemiology of henipavirus disease in humans. Curr. Top. Microbiol. Immunol. **359:**25-40. doi: 10.1007/82_2012_207;10.1007/82_2012_207.

21. **Chua, K. B., C. L. Koh, P. S. Hooi, K. F. Wee, J. H. Khong, B. H. Chua, Y. P. Chan, M. E. Lim, and S. K. Lam.** 2002. Isolation of Nipah virus from Malaysian Island flying-foxes. Microbes Infect. **4:**145-151.

22. **Reynes, J. M., D. Counor, S. Ong, C. Faure, V. Seng, S. Molia, J. Walston, M. C. Georges-Courbot, V. Deubel, and J. L. Sarthou.** 2005. Nipah virus in Lyle's flying foxes, Cambodia. Emerg. Infect. Dis. **11:**1042-1047.

23. **Luby, S. P., M. Rahman, M. J. Hossain, L. S. Blum, M. M. Husain, E. Gurley, R. Khan, B. N. Ahmed, S. Rahman, N. Nahar, E. Kenah, J. A. Comer, and T. G. Ksiazek.** 2006. Foodborne transmission of Nipah virus, Bangladesh. Emerg. Infect. Dis. **12:**1888-1894.

24. **Luby, S. P., E. S. Gurley, and M. J. Hossain.** 2009. Transmission of human infection with Nipah virus. Clin. Infect. Dis. **49:**1743-1748. doi: 10.1086/647951; 10.1086/647951.

25. **Yob, J. M., H. Field, A. M. Rashdi, C. Morrissy, B. van der Heide, P. Rota, A. bin Adzhar, J. White, P. Daniels, A. Jamaluddin, and T. Ksiazek.** 2001. Nipah virus infection in bats (order Chiroptera) in peninsular Malaysia. Emerg. Infect. Dis. **7:**439-441.

26. **Hsu, V. P., M. J. Hossain, U. D. Parashar, M. M. Ali, T. G. Ksiazek, I. Kuzmin, M. Niezgoda, C. Rupprecht, J. Bresee, and R. F. Breiman.** 2004. Nipah virus encephalitis reemergence, Bangladesh. Emerg. Infect. Dis. **10:**2082-2087. doi: 10.3201/eid1012.040701.

27. **Epstein, J. H., V. Prakash, C. S. Smith, P. Daszak, A. B. McLaughlin, G. Meehan, H. E. Field, and A. A. Cunningham.** 2008. Henipavirus infection in fruit bats (Pteropus giganteus), India. Emerg. Infect. Dis. **14:**1309-1311.

28. **O'Brien, G. M.** 1993. Seasonal reproduction in flying foxes, reviewed in the context of other tropical mammals. Reprod. Fertil. Dev. **5:**499-521.

29. **Wacharapluesadee, S., B. Lumlertdacha, K. Boongird, S. Wanghongsa, L. Chanhome, P. Rollin, P. Stockton, C. E. Rupprecht, T. G. Ksiazek, and T. Hemachudha.** 2005. Bat Nipah virus, Thailand. Emerg. Infect. Dis. **11:**1949-1951.

30. **Middleton, D. J., C. J. Morrissy, B. M. van der Heide, G. M. Russell, M. A. Braun, H. A. Westbury, K. Halpin, and P. W. Daniels.** 2007. Experimental Nipah virus infection in pteropid bats (Pteropus poliocephalus). J. Comp. Pathol. **136:**266-272. doi: 10.1016/j.jcpa.2007.03.002.

31. **Chua, K. B.** 2003. A novel approach for collecting samples from fruit bats for isolation of infectious agents. Microbes Infect. **5:**487-490.

32. **Wacharapluesadee, S., K. Boongird, S. Wanghongsa, N. Ratanasetyuth, P. Supavonwong, D. Saengsen, G. N. Gongal, and T. Hemachudha.** 2010. A longitudinal study of the prevalence of Nipah virus in Pteropus lylei bats in Thailand: evidence for seasonal

preference in disease transmission. Vector Borne Zoonotic Dis. **10:**183-190. doi: 10.1089/vbz.2008.0105.

33. **Reeder, D. M., T. H. Kunz, and E. P. Widmaier.** 2004. Baseline and stress-induced glucocorticoids during reproduction in the variable flying fox, Pteropus hypomelanus (Chiroptera: Pteropodidae). J. Exp. Zool. A. Comp. Exp. Biol. **301:**682-690. doi: 10.1002/jez.a.58.

34. **Reeder, D. M., N. S. Kosteczko, T. H. Kunz, and E. P. Widmaier.** 2006. The hormonal and behavioral response to group formation, seasonal changes, and restraint stress in the highly social Malayan Flying Fox (Pteropus vampyrus) and the less social Little Golden-mantled Flying Fox (Pteropus pumilus) (Chiroptera: Pteropodidae). Horm. Behav. **49:**484-500. doi: 10.1016/j.yhbeh.2005.11.001.

35. **Rahman, M. A., M. J. Hossain, S. Sultana, N. Homaira, S. U. Khan, M. Rahman, E. S. Gurley, P. E. Rollin, M. K. Lo, J. A. Comer, L. Lowe, P. A. Rota, T. G. Ksiazek, E. Kenah, Y. Sharker, and S. P. Luby.** 2012. Date palm sap linked to Nipah virus outbreak in Bangladesh, 2008. Vector Borne Zoonotic Dis. **12:**65-72. doi: 10.1089/vbz.2011.0656; 10.1089/vbz.2011.0656.

36. **Rahman, S. A., L. Hassan, J. H. Epstein, Z. C. Mamat, A. M. Yatim, S. S. Hassan, H. E. Field, T. Hughes, J. Westrum, M. S. Naim, A. S. Suri, A. A. Jamaluddin, P. Daszak, and Henipavirus Ecology Research Group.** 2013. Risk Factors for Nipah virus infection among pteropid bats, Peninsular Malaysia. Emerg. Infect. Dis. **19:**51-60. doi: 10.3201/eid1901.120221; 10.3201/eid1901.120221.

37. **Wang, L. F., M. Yu, E. Hansson, L. I. Pritchard, B. Shiell, W. P. Michalski, and B. T. Eaton.** 2000. The exceptionally large genome of Hendra virus: support for creation of a new genus within the family Paramyxoviridae. J. Virol. **74:**9972-9979.

38. **Mayo, M. A.** 2002. Names of viruses and virus species - an editorial note. Arch. Virol. **147:**1463-1464.

39. **Yu, M., E. Hansson, J. P. Langedijk, B. T. Eaton, and L. F. Wang.** 1998. The attachment protein of Hendra virus has high structural similarity but limited primary sequence homology compared with viruses in the genus Paramyxovirus. Virology. **251:**227-233. doi: 10.1006/viro.1998.9302.

40. **Harcourt, B. H., A. Tamin, K. Halpin, T. G. Ksiazek, P. E. Rollin, W. J. Bellini, and P. A. Rota.** 2001. Molecular characterization of the polymerase gene and genomic termini of Nipah virus. Virology. **287:**192-201. doi: 10.1006/viro.2001.1026.

41. **Lo, M. K., L. Lowe, K. B. Hummel, H. M. Sazzad, E. S. Gurley, M. J. Hossain, S. P. Luby, D. M. Miller, J. A. Comer, P. E. Rollin, W. J. Bellini, and P. A. Rota.** 2012. Characterization of Nipah virus from outbreaks in Bangladesh, 2008-2010. Emerg. Infect. Dis. **18:**248-255. doi: 10.3201/eid1802.111492; 10.3201/eid1802.111492.

42. **Marsh, G. A., C. de Jong, J. A. Barr, M. Tachedjian, C. Smith, D. Middleton, M. Yu, S. Todd, A. J. Foord, V. Haring, J. Payne, R. Robinson, I. Broz, G. Crameri, H. E. Field, and L. F. Wang.** 2012. Cedar virus: a novel Henipavirus isolated from Australian bats. PLoS Pathog. **8:**e1002836. doi: 10.1371/journal.ppat.1002836; 10.1371/journal.ppat.1002836.

43. **Murray, K., P. Selleck, P. Hooper, A. Hyatt, A. Gould, L. Gleeson, H. Westbury, L. Hiley, L. Selvey, and B. Rodwell.** 1995. A morbillivirus that caused fatal disease in horses and humans. Science. **268:**94-97.

44. **Hyatt, A. D., S. R. Zaki, C. S. Goldsmith, T. G. Wise, and S. G. Hengstberger.** 2001. Ultrastructure of Hendra virus and Nipah virus within cultured cells and host animals. Microbes Infect. **3:**297-306.

45. **Lamb RA, Parks GD.** Paramyxoviridae: the viruses and their replication. 2007 In: Knipe DM, Howley PM (eds) Fields virology, 5th edn. vols 1 and 2. Lippincott Williams & Wilkins, Philadelphia, 1449–1496.

46. **Jack, P. J., D. B. Boyle, B. T. Eaton, and L. F. Wang.** 2005. The complete genome sequence of J virus reveals a unique genome structure in the family Paramyxoviridae. J. Virol. **79:**10690-10700. doi: 10.1128/JVI.79.16.10690-10700.2005.

47. **Li, Z., M. Yu, H. Zhang, D. E. Magoffin, P. J. Jack, A. Hyatt, H. Y. Wang, and L. F. Wang.** 2006. Beilong virus, a novel paramyxovirus with the largest genome of non-segmented negative-stranded RNA viruses. Virology. **346:**219-228. doi: 10.1016/j.virol.2005.10.039.

48. **Magoffin, D. E., K. Halpin, P. A. Rota, and L. F. Wang.** 2007. Effects of single amino acid substitutions at the E residue in the conserved GDNE motif of the Nipah virus polymerase (L) protein. Arch. Virol. **152:**827-832. doi: 10.1007/s00705-006-0881-1.

49. **Hino, K., H. Sato, A. Sugai, M. Kato, M. Yoneda, and C. Kai.** 2013. Downregulation of Nipah Virus N mRNA Occurs through Interaction between Its 3' Untranslated Region and hnRNP D. J. Virol. **87:**6582-6588. doi: 10.1128/JVI.02495-12;10.1128/JVI.02495-12.

50. **Walpita, P., and C. J. Peters.** 2007. Cis-acting elements in the antigenomic promoter of Nipah virus. J. Gen. Virol. **88:**2542-2551. doi: 10.1099/vir.0.83035-0.

51. **Rodriguez, J. J., and C. M. Horvath.** 2004. Host evasion by emerging paramyxoviruses: Hendra virus and Nipah virus v proteins inhibit interferon signaling. Viral Immunol. **17:**210-219. doi: 10.1089/0882824041310568.

52. **Kulkarni, S., V. Volchkova, C. F. Basler, P. Palese, V. E. Volchkov, and M. L. Shaw.** 2009. Nipah virus edits its P gene at high frequency to express the V and W proteins. J. Virol. **83:**3982-3987. doi: 10.1128/JVI.02599-08; 10.1128/JVI.02599-08.

53. **Halpin, K., B. Bankamp, B. H. Harcourt, W. J. Bellini, and P. A. Rota.** 2004. Nipah virus conforms to the rule of six in a minigenome replication assay. J. Gen. Virol. **85:**701-707.

54. **Tan, W. S., S. T. Ong, M. Eshaghi, S. S. Foo, and K. Yusoff.** 2004. Solubility, immunogenicity and physical properties of the nucleocapsid protein of Nipah virus produced in Escherichia coli. J. Med. Virol. **73:**105-112. doi: 10.1002/jmv.20052.

55. **Ong, S. T., K. Yusoff, C. L. Kho, J. O. Abdullah, and W. S. Tan.** 2009. Mutagenesis of the nucleocapsid protein of Nipah virus involved in capsid assembly. J. Gen. Virol. **90:**392-397. doi: 10.1099/vir.0.005710-0; 10.1099/vir.0.005710-0.

56. **Hausmann, S., J. P. Jacques, and D. Kolakofsky.** 1996. Paramyxovirus RNA editing and the requirement for hexamer genome length. RNA. **2:**1033-1045.

57. **Chan, Y. P., C. L. Koh, S. K. Lam, and L. F. Wang.** 2004. Mapping of domains responsible for nucleocapsid protein-phosphoprotein interaction of Henipaviruses. J. Gen. Virol. **85:**1675-1684.

58. **Blocquel, D., M. Beltrandi, J. Erales, P. Barbier, and S. Longhi.** 2013. Biochemical and structural studies of the oligomerization domain of the Nipah virus phosphoprotein: evidence for an elongated coiled-coil homotrimer. Virology. **446:**162-172. doi: 10.1016/j.virol.2013.07.031; 10.1016/j.virol.2013.07.031.

59. **Huang, M., H. Sato, K. Hagiwara, A. Watanabe, A. Sugai, F. Ikeda, H. Kozuka-Hata, M. Oyama, M. Yoneda, and C. Kai.** 2011. Determination of a phosphorylation site in Nipah virus nucleoprotein and its involvement in virus transcription. J. Gen. Virol. **92:**2133-2141. doi: 10.1099/vir.0.032342-0; 10.1099/vir.0.032342-0.

60. **Yu, F., N. S. Khairullah, S. Inoue, V. Balasubramaniam, S. J. Berendam, L. K. Teh, N. S. Ibrahim, S. Abdul Rahman, S. S. Hassan, F. Hasebe, M. Sinniah, and K. Morita.** 2006. Serodiagnosis using recombinant nipah virus nucleocapsid protein expressed in Escherichia coli. J. Clin. Microbiol. **44:**3134-3138. doi: 10.1128/JCM.00693-06.

61. **Omi-Furutani, M., M. Yoneda, K. Fujita, F. Ikeda, and C. Kai.** 2010. Novel phosphoprotein-interacting region in Nipah virus nucleocapsid protein and its involvement in viral replication. J. Virol. **84:**9793-9799. doi: 10.1128/JVI.00339-10.

62. **Shiell, B. J., D. R. Gardner, G. Crameri, B. T. Eaton, and W. P. Michalski.** 2003. Sites of phosphorylation of P and V proteins from Hendra and Nipah viruses: newly emerged members of Paramyxoviridae. Virus Res. **92:**55-65.

63. **Ciancanelli, M. J., and C. F. Basler.** 2006. Mutation of YMYL in the Nipah virus matrix protein abrogates budding and alters subcellular localization. J. Virol. **80:**12070-12078. doi: 10.1128/JVI.01743-06.

64. **Patch, J. R., Z. Han, S. E. McCarthy, L. Yan, L. F. Wang, R. N. Harty, and C. C. Broder.** 2008. The YPLGVG sequence of the Nipah virus matrix protein is required for budding. Virol. J. **5:**137-422X-5-137. doi: 10.1186/1743-422X-5-137; 10.1186/1743-422X-5-137.

65. **Lamp, B., E. Dietzel, L. Kolesnikova, L. Sauerhering, S. Erbar, H. Weingartl, and A. Maisner.** 2013. Nipah virus entry and egress from polarized epithelial cells. J. Virol. **87:**3143-3154. doi: 10.1128/JVI.02696-12; 10.1128/JVI.02696-12.

66. **Wang, Y. E., A. Park, M. Lake, M. Pentecost, B. Torres, T. E. Yun, M. C. Wolf, M. R. Holbrook, A. N. Freiberg, and B. Lee.** 2010. Ubiquitin-regulated nuclear-cytoplasmic trafficking of the Nipah virus matrix protein is important for viral budding. PLoS Pathog. **6:**e1001186. doi: 10.1371/journal.ppat.1001186.

67. **Bossart, K. N., B. A. Mungall, G. Crameri, L. F. Wang, B. T. Eaton, and C. C. Broder.** 2005. Inhibition of Henipavirus fusion and infection by heptad-derived peptides of the Nipah virus fusion glycoprotein. Virol. J. **2:**57. doi: 10.1186/1743-422X-2-57.

68. **Bowden, T. A., A. R. Aricescu, R. J. Gilbert, J. M. Grimes, E. Y. Jones, and D. I. Stuart.** 2008. Structural basis of Nipah and Hendra virus attachment to their cell-surface receptor ephrin-B2. Nat. Struct. Mol. Biol. **15:**567-572. doi: 10.1038/nsmb.1435; 10.1038/nsmb.1435.

69. **Yu, G., H. Luo, Y. Wu, and J. Wu.** 2003. Ephrin B2 induces T cell costimulation. J. Immunol. **171:**106-114.

70. **Bonaparte, M. I., A. S. Dimitrov, K. N. Bossart, G. Crameri, B. A. Mungall, K. A. Bishop, V. Choudhry, D. S. Dimitrov, L. F. Wang, B. T. Eaton, and C. C. Broder.** 2005. Ephrin-B2 ligand is a functional receptor for Hendra virus and Nipah virus. Proc. Natl. Acad. Sci. U. S. A. **102:**10652-10657. doi: 10.1073/pnas.0504887102.

71. **Negrete, O. A., E. L. Levroney, H. C. Aguilar, A. Bertolotti-Ciarlet, R. Nazarian, S. Tajyar, and B. Lee.** 2005. EphrinB2 is the entry receptor for Nipah virus, an emergent deadly paramyxovirus. Nature. **436:**401-405. doi: 10.1038/nature03838.

72. **Negrete, O. A., M. C. Wolf, H. C. Aguilar, S. Enterlein, W. Wang, E. Muhlberger, S. V. Su, A. Bertolotti-Ciarlet, R. Flick, and B. Lee.** 2006. Two key residues in ephrinB3 are critical for its use as an alternative receptor for Nipah virus. PLoS Pathog. **2:**e7. doi: 10.1371/journal.ppat.0020007.

73. **Erbar, S., S. Diederich, and A. Maisner.** 2008. Selective receptor expression restricts Nipah virus infection of endothelial cells. Virol. J. **5:**142-422X-5-142. doi: 10.1186/1743-422X-5-142; 10.1186/1743-422X-5-142.

74. **Bochenek, M. L., S. Dickinson, J. W. Astin, R. H. Adams, and C. D. Nobes.** 2010. Ephrin-B2 regulates endothelial cell morphology and motility independently of Eph-receptor binding. J. Cell. Sci. **123:**1235-1246. doi: 10.1242/jcs.061903; 10.1242/jcs.061903.

75. **Negrete, O. A., D. Chu, H. C. Aguilar, and B. Lee.** 2007. Single amino acid changes in the Nipah and Hendra virus attachment glycoproteins distinguish ephrinB2 from ephrinB3 usage. J. Virol. **81:**10804-10814. doi: 10.1128/JVI.00999-07.

76. **Hafner, C., S. Meyer, I. Hagen, B. Becker, A. Roesch, M. Landthaler, and T. Vogt.** 2005. Ephrin-B reverse signaling induces expression of wound healing associated genes in IEC-6 intestinal epithelial cells. World J. Gastroenterol. **11:**4511-4518.

77. **Aguilar, H. C., Z. A. Ataman, V. Aspericueta, A. Q. Fang, M. Stroud, O. A. Negrete, R. A. Kammerer, and B. Lee.** 2009. A novel receptor-induced activation site in the Nipah virus attachment glycoprotein (G) involved in triggering the fusion glycoprotein (F). J. Biol. Chem. **284:**1628-1635. doi: 10.1074/jbc.M807469200; 10.1074/jbc.M807469200.

78. **Zhu, Q., S. B. Biering, A. M. Mirza, B. A. Grasseschi, P. J. Mahon, B. Lee, H. C. Aguilar, and R. M. Iorio.** 2013. Individual N-glycans added at intervals along the stalk of the Nipah virus G protein prevent fusion but do not block the interaction with the homologous F protein. J. Virol. **87:**3119-3129. doi: 10.1128/JVI.03084-12; 10.1128/JVI.03084-12.

79. **Liu, Q., J. A. Stone, B. Bradel-Tretheway, J. Dabundo, J. A. Benavides Montano, J. Santos-Montanez, S. B. Biering, A. V. Nicola, R. M. Iorio, X. Lu, and H. C. Aguilar.** 2013. Unraveling a three-step spatiotemporal mechanism of triggering of receptor-induced Nipah virus fusion and cell entry. PLoS Pathog. **9:**e1003770. doi: 10.1371/journal.ppat.1003770 [doi].

80. **Talekar, A., I. DeVito, Z. Salah, S. G. Palmer, A. Chattopadhyay, J. K. Rose, R. Xu, I. A. Wilson, A. Moscona, and M. Porotto.** 2013. Identification of a region in the stalk domain of the Nipah virus receptor binding protein that is critical for fusion activation. J. Virol. **87:**10980-10996. doi: 10.1128/JVI.01646-13 [doi].

81. **Bossart, K. N., L. F. Wang, B. T. Eaton, and C. C. Broder.** 2001. Functional expression and membrane fusion tropism of the envelope glycoproteins of Hendra virus. Virology. **290:**121-135. doi: 10.1006/viro.2001.1158.

82. **Tamin, A., B. H. Harcourt, T. G. Ksiazek, P. E. Rollin, W. J. Bellini, and P. A. Rota.** 2002. Functional properties of the fusion and attachment glycoproteins of Nipah virus. Virology. **296:**190-200. doi: 10.1006/viro.2002.1418.

83. **Diederich, S., M. Moll, H. D. Klenk, and A. Maisner.** 2005. The Nipah virus fusion protein is cleaved within the endosomal compartment. J. Biol. Chem. **280:**29899-29903. doi: 10.1074/jbc.M504598200.

84. **Vogt, C., M. Eickmann, S. Diederich, M. Moll, and A. Maisner.** 2005. Endocytosis of the Nipah virus glycoproteins. J. Virol. **79:**3865-3872. doi: 10.1128/JVI.79.6.3865-3872.2005.

85. **Pager, C. T., W. W. Craft Jr, J. Patch, and R. E. Dutch.** 2006. A mature and fusogenic form of the Nipah virus fusion protein requires proteolytic processing by cathepsin L. Virology. **346:**251-257. doi: 10.1016/j.virol.2006.01.007.

86. **Diederich, S., E. Dietzel, and A. Maisner.** 2009. Nipah virus fusion protein: influence of cleavage site mutations on the cleavability by cathepsin L, trypsin and furin. Virus Res. **145:**300-306. doi: 10.1016/j.virusres.2009.07.020; 10.1016/j.virusres.2009.07.020.

87. **Moll, M., S. Diederich, H. D. Klenk, M. Czub, and A. Maisner.** 2004. Ubiquitous activation of the Nipah virus fusion protein does not require a basic amino acid at the cleavage site. J. Virol. **78:**9705-9712. doi: 10.1128/JVI.78.18.9705-9712.2004 [doi].

88. **Weise, C., S. Erbar, B. Lamp, C. Vogt, S. Diederich, and A. Maisner.** 2010. Tyrosine residues in the cytoplasmic domains affect sorting and fusion activity of the Nipah virus glycoproteins in polarized epithelial cells. J. Virol. **84:**7634-7641. doi: 10.1128/JVI.02576-09.

89. **Erbar, S., and A. Maisner.** 2010. Nipah virus infection and glycoprotein targeting in endothelial cells. Virol. J. **7:**305-422X-7-305. doi: 10.1186/1743-422X-7-305; 10.1186/1743-422X-7-305.

90. **Diederich, S., L. Sauerhering, M. Weis, H. Altmeppen, N. Schaschke, T. Reinheckel, S. Erbar, and A. Maisner.** 2012. Activation of the Nipah virus fusion protein in MDCK cells is mediated by cathepsin B within the endosome-recycling compartment. J. Virol. **86:**3736-3745. doi: 10.1128/JVI.06628-11;10.1128/JVI.06628-11.

91. **Xu, Y., Z. Lou, Y. Liu, D. K. Cole, N. Su, L. Qin, X. Li, Z. Bai, Z. Rao, and G. F. Gao.** 2004. Crystallization and preliminary crystallographic analysis of the fusion core from two new zoonotic paramyxoviruses, Nipah virus and Hendra virus. Acta Crystallogr. D Biol. Crystallogr. **60:**1161-1164. doi: 10.1107/S0907444904009515.

92. **Aguilar, H. C., V. Aspericueta, L. R. Robinson, K. E. Aanensen, and B. Lee.** 2010. A quantitative and kinetic fusion protein-triggering assay can discern distinct steps in the nipah virus membrane fusion cascade. J. Virol. **84:**8033-8041. doi: 10.1128/JVI.00469-10.

93. **Rota, P. A., and M. K. Lo.** 2012. Molecular virology of the henipaviruses. Curr. Top. Microbiol. Immunol. **359:**41-58. doi: 10.1007/82_2012_211;10.1007/82_2012_211.

94. **Lo, M. K., B. H. Harcourt, B. A. Mungall, A. Tamin, M. E. Peeples, W. J. Bellini, and P. A. Rota.** 2009. Determination of the henipavirus phosphoprotein gene mRNA editing frequencies and detection of the C, V and W proteins of Nipah virus in virus-infected cells. J. Gen. Virol. **90:**398-404. doi: 10.1099/vir.0.007294-0.

95. **Lo, M. K., D. Miller, M. Aljofan, B. A. Mungall, P. E. Rollin, W. J. Bellini, and P. A. Rota.** 2010. Characterization of the antiviral and inflammatory responses against Nipah virus in endothelial cells and neurons. Virology. doi: 10.1016/j.virol.2010.05.005.

96. **Rodriguez, J. J., J. P. Parisien, and C. M. Horvath.** 2002. Nipah virus V protein evades alpha and gamma interferons by preventing STAT1 and STAT2 activation and nuclear accumulation. J. Virol. **76:**11476-11483.

97. **Shaw, M. L., A. Garcia-Sastre, P. Palese, and C. F. Basler.** 2004. Nipah virus V and W proteins have a common STAT1-binding domain yet inhibit STAT1 activation from the cytoplasmic and nuclear compartments, respectively. J. Virol. **78:**5633-5641. doi: 10.1128/JVI.78.11.5633-5641.2004.

98. **Sleeman, K., B. Bankamp, K. B. Hummel, M. K. Lo, W. J. Bellini, and P. A. Rota.** 2008. The C, V and W proteins of Nipah virus inhibit minigenome replication. J. Gen. Virol. **89:**1300-1308. doi: 10.1099/vir.0.83582-0; 10.1099/vir.0.83582-0.

99. **Yoneda, M., V. Guillaume, H. Sato, K. Fujita, M. C. Georges-Courbot, F. Ikeda, M. Omi, Y. Muto-Terao, T. F. Wild, and C. Kai.** 2010. The nonstructural proteins of Nipah virus play a key role in pathogenicity in experimentally infected animals. PLoS One. **5:**e12709. doi: 10.1371/journal.pone.0012709.

100. **Rodriguez, J. J., C. D. Cruz, and C. M. Horvath.** 2004. Identification of the nuclear export signal and STAT-binding domains of the Nipah virus V protein reveals mechanisms underlying interferon evasion. J. Virol. **78:**5358-5367.

101. **Shaw, M. L., W. B. Cardenas, D. Zamarin, P. Palese, and C. F. Basler.** 2005. Nuclear localization of the Nipah virus W protein allows for inhibition of both virus- and toll-like receptor 3-triggered signaling pathways. J. Virol. **79:**6078-6088. doi: 10.1128/JVI.79.10.6078-6088.2005.

102. **Rodriguez, J. J., L. F. Wang, and C. M. Horvath.** 2003. Hendra virus V protein inhibits interferon signaling by preventing STAT1 and STAT2 nuclear accumulation. J. Virol. **77:**11842-11845.

103. **Hagmaier, K., N. Stock, S. Goodbourn, L. F. Wang, and R. Randall.** 2006. A single amino acid substitution in the V protein of Nipah virus alters its ability to block interferon signalling in cells from different species. J. Gen. Virol. **87:**3649-3653. doi: 10.1099/vir.0.82261-0.

104. **Childs, K., N. Stock, C. Ross, J. Andrejeva, L. Hilton, M. Skinner, R. Randall, and S. Goodbourn.** 2007. mda-5, but not RIG-I, is a common target for paramyxovirus V proteins. Virology. **359:**190-200. doi: 10.1016/j.virol.2006.09.023.

105. **Parisien, J. P., D. Bamming, A. Komuro, A. Ramachandran, J. J. Rodriguez, G. Barber, R. D. Wojahn, and C. M. Horvath.** 2009. A shared interface mediates paramyxovirus interference with antiviral RNA helicases MDA5 and LGP2. J. Virol. **83:**7252-7260. doi: 10.1128/JVI.00153-09; 10.1128/JVI.00153-09.

106. **Park, M. S., M. L. Shaw, J. Munoz-Jordan, J. F. Cros, T. Nakaya, N. Bouvier, P. Palese, A. Garcia-Sastre, and C. F. Basler.** 2003. Newcastle disease virus (NDV)-based assay demonstrates interferon-antagonist activity for the NDV V protein and the Nipah virus V, W, and C proteins. J. Virol. **77:**1501-1511.

107. **Yoneda, M., K. Fujita, H. Sato, and C. Kai.** 2009. Reverse genetics of Nipah virus to probe viral pathogenicity. Methods Mol. Biol. **515:**329-337. doi: 10.1007/978-1-59745-559-6_23; 10.1007/978-1-59745-559-6_23.

108. **Mathieu, C., V. Guillaume, V. A. Volchkova, C. Pohl, F. Jacquot, R. Y. Looi, K. T. Wong, C. Legras-Lachuer, V. E. Volchkov, J. Lachuer, and B. Horvat.** 2012. Nonstructural Nipah virus C protein regulates both the early host proinflammatory response and viral virulence. J. Virol. **86:**10766-10775. doi: 10.1128/JVI.01203-12;10.1128/JVI.01203-12.

109. **Lo, M. K., M. E. Peeples, W. J. Bellini, S. T. Nichol, P. A. Rota, and C. F. Spiropoulou.** 2012. Distinct and overlapping roles of Nipah virus P gene products in modulating the human endothelial cell antiviral response. PLoS One. **7:**e47790. doi: 10.1371/journal.pone.0047790;10.1371/journal.pone.0047790.

110. **Yamaguchi, M., Y. Kitagawa, M. Zhou, M. Itoh, and B. Gotoh.** 2014. An anti-interferon activity shared by paramyxovirus C proteins: inhibition of Toll-like receptor 7/9-dependent alpha interferon induction. FEBS Lett. **588:**28-34. doi: 10.1016/j.febslet.2013.11.015; 10.1016/j.febslet.2013.11.015.

111. **Pernet, O., C. Pohl, M. Ainouze, H. Kweder, and R. Buckland.** 2009. Nipah virus entry can occur by macropinocytosis. Virology. **395:**298-311. doi: 10.1016/j.virol.2009.09.016; 10.1016/j.virol.2009.09.016.

112. **Bossart, K. N., L. F. Wang, M. N. Flora, K. B. Chua, S. K. Lam, B. T. Eaton, and C. C. Broder.** 2002. Membrane fusion tropism and heterotypic functional activities of the Nipah virus and Hendra virus envelope glycoproteins. J. Virol. **76:**11186-11198.

113. **Cargnello, M., and P. P. Roux.** 2011. Activation and function of the MAPKs and their substrates, the MAPK-activated protein kinases. Microbiol. Mol. Biol. Rev. **75:**50-83. doi: 10.1128/MMBR.00031-10; 10.1128/MMBR.00031-10.

114. **Wong, K. T., W. J. Shieh, S. Kumar, K. Norain, W. Abdullah, J. Guarner, C. S. Goldsmith, K. B. Chua, S. K. Lam, C. T. Tan, K. J. Goh, H. T. Chong, R. Jusoh, P. E. Rollin, T. G. Ksiazek, S. R. Zaki, and Nipah Virus Pathology Working Group.** 2002. Nipah virus infection: pathology and pathogenesis of an emerging paramyxoviral zoonosis. Am. J. Pathol. **161:**2153-2167.

115. **Tan, C. T., K. J. Goh, K. T. Wong, S. A. Sarji, K. B. Chua, N. K. Chew, P. Murugasu, Y. L. Loh, H. T. Chong, K. S. Tan, T. Thayaparan, S. Kumar, and M. R. Jusoh.** 2002. Relapsed and late-onset Nipah encephalitis. Ann. Neurol. **51:**703-708. doi: 10.1002/ana.10212.

116. **Wong, K. T., T. Robertson, B. B. Ong, J. W. Chong, K. C. Yaiw, L. F. Wang, A. J. Ansford, and A. Tannenberg.** 2009. Human Hendra virus infection causes acute and relapsing encephalitis. Neuropathol. Appl. Neurobiol. **35:**296-305. doi: 10.1111/j.1365-2990.2008.00991.x; 10.1111/j.1365-2990.2008.00991.x.

117. **Chua, K. B., S. K. Lam, K. J. Goh, P. S. Hooi, T. G. Ksiazek, A. Kamarulzaman, J. Olson, and C. T. Tan.** 2001. The presence of Nipah virus in respiratory secretions and urine of patients during an outbreak of Nipah virus encephalitis in Malaysia. J. Infect. **42:**40-43. doi: 10.1053/jinf.2000.0782 [doi].

118. **Wong, K. T., and K. C. Ong.** 2011. Pathology of acute henipavirus infection in humans and animals. Patholog Res. Int. **2011:**567248. doi: 10.4061/2011/567248; 10.4061/2011/567248.

119. **Mathieu, C., C. Pohl, J. Szecsi, S. Trajkovic-Bodennec, S. Devergnas, H. Raoul, F. L. Cosset, D. Gerlier, T. F. Wild, and B. Horvat.** 2011. Nipah Virus uses leukocytes for efficient dissemination within a host. J. Virol. . doi: 10.1128/JVI.00549-11.

120. **Chua, K. B., S. K. Lam, C. T. Tan, P. S. Hooi, K. J. Goh, N. K. Chew, K. S. Tan, A. Kamarulzaman, and K. T. Wong.** 2000. High mortality in Nipah encephalitis is associated with presence of virus in cerebrospinal fluid. Ann. Neurol. **48:**802-805.

121. **Dhondt, K. P., C. Mathieu, M. Chalons, J. M. Reynaud, A. Vallve, H. Raoul, and B. Horvat.** 2013. Type I interferon signaling protects mice from lethal henipavirus infection. J. Infect. Dis. **207:**142-151. doi: 10.1093/infdis/jis653; 10.1093/infdis/jis653.

122. **Hooper, P. T., H. A. Westbury, and G. M. Russell.** 1997. The lesions of experimental equine morbillivirus disease in cats and guinea pigs. Vet. Pathol. **34:**323-329.

123. **Williamson, M. M., P. T. Hooper, P. W. Selleck, H. A. Westbury, and R. F. Slocombe.** 2000. Experimental hendra virus infectionin pregnant guinea-pigs and fruit Bats (Pteropus poliocephalus). J. Comp. Pathol. **122:**201-207. doi: 10.1053/jcpa.1999.0364.

124. **Torres-Velez, F. J., W. J. Shieh, P. E. Rollin, T. Morken, C. Brown, T. G. Ksiazek, and S. R. Zaki.** 2008. Histopathologic and immunohistochemical characterization of Nipah virus infection in the guinea pig. Vet. Pathol. **45:**576-585. doi: 10.1354/vp.45-4-576; 10.1354/vp.45-4-576.

125. **Middleton, D. J., H. A. Westbury, C. J. Morrissy, B. M. van der Heide, G. M. Russell, M. A. Braun, and A. D. Hyatt.** 2002. Experimental Nipah virus infection in pigs and cats. J. Comp. Pathol. **126:**124-136. doi: 10.1053/jcpa.2001.0532.

126. **Mungall, B. A., D. Middleton, G. Crameri, K. Halpin, J. Bingham, B. T. Eaton, and C. C. Broder.** 2007. Vertical transmission and fetal replication of Nipah virus in an experimentally infected cat. J. Infect. Dis. **196:**812-816. doi: 10.1086/520818.

127. **McEachern, J. A., J. Bingham, G. Crameri, D. J. Green, T. J. Hancock, D. Middleton, Y. R. Feng, C. C. Broder, L. F. Wang, and K. N. Bossart.** 2008. A recombinant subunit vaccine formulation protects against lethal Nipah virus challenge in cats. Vaccine. **26:**3842-3852. doi: 10.1016/j.vaccine.2008.05.016; 10.1016/j.vaccine.2008.05.016.

128. **Guillaume, V., H. Contamin, P. Loth, M. C. Georges-Courbot, A. Lefeuvre, P. Marianneau, K. B. Chua, S. K. Lam, R. Buckland, V. Deubel, and T. F. Wild.** 2004. Nipah virus: vaccination and passive protection studies in a hamster model. J. Virol. **78:**834-840.

129. **Guillaume, V., K. T. Wong, R. Y. Looi, M. C. Georges-Courbot, L. Barrot, R. Buckland, T. F. Wild, and B. Horvat.** 2009. Acute Hendra virus infection: Analysis of the

pathogenesis and passive antibody protection in the hamster model. Virology. **387:**459-465. doi: 10.1016/j.virol.2009.03.001;10.1016/j.virol.2009.03.001.

130. **Rockx, B., D. Brining, J. Kramer, J. Callison, H. Ebihara, K. Mansfield, and H. Feldmann.** 2011. Clinical outcome of henipavirus infection in hamsters is determined by the route and dose of infection. J. Virol. **85:**7658-7671. doi: 10.1128/JVI.00473-11; 10.1128/JVI.00473-11.

131. **Bossart, K. N., Z. Zhu, D. Middleton, J. Klippel, G. Crameri, J. Bingham, J. A. McEachern, D. Green, T. J. Hancock, Y. P. Chan, A. C. Hickey, D. S. Dimitrov, L. F. Wang, and C. C. Broder.** 2009. A neutralizing human monoclonal antibody protects against lethal disease in a new ferret model of acute Nipah virus infection. PLoS Pathog. **5:**e1000642. doi: 10.1371/journal.ppat.1000642;10.1371/journal.ppat.1000642.

132. **Pallister, J., D. Middleton, G. Crameri, M. Yamada, R. Klein, T. J. Hancock, A. Foord, B. Shiell, W. Michalski, C. C. Broder, and L. F. Wang.** 2009. Chloroquine administration does not prevent Nipah virus infection and disease in ferrets. J. Virol. **83:**11979-11982. doi: 10.1128/JVI.01847-09; 10.1128/JVI.01847-09.

133. **Geisbert, T. W., K. M. Daddario-DiCaprio, A. C. Hickey, M. A. Smith, Y. P. Chan, L. F. Wang, J. J. Mattapallil, J. B. Geisbert, K. N. Bossart, and C. C. Broder.** 2010. Development of an acute and highly pathogenic nonhuman primate model of Nipah virus infection. PLoS One. **5:**e10690. doi: 10.1371/journal.pone.0010690.

134. **Hooper, P., S. Zaki, P. Daniels, and D. Middleton.** 2001. Comparative pathology of the diseases caused by Hendra and Nipah viruses. Microbes Infect. **3:**315-322.

135. **Tanimura, N., T. Imada, Y. Kashiwazaki, S. Shamusudin, S. Syed Hassan, A. Jamaluddin, G. Russell, and J. White.** 2004. Reactivity of anti-Nipah virus monoclonal antibodies to formalin-fixed, paraffin-embedded lung tissues from experimental Nipah and Hendra virus infections. J. Vet. Med. Sci. **66:**1263-1266.

136. **Weingartl, H., S. Czub, J. Copps, Y. Berhane, D. Middleton, P. Marszal, J. Gren, G. Smith, S. Ganske, L. Manning, and M. Czub.** 2005. Invasion of the central nervous system in a porcine host by Nipah virus. J. Virol. **79:**7528-7534. doi: 10.1128/JVI.79.12.7528-7534.2005.

137. **Berhane, Y., H. M. Weingartl, J. Lopez, J. Neufeld, S. Czub, C. Embury-Hyatt, M. Goolia, J. Copps, and M. Czub.** 2008. Bacterial infections in pigs experimentally infected with Nipah virus. Transbound Emerg. Dis. **55:**165-174. doi: 10.1111/j.1865-1682.2008.01021.x.

138. **Weingartl, H. M., Y. Berhane, J. L. Caswell, S. Loosmore, J. C. Audonnet, J. A. Roth, and M. Czub.** 2006. Recombinant nipah virus vaccines protect pigs against challenge. J. Virol. **80:**7929-7938. doi: 10.1128/JVI.00263-06.

139. **Weingartl, H. M., Y. Berhane, T. Hisanaga, J. Neufeld, H. Kehler, C. Emburry-Hyatt, K. Hooper-McGreevy, S. Kasloff, B. Dalman, J. Bystrom, S. Alexandersen, Y. Li, and J.**

Pasick. 2010. Genetic and pathobiologic characterization of pandemic H1N1 2009 influenza viruses from a naturally infected swine herd. J. Virol. **84:**2245-2256. doi: 10.1128/JVI.02118-09.

140. **Biron, C. A.** 1999. Initial and innate responses to viral infections--pattern setting in immunity or disease. Curr. Opin. Microbiol. **2:**374-381.

141. **Akira, S., K. Takeda, and T. Kaisho.** 2001. Toll-like receptors: critical proteins linking innate and acquired immunity. Nat. Immunol. **2:**675-680. doi: 10.1038/90609.

142. **Yang, L., and E. Seki.** 2012. Toll-like receptors in liver fibrosis: cellular crosstalk and mechanisms. Front. Physiol. **3:**138. doi: 10.3389/fphys.2012.00138 [doi].

143. **Prakash, A., E. Smith, C. K. Lee, and D. E. Levy.** 2005. Tissue-specific positive feedback requirements for production of type I interferon following virus infection. J. Biol. Chem. **280:**18651-18657. doi: 10.1074/jbc.M501289200.

144. **Kitagawa, Y., M. Yamaguchi, M. Zhou, T. Komatsu, M. Nishio, T. Sugiyama, K. Takeuchi, M. Itoh, and B. Gotoh.** 2011. A tryptophan-rich motif in the human parainfluenza virus type 2 V protein is critical for the blockade of toll-like receptor 7 (TLR7)- and TLR9-dependent signaling. J. Virol. **85:**4606-4611. doi: 10.1128/JVI.02012-10 [doi].

145. **Thompson, M. R., J. J. Kaminski, E. A. Kurt-Jones, and K. A. Fitzgerald.** 2011. Pattern recognition receptors and the innate immune response to viral infection. Viruses. **3:**920-940. doi: 10.3390/v3060920; 10.3390/v3060920.

146. **Kawai, T., K. Takahashi, S. Sato, C. Coban, H. Kumar, H. Kato, K. J. Ishii, O. Takeuchi, and S. Akira.** 2005. IPS-1, an adaptor triggering RIG-I- and Mda5-mediated type I interferon induction. Nat. Immunol. **6:**981-988. doi: 10.1038/ni1243.

147. **Seth, R. B., L. Sun, C. K. Ea, and Z. J. Chen.** 2005. Identification and characterization of MAVS, a mitochondrial antiviral signaling protein that activates NF-kappaB and IRF 3. Cell. **122:**669-682. doi: 10.1016/j.cell.2005.08.012.

148. **Xu, L. G., Y. Y. Wang, K. J. Han, L. Y. Li, Z. Zhai, and H. B. Shu.** 2005. VISA is an adapter protein required for virus-triggered IFN-beta signaling. Mol. Cell. **19:**727-740. doi: 10.1016/j.molcel.2005.08.014.

149. **Meylan, E., and J. Tschopp.** 2006. Toll-like receptors and RNA helicases: two parallel ways to trigger antiviral responses. Mol. Cell. **22:**561-569. doi: 10.1016/j.molcel.2006.05.012.

150. **Kawai, T., and S. Akira.** 2007. Antiviral signaling through pattern recognition receptors. J. Biochem. **141:**137-145. doi: 10.1093/jb/mvm032.

151. **Habjan, M., I. Andersson, J. Klingstrom, M. Schumann, A. Martin, P. Zimmermann, V. Wagner, A. Pichlmair, U. Schneider, E. Muhlberger, A. Mirazimi, and F. Weber.** 2008. Processing of genome 5' termini as a strategy of negative-strand RNA viruses to avoid RIG-I-

dependent interferon induction. PLoS One. **3:**e2032. doi: 10.1371/journal.pone.0002032; 10.1371/journal.pone.0002032.

152. **Stark, G. R.** 2007. How cells respond to interferons revisited: from early history to current complexity. Cytokine Growth Factor Rev. **18:**419-423. doi: 10.1016/j.cytogfr.2007.06.013.

153. **Randall, R. E., and S. Goodbourn.** 2008. Interferons and viruses: an interplay between induction, signalling, antiviral responses and virus countermeasures. J. Gen. Virol. **89:**1-47. doi: 10.1099/vir.0.83391-0.

154. **Theofilopoulos, A. N., R. Baccala, B. Beutler, and D. H. Kono.** 2005. Type I interferons (alpha/beta) in immunity and autoimmunity. Annu. Rev. Immunol. **23:**307-336. doi: 10.1146/annurev.immunol.23.021704.115843.

155. **Stahl, N., T. J. Farruggella, T. G. Boulton, Z. Zhong, J. E. Darnell Jr, and G. D. Yancopoulos.** 1995. Choice of STATs and other substrates specified by modular tyrosine-based motifs in cytokine receptors. Science. **267:**1349-1353.

156. **Improta, T., C. Schindler, C. M. Horvath, I. M. Kerr, G. R. Stark, and J. E. Darnell Jr.** 1994. Transcription factor ISGF-3 formation requires phosphorylated Stat91 protein, but Stat113 protein is phosphorylated independently of Stat91 protein. Proc. Natl. Acad. Sci. U. S. A. **91:**4776-4780.

157. **Fu, X. Y., D. S. Kessler, S. A. Veals, D. E. Levy, and J. E. Darnell Jr.** 1990. ISGF3, the transcriptional activator induced by interferon alpha, consists of multiple interacting polypeptide chains. Proc. Natl. Acad. Sci. U. S. A. **87:**8555-8559.

158. **Kessler, D. S., S. A. Veals, X. Y. Fu, and D. E. Levy.** 1990. Interferon-alpha regulates nuclear translocation and DNA-binding affinity of ISGF3, a multimeric transcriptional activator. Genes Dev. **4:**1753-1765.

159. **Reich, N., B. Evans, D. Levy, D. Fahey, E. Knight Jr, and J. E. Darnell Jr.** 1987. Interferon-induced transcription of a gene encoding a 15-kDa protein depends on an upstream enhancer element. Proc. Natl. Acad. Sci. U. S. A. **84:**6394-6398.

160. **Levy, D. E., D. S. Kessler, R. Pine, N. Reich, and J. E. Darnell Jr.** 1988. Interferon-induced nuclear factors that bind a shared promoter element correlate with positive and negative transcriptional control. Genes Dev. **2:**383-393.

161. **Levy, D. E., D. J. Lew, T. Decker, D. S. Kessler, and J. E. Darnell Jr.** 1990. Synergistic interaction between interferon-alpha and interferon-gamma through induced synthesis of one subunit of the transcription factor ISGF3. EMBO J. **9:**1105-1111.

162. **Shuai, K.** 1994. Interferon-activated signal transduction to the nucleus. Curr. Opin. Cell Biol. **6:**253-259.

163. **Decker, T., D. J. Lew, and J. E. Darnell Jr.** 1991. Two distinct alpha-interferon-dependent signal transduction pathways may contribute to activation of transcription of the guanylate-binding protein gene. Mol. Cell. Biol. **11:**5147-5153.

164. **Uddin, S., B. Majchrzak, J. Woodson, P. Arunkumar, Y. Alsayed, R. Pine, P. R. Young, E. N. Fish, and L. C. Platanias.** 1999. Activation of the p38 mitogen-activated protein kinase by type I interferons. J. Biol. Chem. **274:**30127-30131.

165. **Arora, T., G. Floyd-Smith, M. J. Espy, and D. F. Jelinek.** 1999. Dissociation between IFN-alpha-induced anti-viral and growth signaling pathways. J. Immunol. **162:**3289-3297.

166. **Zhao, L. J., X. Hua, S. F. He, H. Ren, and Z. T. Qi.** 2011. Interferon alpha regulates MAPK and STAT1 pathways in human hepatoma cells. Virol. J. **8:**157-422X-8-157. doi: 10.1186/1743-422X-8-157; 10.1186/1743-422X-8-157.

167. **Chan, E. D., B. W. Winston, S. T. Uh, M. W. Wynes, D. M. Rose, and D. W. Riches.** 1999. Evaluation of the role of mitogen-activated protein kinases in the expression of inducible nitric oxide synthase by IFN-gamma and TNF-alpha in mouse macrophages. J. Immunol. **162:**415-422.

168. **Li, Y., S. Batra, A. Sassano, B. Majchrzak, D. E. Levy, M. Gaestel, E. N. Fish, R. J. Davis, and L. C. Platanias.** 2005. Activation of mitogen-activated protein kinase kinase (MKK) 3 and MKK6 by type I interferons. J. Biol. Chem. **280:**10001-10010. doi: 10.1074/jbc.M410972200.

169. **Blank, V. C., C. Pena, and L. P. Roguin.** 2010. STAT1, STAT3 and p38MAPK are involved in the apoptotic effect induced by a chimeric cyclic interferon-alpha2b peptide. Exp. Cell Res. **316:**603-614. doi: 10.1016/j.yexcr.2009.11.016; 10.1016/j.yexcr.2009.11.016.

170. **Marchant, D., G. K. Singhera, S. Utokaparch, T. L. Hackett, J. H. Boyd, Z. Luo, X. Si, D. R. Dorscheid, B. M. McManus, and R. G. Hegele.** 2010. Toll-like receptor 4-mediated activation of p38 mitogen-activated protein kinase is a determinant of respiratory virus entry and tropism. J. Virol. **84:**11359-11373. doi: 10.1128/JVI.00804-10; 10.1128/JVI.00804-10.

171. **Junttila, M. R., S. P. Li, and J. Westermarck.** 2008. Phosphatase-mediated crosstalk between MAPK signaling pathways in the regulation of cell survival. FASEB J. **22:**954-965. doi: 10.1096/fj.06-7859rev.

172. **Schaeffer, H. J., and M. J. Weber.** 1999. Mitogen-activated protein kinases: specific messages from ubiquitous messengers. Mol. Cell. Biol. **19:**2435-2444.

173. **Davis, R. J.** 2000. Signal transduction by the JNK group of MAP kinases. Cell. **103:**239-252.

174. **Zhao, L. J., L. Wang, H. Ren, J. Cao, L. Li, J. S. Ke, and Z. T. Qi.** 2005. Hepatitis C virus E2 protein promotes human hepatoma cell proliferation through the MAPK/ERK signaling pathway via cellular receptors. Exp. Cell Res. **305:**23-32. doi: 10.1016/j.yexcr.2004.12.024.

175. **Mazzocca, A., S. C. Sciammetta, V. Carloni, L. Cosmi, F. Annunziato, T. Harada, S. Abrignani, and M. Pinzani.** 2005. Binding of hepatitis C virus envelope protein E2 to CD81 up-regulates matrix metalloproteinase-2 in human hepatic stellate cells. J. Biol. Chem. **280:**11329-11339. doi: 10.1074/jbc.M410161200.

176. **Balabanian, K., J. Harriague, C. Decrion, B. Lagane, S. Shorte, F. Baleux, J. L. Virelizier, F. Arenzana-Seisdedos, and L. A. Chakrabarti.** 2004. CXCR4-tropic HIV-1 envelope glycoprotein functions as a viral chemokine in unstimulated primary CD4+ T lymphocytes. J. Immunol. **173:**7150-7160.

177. **Torres, NI., Castilla, V., Washsman, M.,** 2012. DHEA inhibits measles virus through a mechanism independent of its ability to modulate the RAF/MEK/ERK signaling pathway. Future Virol. 7, 1115-1125.

178. **Kong, X., H. San Juan, A. Behera, M. E. Peeples, J. Wu, R. F. Lockey, and S. S. Mohapatra.** 2004. ERK-1/2 activity is required for efficient RSV infection. FEBS Lett. **559:**33-38. doi: 10.1016/S0014-5793(04)00002-X.

179. **Takeyama, K., K. Dabbagh, H. M. Lee, C. Agusti, J. A. Lausier, I. F. Ueki, K. M. Grattan, and J. A. Nadel.** 1999. Epidermal growth factor system regulates mucin production in airways. Proc. Natl. Acad. Sci. U. S. A. **96:**3081-3086.

180. **Zhu, L., P. K. Lee, W. M. Lee, Y. Zhao, D. Yu, and Y. Chen.** 2009. Rhinovirus-induced major airway mucin production involves a novel TLR3-EGFR-dependent pathway. Am. J. Respir. Cell Mol. Biol. **40:**610-619. doi: 10.1165/rcmb.2008-0223OC [doi].

181. **Griego, S. D., C. B. Weston, J. L. Adams, R. Tal-Singer, and S. B. Dillon.** 2000. Role of p38 mitogen-activated protein kinase in rhinovirus-induced cytokine production by bronchial epithelial cells. J. Immunol. **165:**5211-5220.

182. **Banerjee, S., K. Narayanan, T. Mizutani, and S. Makino.** 2002. Murine coronavirus replication-induced p38 mitogen-activated protein kinase activation promotes interleukin-6 production and virus replication in cultured cells. J. Virol. **76:**5937-5948.

183. **Lee, C., B. Tomkowicz, B. D. Freedman, and R. G. Collman.** 2005. HIV-1 gp120-induced TNF-{alpha} production by primary human macrophages is mediated by phosphatidylinositol-3 (PI-3) kinase and mitogen-activated protein (MAP) kinase pathways. J. Leukoc. Biol. **78:**1016-1023. doi: 10.1189/jlb.0105056.

184. **Regan, A. D., R. D. Cohen, and G. R. Whittaker.** 2009. Activation of p38 MAPK by feline infectious peritonitis virus regulates pro-inflammatory cytokine production in primary

blood-derived feline mononuclear cells. Virology. **384:**135-143. doi: 10.1016/j.virol.2008.11.006; 10.1016/j.virol.2008.11.006.

185. **Rincon, M., H. Enslen, J. Raingeaud, M. Recht, T. Zapton, M. S. Su, L. A. Penix, R. J. Davis, and R. A. Flavell.** 1998. Interferon-gamma expression by Th1 effector T cells mediated by the p38 MAP kinase signaling pathway. EMBO J. **17:**2817-2829. doi: 10.1093/emboj/17.10.2817.

186. **Dong, C., R. J. Davis, and R. A. Flavell.** 2002. MAP kinases in the immune response. Annu. Rev. Immunol. **20:**55-72. doi: 10.1146/annurev.immunol.20.091301.131133.

187. **Dodeller, F., and H. Schulze-Koops.** 2006. The p38 mitogen-activated protein kinase signaling cascade in CD4 T cells. Arthritis Res. Ther. **8:**205. doi: 10.1186/ar1905.

188. **Goodbourn, S., L. Didcock, and R. E. Randall.** 2000. Interferons: cell signalling, immune modulation, antiviral response and virus countermeasures. J. Gen. Virol. **81:**2341-2364.

189. **Lu, G., J. T. Reinert, I. Pitha-Rowe, A. Okumura, M. Kellum, K. P. Knobeloch, B. Hassel, and P. M. Pitha.** 2006. ISG15 enhances the innate antiviral response by inhibition of IRF-3 degradation. Cell. Mol. Biol. (Noisy-Le-Grand). **52:**29-41.

190. **Virtue, E. R., G. A. Marsh, and L. F. Wang.** 2011. Interferon signaling remains functional during henipavirus infection of human cell lines. J. Virol. **85:**4031-4034. doi: 10.1128/JVI.02412-10.

191. **Nanduri, S., F. Rahman, B. R. Williams, and J. Qin.** 2000. A dynamically tuned double-stranded RNA binding mechanism for the activation of antiviral kinase PKR. EMBO J. **19:**5567-5574. doi: 10.1093/emboj/19.20.5567.

192. **Garcia, M. A., J. Gil, I. Ventoso, S. Guerra, E. Domingo, C. Rivas, and M. Esteban.** 2006. Impact of protein kinase PKR in cell biology: from antiviral to antiproliferative action. Microbiol. Mol. Biol. Rev. **70:**1032-1060. doi: 10.1128/MMBR.00027-06.

193. **Kakugawa, S., M. Shimojima, H. Goto, T. Horimoto, N. Oshimori, G. Neumann, T. Yamamoto, and Y. Kawaoka.** 2009. Mitogen-activated protein kinase-activated kinase RSK2 plays a role in innate immune responses to influenza virus infection. J. Virol. **83:**2510-2517. doi: 10.1128/JVI.02416-08; 10.1128/JVI.02416-08.

194. **Dauber, B., L. Martinez-Sobrido, J. Schneider, R. Hai, Z. Waibler, U. Kalinke, A. Garcia-Sastre, and T. Wolff.** 2009. Influenza B virus ribonucleoprotein is a potent activator of the antiviral kinase PKR. PLoS Pathog. **5:**e1000473. doi: 10.1371/journal.ppat.1000473; 10.1371/journal.ppat.1000473.

195. **Meurs, E., K. Chong, J. Galabru, N. S. Thomas, I. M. Kerr, B. R. Williams, and A. G. Hovanessian.** 1990. Molecular cloning and characterization of the human double-stranded RNA-activated protein kinase induced by interferon. Cell. **62:**379-390.

196. **Haller, O., P. Staeheli, and G. Kochs.** 2007. Interferon-induced Mx proteins in antiviral host defense. Biochimie. **89:**812-818. doi: 10.1016/j.biochi.2007.04.015.

197. **Kang, J. I., S. N. Kwon, S. H. Park, Y. K. Kim, S. Y. Choi, J. P. Kim, and B. Y. Ahn.** 2009. PKR protein kinase is activated by hepatitis C virus and inhibits viral replication through translational control. Virus Res. **142:**51-56. doi: 10.1016/j.virusres.2009.01.007; 10.1016/j.virusres.2009.01.007.

198. **Silverman, R. H.** 2007. Viral encounters with 2',5'-oligoadenylate synthetase and RNase L during the interferon antiviral response. J. Virol. **81:**12720-12729. doi: 10.1128/JVI.01471-07.

199. **Williams, M. A., and M. J. Bevan.** 2007. Effector and memory CTL differentiation. Annu. Rev. Immunol. **25:**171-192. doi: 10.1146/annurev.immunol.25.022106.141548.

200. **Le Bon, A., N. Etchart, C. Rossmann, M. Ashton, S. Hou, D. Gewert, P. Borrow, and D. F. Tough.** 2003. Cross-priming of CD8+ T cells stimulated by virus-induced type I interferon. Nat. Immunol. **4:**1009-1015. doi: 10.1038/ni978.

201. **Lawrence, C. W., R. M. Ream, and T. J. Braciale.** 2005. Frequency, specificity, and sites of expansion of CD8+ T cells during primary pulmonary influenza virus infection. J. Immunol. **174:**5332-5340.

202. **Yoon, H., K. L. Legge, S. S. Sung, and T. J. Braciale.** 2007. Sequential activation of CD8+ T cells in the draining lymph nodes in response to pulmonary virus infection. J. Immunol. **179:**391-399.

203. **Zhu, J., H. Yamane, and W. E. Paul.** 2010. Differentiation of effector CD4 T cell populations (*). Annu. Rev. Immunol. **28:**445-489. doi: 10.1146/annurev-immunol-030409-101212; 10.1146/annurev-immunol-030409-101212.

204. **Binns, R. M., and R. Pabst.** 1994. Lymphoid tissue structure and lymphocyte trafficking in the pig. Vet. Immunol. Immunopathol. **43:**79-87.

205. **Reddy, N. R., P. Borgs, and B. N. Wilkie.** 2000. Cytokine mRNA expression in leukocytes of efferent lymph from stimulated lymph nodes in pigs. Vet. Immunol. Immunopathol. **74:**31-46.

206. **Binns, R. M., I. A. Duncan, S. J. Powis, A. Hutchings, and G. W. Butcher.** 1992. Subsets of null and gamma delta T-cell receptor+ T lymphocytes in the blood of young pigs identified by specific monoclonal antibodies. Immunology. **77:**219-227.

207. **Zuckermann, F. A., and R. J. Husmann.** 1996. Functional and phenotypic analysis of porcine peripheral blood CD4/CD8 double-positive T cells. Immunology. **87:**500-512.

208. **Narita, M., K. Kawashima, K. Kimura, O. Mikami, T. Shibahara, S. Yamada, and Y. Sakoda.** 2000. Comparative immunohistopathology in pigs infected with highly virulent or less virulent strains of hog cholera virus. Vet. Pathol. **37:**402-408.

209. **Yang, H., and R. M. Parkhouse.** 1996. Phenotypic classification of porcine lymphocyte subpopulations in blood and lymphoid tissues. Immunology. **89:**76-83.

210. **Charerntantanakul, W., R. Platt, and J. A. Roth.** 2006. Effects of porcine reproductive and respiratory syndrome virus-infected antigen-presenting cells on T cell activation and antiviral cytokine production. Viral Immunol. **19:**646-661. doi: 10.1089/vim.2006.19.646.

211. **Chong, H. T., A. Kamarulzaman, C. T. Tan, K. J. Goh, T. Thayaparan, S. R. Kunjapan, N. K. Chew, K. B. Chua, and S. K. Lam.** 2001. Treatment of acute Nipah encephalitis with ribavirin. Ann. Neurol. **49:**810-813.

212. **Georges-Courbot, M. C., H. Contamin, C. Faure, P. Loth, S. Baize, P. Leyssen, J. Neyts, and V. Deubel.** 2006. Poly(I)-poly(C12U) but not ribavirin prevents death in a hamster model of Nipah virus infection. Antimicrob. Agents Chemother. **50:**1768-1772. doi: 10.1128/AAC.50.5.1768-1772.2006.

213. **Freiberg, A. N., M. N. Worthy, B. Lee, and M. R. Holbrook.** 2010. Combined chloroquine and ribavirin treatment does not prevent death in a hamster model of Nipah and Hendra virus infection. J. Gen. Virol. **91:**765-772. doi: 10.1099/vir.0.017269-0; 10.1099/vir.0.017269-0.

214. **Guillaume, V., H. Contamin, P. Loth, I. Grosjean, M. C. Courbot, V. Deubel, R. Buckland, and T. F. Wild.** 2006. Antibody prophylaxis and therapy against Nipah virus infection in hamsters. J. Virol. **80:**1972-1978. doi: 10.1128/JVI.80.4.1972-1978.2006.

215. **Zhu, Z., A. S. Dimitrov, K. N. Bossart, G. Crameri, K. A. Bishop, V. Choudhry, B. A. Mungall, Y. R. Feng, A. Choudhary, M. Y. Zhang, Y. Feng, L. F. Wang, X. Xiao, B. T. Eaton, C. C. Broder, and D. S. Dimitrov.** 2006. Potent neutralization of Hendra and Nipah viruses by human monoclonal antibodies. J. Virol. **80:**891-899. doi: 10.1128/JVI.80.2.891-899.2006.

216. **Chua, K. B.** 2010. Epidemiology, surveillance and control of Nipah virus infections in Malaysia. Malays. J. Pathol. **32:**69-73.

217. **Kong, D., Z. Wen, H. Su, J. Ge, W. Chen, X. Wang, C. Wu, C. Yang, H. Chen, and Z. Bu.** 2012. Newcastle disease virus-vectored Nipah encephalitis vaccines induce B and T cell responses in mice and long-lasting neutralizing antibodies in pigs. Virology. **432:**327-335. doi: 10.1016/j.virol.2012.06.001 [doi].

218. **Yoneda, M., M. C. Georges-Courbot, F. Ikeda, M. Ishii, N. Nagata, F. Jacquot, H. Raoul, H. Sato, and C. Kai.** 2013. Recombinant measles virus vaccine expressing the Nipah

virus glycoprotein protects against lethal Nipah virus challenge. PLoS One. **8:**e58414. doi: 10.1371/journal.pone.0058414 [doi].

219. **Chattopadhyay, A., and J. K. Rose.** 2010. Complementing defective viruses expressing separate paramyxovirus glycoproteins provide a new vaccine vector approach. J. Virol. . doi: 10.1128/JVI.01852-10.

220. **Mire, C. E., K. M. Versteeg, R. W. Cross, K. N. Agans, K. A. Fenton, M. A. Whitt, and T. W. Geisbert.** 2013. Single injection recombinant vesicular stomatitis virus vaccines protect ferrets against lethal Nipah virus disease. Virol. J. **10:**353-422X-10-353. doi: 10.1186/1743-422X-10-353 [doi].

221. **DeBuysscher, B. L., E. de Wit, V. J. Munster, D. Scott, H. Feldmann, and J. Prescott.** 2013. Comparison of the pathogenicity of Nipah virus isolates from Bangladesh and Malaysia in the Syrian hamster. PLoS Negl Trop. Dis. **7:**e2024. doi: 10.1371/journal.pntd.0002024; 10.1371/journal.pntd.0002024.

222. **Broder, C. C., T. W. Geisbert, K. Xu, D. B. Nikolov, L. F. Wang, D. Middleton, J. Pallister, and K. N. Bossart.** 2012. Immunization strategies against henipaviruses. Curr. Top. Microbiol. Immunol. **359:**197-223. doi: 10.1007/82_2012_213; 10.1007/82_2012_213.

223. **Pallister, J. A., R. Klein, R. Arkinstall, J. Haining, F. Long, J. R. White, J. Payne, Y. R. Feng, L. F. Wang, C. C. Broder, and D. Middleton.** 2013. Vaccination of ferrets with a recombinant G glycoprotein subunit vaccine provides protection against Nipah virus disease for over 12 months. Virol. J. **10:**237-422X-10-237. doi: 10.1186/1743-422X-10-237 [doi].

224. **Bossart, K. N., B. Rockx, F. Feldmann, D. Brining, D. Scott, R. LaCasse, J. B. Geisbert, Y. R. Feng, Y. P. Chan, A. C. Hickey, C. C. Broder, H. Feldmann, and T. W. Geisbert.** 2012. A Hendra virus G glycoprotein subunit vaccine protects African green monkeys from Nipah virus challenge. Sci. Transl. Med. **4:**146ra107. doi: 10.1126/scitranslmed.3004241 [doi].

225. **Richmond, R.** 2012. The Hendra vaccine has arrived. Aust. Vet. J. **90:**N2-0813.2012.00087.GRP.x. doi: 10.1111/j.1751-0813.2012.00087.GRP.x [doi].

226. **Goh, K. C., S. J. Haque, and B. R. Williams.** 1999. p38 MAP kinase is required for STAT1 serine phosphorylation and transcriptional activation induced by interferons. EMBO J. **18:**5601-5608. doi: 10.1093/emboj/18.20.5601.

227. **Mayer, I. A., A. Verma, I. M. Grumbach, S. Uddin, F. Lekmine, F. Ravandi, B. Majchrzak, S. Fujita, E. N. Fish, and L. C. Platanias.** 2001. The p38 MAPK pathway mediates the growth inhibitory effects of interferon-alpha in BCR-ABL-expressing cells. J. Biol. Chem. **276:**28570-28577. doi: 10.1074/jbc.M011685200.

228. **Charerntantanakul, W., and J. A. Roth.** 2006. Biology of porcine T lymphocytes. Anim. Health. Res. Rev. **7:**81-96. doi: 10.1017/S1466252307001235.

229. **Griffin, D. E.** 1995. Immune responses during measles virus infection. Curr. Top. Microbiol. Immunol. **191:**117-134.

230. **Slifka, M. K., D. Homann, A. Tishon, R. Pagarigan, and M. B. Oldstone.** 2003. Measles virus infection results in suppression of both innate and adaptive immune responses to secondary bacterial infection. J. Clin. Invest. **111:**805-810. doi: 10.1172/JCI13603 [doi].

231. **Riddell, M. A., W. J. Moss, D. Hauer, M. Monze, and D. E. Griffin.** 2007. Slow clearance of measles virus RNA after acute infection. J. Clin. Virol. **39:**312-317. doi: S1386-6532(07)00180-1 [pii].

232. **Weingartl, H. M., M. Sabara, J. Pasick, E. van Moorlehem, and L. Babiuk.** 2002. Continuous porcine cell lines developed from alveolar macrophages: partial characterization and virus susceptibility. J. Virol. Methods. **104:**203-216.

233. **Volf, J., F. Boyen, M. Faldyna, B. Pavlova, J. Navratilova, and I. Rychlik.** 2007. Cytokine response of porcine cell lines to Salmonella enterica serovar typhimurium and its hilA and ssrA mutants. Zoonoses Public. Health. **54:**286-293. doi: 10.1111/j.1863-2378.2007.01064.x.

234. **Dawson, H. D., E. Beshah, S. Nishi, G. Solano-Aguilar, M. Morimoto, A. Zhao, K. B. Madden, T. K. Ledbetter, J. P. Dubey, T. Shea-Donohue, J. K. Lunney, and J. F. Urban Jr.** 2005. Localized multigene expression patterns support an evolving Th1/Th2-like paradigm in response to infections with Toxoplasma gondii and Ascaris suum. Infect. Immun. **73:**1116-1128. doi: 10.1128/IAI.73.2.1116-1128.2005.

235. **Livak, K. J., and T. D. Schmittgen.** 2001. Analysis of relative gene expression data using real-time quantitative PCR and the 2(-Delta Delta C(T)) Method. Methods. **25:**402-408. doi: 10.1006/meth.2001.1262.

236. **Silversides, D. W., N. Music, M. Jacques, C. A. Gagnon, and R. Webby.** 2010. Investigation of the species origin of the St. Jude Porcine Lung epithelial cell line (SJPL) made available to researchers. J. Virol. **84:**5454-5455. doi: 10.1128/JVI.00042-10 [doi].

237. **Mikkelsen, S. S., S. B. Jensen, S. Chiliveru, J. Melchjorsen, I. Julkunen, M. Gaestel, J. S. Arthur, R. A. Flavell, S. Ghosh, and S. R. Paludan.** 2009. RIG-I-mediated activation of p38 MAPK is essential for viral induction of interferon and activation of dendritic cells: dependence on TRAF2 and TAK1. J. Biol. Chem. **284:**10774-10782. doi: 10.1074/jbc.M807272200 [doi].

238. **McCullough, K. C., N. Ruggli, and A. Summerfield.** 2009. Dendritic cells--at the front-line of pathogen attack. Vet. Immunol. Immunopathol. **128:**7-15. doi: 10.1016/j.vetimm.2008.10.290.

239. **Goolia M**. 2008. The expression and localization of V and W accessory proteins in porcine and human cells infected with Nipah virus. Department of Medical Microbiology, University of Manitoba. Winnipeg, Manitoba, Canada.

240. **Beck, M. A., N. M. Chapman, B. M. McManus, J. C. Mullican, and S. Tracy.** 1990. Secondary enterovirus infection in the murine model of myocarditis. Pathologic and immunologic aspects. Am. J. Pathol. **136:**669-681.

241. **Goh, K. C., M. J. deVeer, and B. R. Williams.** 2000. The protein kinase PKR is required for p38 MAPK activation and the innate immune response to bacterial endotoxin. EMBO J. **19:**4292-4297. doi: 10.1093/emboj/19.16.4292.

242. **Uddin, S., F. Lekmine, N. Sharma, B. Majchrzak, I. Mayer, P. R. Young, G. M. Bokoch, E. N. Fish, and L. C. Platanias.** 2000. The Rac1/p38 mitogen-activated protein kinase pathway is required for interferon alpha-dependent transcriptional activation but not serine phosphorylation of Stat proteins. J. Biol. Chem. **275:**27634-27640. doi: 10.1074/jbc.M003170200.

243. **Davies, S. P., H. Reddy, M. Caivano, and P. Cohen.** 2000. Specificity and mechanism of action of some commonly used protein kinase inhibitors. Biochem. J. **351:**95-105.

244. **Adler, V., Y. Qu, S. J. Smith, L. Izotova, S. Pestka, H. F. Kung, M. Lin, F. K. Friedman, L. Chie, D. Chung, M. Boutjdir, and M. R. Pincus.** 2005. Functional interactions of Raf and MEK with Jun-N-terminal kinase (JNK) result in a positive feedback loop on the oncogenic Ras signaling pathway. Biochemistry. **44:**10784-10795. doi: 10.1021/bi050619j.

245. **Ohori, M., T. Kinoshita, M. Okubo, K. Sato, A. Yamazaki, H. Arakawa, S. Nishimura, N. Inamura, H. Nakajima, M. Neya, H. Miyake, and T. Fujii.** 2005. Identification of a selective ERK inhibitor and structural determination of the inhibitor-ERK2 complex. Biochem. Biophys. Res. Commun. **336:**357-363. doi: 10.1016/j.bbrc.2005.08.082.

246. **Gerner, W., T. Kaser, and A. Saalmuller.** 2009. Porcine T lymphocytes and NK cells--an update. Dev. Comp. Immunol. **33:**310-320. doi: 10.1016/j.dci.2008.06.003.

247. **Saalmuller, A., G. Kuebart, E. Hollemweguer, Z. Chen, J. Nielsen, F. Zuckermann, and K. Haverson.** 2001. Summary of workshop findings for porcine T-lymphocyte-specific monoclonal antibodies. Vet. Immunol. Immunopathol. **80:**35-52.

248. **Escoffier, C., S. Manie, S. Vincent, C. P. Muller, M. Billeter, and D. Gerlier.** 1999. Nonstructural C protein is required for efficient measles virus replication in human peripheral blood cells. J. Virol. **73:**1695-1698.

249. **De Bruin, T. G., E. M. Van Rooij, Y. E. De Visser, and A. T. Bianchi.** 2000. Cytolytic function for pseudorabies virus-stimulated porcine CD4+ CD8dull+ lymphocytes. Viral Immunol. **13:**511-520.

250. **Ober, B. T., A. Summerfield, C. Mattlinger, K. H. Wiesmuller, G. Jung, E. Pfaff, A. Saalmuller, and H. J. Rziha.** 1998. Vaccine-induced, pseudorabies virus-specific, extrathymic CD4+CD8+ memory T-helper cells in swine. J. Virol. **72:**4866-4873.

251. **Abbas, A. K., M. E. Williams, H. J. Burstein, T. L. Chang, P. Bossu, and A. H. Lichtman.** 1991. Activation and functions of CD4+ T-cell subsets. Immunol. Rev. **123:**5-22.

252. **Zheng, L., G. Fisher, R. E. Miller, J. Peschon, D. H. Lynch, and M. J. Lenardo.** 1995. Induction of apoptosis in mature T cells by tumour necrosis factor. Nature. **377:**348-351. doi: 10.1038/377348a0 [doi].

253. **van Reeth, K., and H. Nauwynck.** 2000. Proinflammatory cytokines and viral respiratory disease in pigs. Vet. Res. **31:**187-213. doi: 10.1051/vetres:2000113.

254. **Bianchi, A. T., R. J. Zwart, S. H. Jeurissen, and H. W. Moonen-Leusen.** 1992. Development of the B- and T-cell compartments in porcine lymphoid organs from birth to adult life: an immunohistological approach. Vet. Immunol. Immunopathol. **33:**201-221.

255. **Bohdanowicz, M., D. Schlam, M. Hermansson, D. Rizzuti, G. D. Fairn, T. Ueyama, P. Somerharju, G. Du, and S. Grinstein.** 2013. Phosphatidic acid is required for the constitutive ruffling and macropinocytosis of phagocytes. Mol. Biol. Cell. **24:**1700-12, S1-7. doi: 10.1091/mbc.E12-11-0789; 10.1091/mbc.E12-11-0789.

256. **Sharma, N. R., P. Mani, N. Nandwani, R. Mishra, A. Rana, and D. P. Sarkar.** 2010. Reciprocal regulation of AKT and MAP kinase dictates virus-host cell fusion. J. Virol. **84:**4366-4382. doi: 10.1128/JVI.01940-09; 10.1128/JVI.01940-09.

257. **Merritt, C., H. Enslen, N. Diehl, D. Conze, R. J. Davis, and M. Rincon.** 2000. Activation of p38 mitogen-activated protein kinase in vivo selectively induces apoptosis of CD8(+) but not CD4(+) T cells. Mol. Cell. Biol. **20:**936-946.

258. **Haller, O., G. Kochs, and F. Weber.** 2006. The interferon response circuit: induction and suppression by pathogenic viruses. Virology. **344:**119-130. doi: 10.1016/j.virol.2005.09.024.

259. **Sumbayev, V. V., and I. M. Yasinska.** 2006. Role of MAP kinase-dependent apoptotic pathway in innate immune responses and viral infection. Scand. J. Immunol. **63:**391-400. doi: 10.1111/j.1365-3083.2006.001764.x.

260. **Seo, Y. J., and B. Hahm.** 2010. Type I interferon modulates the battle of host immune system against viruses. Adv. Appl. Microbiol. **73:**83-101. doi: 10.1016/S0065-2164(10)73004-5.

261. **Katsoulidis, E., Y. Li, H. Mears, and L. C. Platanias.** 2005. The p38 mitogen-activated protein kinase pathway in interferon signal transduction. J. Interferon Cytokine Res. **25:**749-756. doi: 10.1089/jir.2005.25.749.

262. **Saccani, S., S. Pantano, and G. Natoli.** 2002. p38-Dependent marking of inflammatory genes for increased NF-kappa B recruitment. Nat. Immunol. **3:**69-75. doi: 10.1038/ni748.

263. **Muthumani, K., S. A. Wadsworth, N. S. Dayes, D. S. Hwang, A. Y. Choo, H. R. Abeysinghe, J. J. Siekierka, and D. B. Weiner.** 2004. Suppression of HIV-1 viral replication and cellular pathogenesis by a novel p38/JNK kinase inhibitor. AIDS. **18:**739-748.

264. **Chang, W. W., I. J. Su, W. T. Chang, W. Huang, and H. Y. Lei.** 2008. Suppression of p38 mitogen-activated protein kinase inhibits hepatitis B virus replication in human hepatoma cell: the antiviral role of nitric oxide. J. Viral Hepat. **15:**490-497. doi: 10.1111/j.1365-2893.2007.00968.x; 10.1111/j.1365-2893.2007.00968.x.

265. **Luig, C., K. Kother, S. E. Dudek, M. Gaestel, J. Hiscott, V. Wixler, and S. Ludwig.** 2010. MAP kinase-activated protein kinases 2 and 3 are required for influenza A virus propagation and act via inhibition of PKR. FASEB J. **24:**4068-4077. doi: 10.1096/fj.10-158766; 10.1096/fj.10-158766.

266. **Ludlow, L. E., M. K. Lo, J. J. Rodriguez, P. A. Rota, and C. M. Horvath.** 2008. Henipavirus V protein association with Polo-like kinase reveals functional overlap with STAT1 binding and interferon evasion. J. Virol. **82:**6259-6271. doi: 10.1128/JVI.00409-08; 10.1128/JVI.00409-08.

267. **Mace, G., M. Miaczynska, M. Zerial, and A. R. Nebreda.** 2005. Phosphorylation of EEA1 by p38 MAP kinase regulates mu opioid receptor endocytosis. EMBO J. **24:**3235-3246. doi: 10.1038/sj.emboj.7600799.

268. **Zwang, Y., and Y. Yarden.** 2006. p38 MAP kinase mediates stress-induced internalization of EGFR: implications for cancer chemotherapy. EMBO J. **25:**4195-4206. doi: 10.1038/sj.emboj.7601297.

269. **Garrett, W. S., L. M. Chen, R. Kroschewski, M. Ebersold, S. Turley, S. Trombetta, J. E. Galan, and I. Mellman.** 2000. Developmental control of endocytosis in dendritic cells by Cdc42. Cell. **102:**325-334.

270. **Liu, N. Q., A. S. Lossinsky, W. Popik, X. Li, C. Gujuluva, B. Kriederman, J. Roberts, T. Pushkarsky, M. Bukrinsky, M. Witte, M. Weinand, and M. Fiala.** 2002. Human immunodeficiency virus type 1 enters brain microvascular endothelia by macropinocytosis dependent on lipid rafts and the mitogen-activated protein kinase signaling pathway. J. Virol. **76:**6689-6700.

271. **Diederich, S., L. Thiel, and A. Maisner.** 2008. Role of endocytosis and cathepsin-mediated activation in Nipah virus entry. Virology. **375:**391-400. doi: 10.1016/j.virol.2008.02.019; 10.1016/j.virol.2008.02.019.

272. **Marshall, C. J.** 1995. Specificity of receptor tyrosine kinase signaling: transient versus sustained extracellular signal-regulated kinase activation. Cell. **80:**179-185.

273. **Rusnati, M., C. Urbinati, B. Musulin, D. Ribatti, A. Albini, D. Noonan, C. Marchisone, J. Waltenberger, and M. Presta.** 2001. Activation of endothelial cell mitogen activated protein

kinase ERK(1/2) by extracellular HIV-1 Tat protein. Endothelium. **8:**65-74. doi: 10.3109/10623320109063158.

274. **Chang, L. Y., A. R. Ali, S. S. Hassan, and S. AbuBakar.** 2006. Nipah virus RNA synthesis in cultured pig and human cells. J. Med. Virol. **78:**1105-1112. doi: 10.1002/jmv.20669.

275. **Wong, K. T., I. Grosjean, C. Brisson, B. Blanquier, M. Fevre-Montange, A. Bernard, P. Loth, M. C. Georges-Courbot, M. Chevallier, H. Akaoka, P. Marianneau, S. K. Lam, T. F. Wild, and V. Deubel.** 2003. A golden hamster model for human acute Nipah virus infection. Am. J. Pathol. **163:**2127-2137. doi: 10.1016/S0002-9440(10)63569-9.

276. **Ofori-Acquah, S. F., J. King, N. Voelkel, K. L. Schaphorst, and T. Stevens.** 2008. Heterogeneity of barrier function in the lung reflects diversity in endothelial cell junctions. Microvasc. Res. **75:**391-402. doi: 10.1016/j.mvr.2007.10.006.

277. **Lee, B. P., and B. A. Imhof.** 2008. Lymphocyte transmigration in the brain: a new way of thinking. Nat. Immunol. **9:**117-118. doi: 10.1038/ni0208-117.

278. **Gupta, M., M. K. Lo, and C. F. Spiropoulou.** 2013. Activation and cell death in human dendritic cells infected with Nipah virus. Virology. **441:**49-56. doi: 10.1016/j.virol.2013.03.004; 10.1016/j.virol.2013.03.004.

279. **Kujime, K., S. Hashimoto, Y. Gon, K. Shimizu, and T. Horie.** 2000. p38 mitogen-activated protein kinase and c-jun-NH2-terminal kinase regulate RANTES production by influenza virus-infected human bronchial epithelial cells. J. Immunol. **164:**3222-3228.

280. **Mori, I., F. Goshima, T. Koshizuka, N. Koide, T. Sugiyama, T. Yoshida, T. Yokochi, Y. Nishiyama, and Y. Kimura.** 2003. Differential activation of the c-Jun N-terminal kinase/stress-activated protein kinase and p38 mitogen-activated protein kinase signal transduction pathways in the mouse brain upon infection with neurovirulent influenza A virus. J. Gen. Virol. **84:**2401-2408.

281. **Yurochko, A. D., and E. S. Huang.** 1999. Human cytomegalovirus binding to human monocytes induces immunoregulatory gene expression. J. Immunol. **162:**4806-4816.

282. **Holloway, G., and B. S. Coulson.** 2006. Rotavirus activates JNK and p38 signaling pathways in intestinal cells, leading to AP-1-driven transcriptional responses and enhanced virus replication. J. Virol. **80:**10624-10633. doi: 10.1128/JVI.00390-06.

283. **Lee, Y. J., and C. Lee.** 2012. Stress-activated protein kinases are involved in porcine reproductive and respiratory syndrome virus infection and modulate virus-induced cytokine production. Virology. **427:**80-89. doi: 10.1016/j.virol.2012.02.017;10.1016/j.virol.2012.02.017.

284. **Coulthard, L. R., D. E. White, D. L. Jones, M. F. McDermott, and S. A. Burchill.** 2009. p38(MAPK): stress responses from molecular mechanisms to therapeutics. Trends Mol. Med. **15:**369-379. doi: 10.1016/j.molmed.2009.06.005;10.1016/j.molmed.2009.06.005.

6.0 Appendix

6.1 Primary and Secondary Antibodies

Antibody	Species	Type	Source	Dilutions	
				Western Blot	IFA
NiV P58	Mouse	Monoclonal	Produced by NCFAD	1:1000	1:100
NiV – P, W,V	Rabbit	Polyclonal	From Dr. C. Kai (U.of Tokyo)	1:100	1:50, 1:100
NiV – N	Mouse	Monoclonal	Produced by NCFAD	1:1000	N/A
Anti-STAT1	Rabbit or Mouse	Polyclonal	Santa Cruz Biotechnology	1:500	1:200
Alexa Fluor 594 Anti-mouse	Goat	Fluorescent Red	Molecular Probes, Invitrogen	N/A	1:1000
Alexa Fluor 488 Anti-rabbit	Goat	Fluorescent Green	Molecular Probes, Invitrogen	N/A	1:1000
				Western Blot	
Beta-actin	rabbit	monoclonal	Cell Signaling	1:1000	
eIF2α phosphorylated	rabbit	monoclonal	Cell Signaling	1:1000	
eIF2α Total	mouse	monoclonal	Cell Signaling	1:1000	
ERK phosphorylated	rabbit	monoclonal	Cell Signaling	1:1000	
ERK total	rabbit	monoclonal	Cell Signaling	1:1000	
p38 MAPK phosphorylated	rabbit	monoclonal	Cell Signaling	1:1000	
p38 MAPK Total	rabbit	monoclonal	Cell Signaling	1:1000	
HRP conjugated secondary antibody	rabbit or mouse (IgG) H&L		KPL Mandel Scientific	1:5000	
				PBMC Separation	
CD6 anti-porcine	mouse	monoclonal	AbD SeroTec	1:100	
CD21 anti-human	mouse	monoclonal	AbD SeroTec	1:100	

CD16 anti-porcine	mouse	monoclonal	AbD SeroTec	1:100
				Flow cytometry
NiV – N	mouse	monoclonal	Produced by NCFAD	1:50
Guinea Pig Sera	guinea Pig	polyclonal	From infected animals (NCFAD)	1:100
Alexa Fluor 594 Anti-guinea pig	goat	Fluorescent Red	Molecular Probes, Invitrogen	1:1000
Alexa Fluor 488 Anti-mouse	goat	Fluorescent green	Molecular Probes, Invitrogen	1:1000
CD3 anti-porcine	mouse	FITC	BD Pharmingen	1:100
CD4 anti-porcine	mouse	FITC or PE	BD Pharmingen	1:100
CD8 anti-porcine	mouse	FITC or PE	BD Pharmingen	1:100
Isotype-IgG2a,k	mouse		BD Pharmingen	
Isotype-IgG2b,k	mouse		BD Pharmingen	
Isotype-IgG1	mouse		BD Pharmingen	
Isotype-IgG2a	mouse		BD Pharmingen	

6.2 Optimization of real time qRT-PCR for cytokine expression

The genes used for qRT-PCR were selected based on previous studies (235, 236). The commonly used HPRT and cyclophilin were selected as the reference genes. Figure 27A shows the plasmid constructs with each cytokine of interest and the house gene. Inserts were verified by sequencing and correct inserts were cloned. Nine-fold serial dilution of the plasmid DNA were prepared and used as template for the generation of the standard curve. In each run, the 96 well microliter plate contained each cDNA sample, plasmid for the standard curves and no template control. A no template control (NTC) was included in each run for each gene to check for

contamination. Quantitative real time RT-PCR was set using 2 µl of first strand cDNA template, the protocol was set up as described in the methods. Based on the Ct values for all dilution points in a series, a standard curve was generated (Fig. 27B), the PCR amplification efficiency of each primer was calculated from the slope of a standard curve. Melting curve analysis was constructed to verify presence of gene specific peaks and the absence of primer dimers. All the cytokine primers and housekeeping were specific and no primer dimers were detected at the final concentration used for the qRT-PCR. In addition agarose gel electrophoresis was performed to test specificity of all the amplicons and results were correct for each primer. Next, the expression levels of the candidate reference genes were evaluated with different stimuli such as NiV, PMA and ConA (Fig. 28). The cycle threshold (Ct) obtained did not differ with each stimuli however there was a difference in Ct with each housekeeping gene. When expression values were compared between cyclophilin and HPRT, HPRT mRNA difference was significant lower than cyclophilin as shown in Figure 28. Therefore the cyclophilin primers were used for normalization for the data present here since this gene was more stable and showed no significant difference between samples.

A

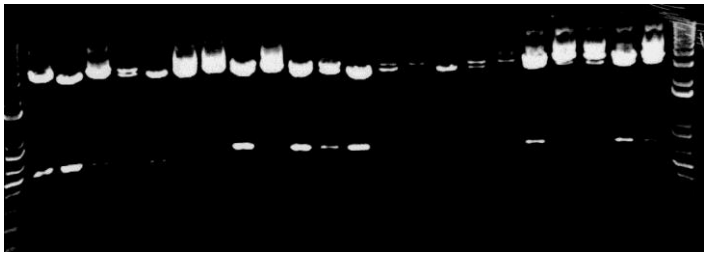

B

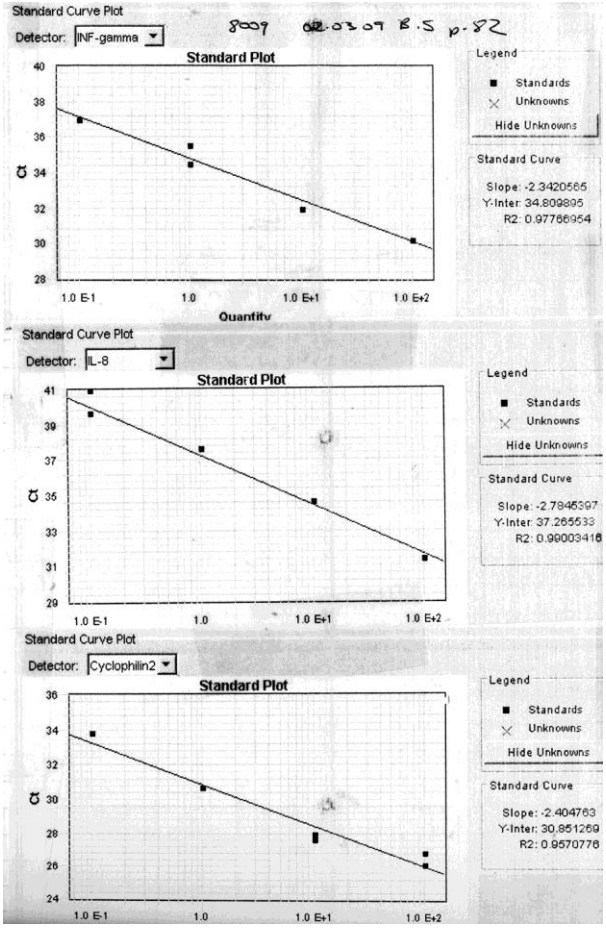

Figure 27 Preparation and testing of cytokine plasmid controls. (**A**) The agarose gel shows plasmid insertions from PCR fragments of each cytokine and housekeeping gene**. (B)** Using specific primers for each plasmid a concentration gradient was generated to determine the sensitivity of detection for the designed protocol.

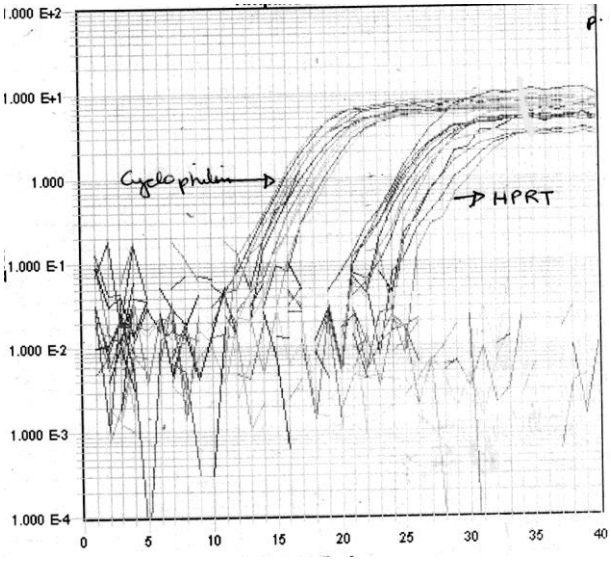

Figure 28 Different concentrations and induction protocols to test variation and sensitivity in housekeeping gene expression with optimized RT-PCR protocol.